CHAPTER V

RESULTS AND DISCUSSION

5.1 Definition of removal efficiency

This section describes the various definitions of the removal efficiency.

5.1.1 Apparent removal efficiency

$$\psi = \frac{(C_{in} - C_{out,anymA})}{C_{in}} \quad [-] \qquad (5.1)$$

5.1.2 Removal efficiency (by discharge effect only)

$$\psi' = \frac{(C_{out,0\,mA} - C_{out\ at\ any\ mA})}{C_{out,0\,mA}} \quad [-] \qquad (5.2)$$

In this definition, ψ represents the sole effect of corona discharge and excludes any effect of possible low-temperature adsorption and thermal decomposition inside the reactor system.

5.1.3 Removal efficiency per unit residence time

$$\psi'' = \frac{\psi' \times residence\ \ time\ at\ 25\ ^{0}C}{residence\ \ time\ at\ T\ ^{0}C} \qquad (5.3)$$

At steady state, the equation of continuity requires that $\rho_1 \langle \upsilon_1 \rangle A_1 = \rho_2 \langle \upsilon_2 \rangle A_2$. Since $A_1 = A_2$ and ρ is a function of the gas temperature, the gas velocity at temperature T_2 will be faster than its velocity at room temperature T_1. Thus the

mean residence time $\theta_2 = \frac{V_r}{\langle \upsilon_2 \rangle A_2}$ of this gas at T_2 is shorter than $\theta_1 = \frac{V_r}{\langle \upsilon_1 \rangle A_1}$ at room temperature. Here V_r is the effective volume of the corona discharge reactor. The removal efficiency per unit residence time is defined so as to take into account the effect of shortened residence time on the observed removal efficiency as the reactor temperature is increased.

5.1.3 Electron-based efficiency

$$\psi_{elec} = \frac{N_r}{N_{e0}} \tag{5.4}$$

The electron-based efficiency ψ_{elec} (-) is defined as the number of gas molecules removed by one discharged electron.

5.1.4 Energy-based efficiency

The energy-based efficiency ψ_{ener} (mol gas .J^{-1}) is defined as the mole of gas removed per energy consumption (J), as in Eq. (5.5).

$$\psi_{ener} = \frac{(q_{out,0\,mA} - q_{out\ at\ any\ mA})}{P} \tag{5.5}$$

Where $q_{out,\ 0\ mA}$, $q_{out\ at\ any\ mA}$, P are the molar flow rate of the target gases at the reactor outlet when using zero current, the molar flow rate of the target gases at the reactor outlet when using non-zero current and the power consumption, respectively.

5.2 Influence of temperature

5.2.1 Influence of temperature on electron energy

The voltages required to generate corona discharge are measured at different gas temperatures. From the experimental results, the voltages required to generate 0.2 mA in the removal of 200 ppm CH_3CHO, 200 ppm NH_3, and 200 ppm $(CH_3)_3N$ from N_2 - CO_2 are, respectively, 12.5, 8.6 and 11.5 kV at room temperature, and these voltages decrease to 4.6 , 4.2 and 6 kV, respectively, as temperature rises to 300°C. These voltages are approximately 30% higher when the target gases are removed from N_2 - O_2 - CO_2 mixture. Their values correspond to the profile changes in the electric field strength, E, inside the reactor. Meanwhile the gas temperature also affects the gas density, N. Thus it is important to note that the electron energy corresponds to the electric field strength divided by the gas density, E/N. To approximate E/N, the electric field strength described by Eq. (5.6) is used.

$$E = V / \{r \ln (D_1/D_o)\} \qquad (5.6)$$

V, r, D_1, D_o are the applied voltage, radial distance from the cylindrical axis, inner diameter of the cylindrical anode, and diameter of the wire cathode, respectively. Thus, the mean E/N is approximated by Eq. (5.7) (Tanthapanichakoon et al. 1998).

$$\langle E/N \rangle = \frac{\int_{D_0/2}^{D_1/2} (2\pi r)(E/N)\, dr}{\pi \left((D_1/2)^2 - (D_0/2)^2 \right)}$$

$$= \frac{4V}{N(D_1 + D_0)\ln(D_1/D_0)} \qquad (5.7)$$

N is calculated as $p/\{R\ (273+T)\}$, where p, R, T are total pressure, gas constant, and gas temperature, respectively. From this correlation, the average $\langle E/N \rangle$ in the case of CH_3CHO is 7.0 kV m^2 mol^{-1} and 5.8 kV m^2 mol^{-1} at room temperature and 300°C, respectively. E positively affects the electron energy because the electrons

emitted by the corona discharge are accelerated by E. On the other hand, N negatively affects the electron energy because the frequency of collisions between electrons and gas molecules becomes higher as N increases. In the case of toluene removal at high temperatures, there exists a general tendency that $\langle E/N \rangle$, the averaged value of E/N across section of the reactor, in both N_2 and air decreases with temperature in the high temperature range (Dhattavorn, 2000). A similar tendency is also observed for the present cases of CH_3CHO, NH_3 and $(CH_3)_3N$. This is primarily caused by a decrease in the required voltage associated with the temperature elevation. This voltage drop associated with temperature elevation may be explained as follows: (1) the voltage required for "corona discharge breakdown" which initiates ionization around the cathode is inversely proportional to the reactor temperature (Uhm, 1999). (2) Gas heating leads to more frequent electron detachment and decomposition of ion clusters that release the electron component so that the effective mobility of negative charges in the gas becomes high (Mnatsakanyan et al., 1987). (3) Gas expansion results in a longer mean free path of charged particles (Uhm, 1999). In spite of the voltage drop associated with the temperature elevation, if the negative thinning effect of gas expansion on N is relatively more significant than that of the temperature-induced voltage drop, the temperature dependency of $\langle E/N \rangle$ may become reversed. This phenomenon is often observed when T is below 200°C in N_2.

Since the electric field strength decreases only slightly when the temperature is elevated, the electron energy at 300°C turns out to be approximately 17% lower than at room temperature. Generally, the electron energy level should affect the reaction mechanism. For example, electron attachment tends to occur when electron energy is relatively low (Massey, 1976; Moruzzi, 1966; Caledonia, 1975), while formation of radicals may take place when electron energy is very high.

5.2.2 Influence of temperature on removal mechanism

Rigorously speaking, the relevant reactions contributing to the removal of CH_3CHO, NH_3 and $(CH_3)_3N$ are affected not only by the change in electron energy level but also by other effects of the elevated temperature. To consider the reaction mechanism, one must take byproduct formation into account. As for the gaseous byproducts, CO and O_3 were detected mainly in the low and NO_x in the high temperature ranges. In fact, the measurements of O_3 concentration during the removal of toluene from N_2 - O_2 mixture reveal that O_3 is produced up to 1370 ppm at room temperature but it rapidly drops down to 430 ppm at 100°C. When *T* is further increased above 300°C, O_3 concentration becomes negligible (Dhattavorn, 2000). This is because O_3 is unstable at high temperature (Peyrous, Pignolet and Held, 1989; Devins, 1956). Therefore, oxidation by O_3 should play a negligible role in the high temperature range.

Contrary to O_3 formation, it is known that production of NO_x by the discharge process is favored at high temperature. This is also confirmed in our experiments. While the outlet concentration of NO_x was negligible at room temperature, its concentration gradually increased with temperature and reached 300ppm at 400°C. Since NO_x formation can be attributed to the reaction of discharge-induced N radicals with O_2 (Lowke and Morrow, 1995; Mukkavilli et al., 1988), N radicals should also contribute to the removal of styrene and/or NH_3 from both N_2 and air at high temperatures. In addition, in the removal from air, there should be the extra effect of O radicals produced by electron impact to O_2 and by O_3 decomposition (Peyrous et al., 1989; Loiseau et al., 1966; Hadj-Ziane et al., 1990). Therefore, the removal efficiency from air at high temperatures should be enhanced by O radicals, though O_3 oxidation is not effective. In fact Peyrous et al. (1989) simulated the concentrations of O_3 and O radicals in pulsed corona discharge in the presence of O_2, and showed that temperature elevation brings about higher O radical concentration and lower O_3.

When H_2O is present in the gas stream, H^-, OH^- and a few O^- anions are expected to be produced by dissociative electron attachment to H_2O molecules at low temperature (Massey, 1976; Moruzzi and Phelps, 1966). The selectivity for

these ionic products should depend on the gas temperature and electron energy. At high temperature, electron detachment would become significant so that radicals of O, H, and OH may play a more important role than their anionic counterparts. These radicals are also expected to contribute to the removal of the target gases. More specifically, OH is believed to dissociate NH_3 to produce an aminogen radical (NH_2) and H_2O (Bityurin, Potapkin and Demisky, 2000).

In non-thermal corona discharge in the air at room temperature, electrons are sometimes captured by O_2 to form negative ions, O^-, O_2^-, O_3^-, and clusters via electron attachment. The reversed electron detachment process, however, becomes significant at high temperature, causing ion clusters to become unstable (Mnatsakanyan, Naydis and Solozobov, 1987). Several previous works indicate that the corona discharge reactor plays host to electron attachment reactions and relevant ion cluster formation at room temperature (Sano et al., 1997; Tamon, Sano and Okasaki, 1996). However, because of high temperature effects such as electron detachment and radical formation, electron attachment and ion clustering would be less and less important as the temperature rises.

In fluidized bed combustion conditions, the effect of coexisting gases, CO_2 and H_2O, on catalytic decomposition of NH_3 over limestone has been reported. In the absence of CO_2 and H_2O, NH_3 was decomposed to N_2. From a NH_3 - CO_2 mixture, $(NH_2)_2CO$ was formed through NH_3 decomposition over both calcined limestone and CO_2. However, from the NH_3 - CO_2 - H_2O mixture, $(NH_2)_2CO$ was not formed (Tadaaki Shimizu et al., 1995). CO_2 is perceived to be less reactive and its efficient catalytic conversion has remained elusive. Since CO_2 is a highly oxidized, thermodynamically stable compound, its utilization requires reaction with certain high energy substances or electro reductive processes. Catalytic hydrogenation is one of the most promising approaches to CO_2 fixation. Recent research has shown that high catalytic efficiency, yield, and rate of reaction can be obtained from CO_2 with the used of optimum conditions and catalysts (Ryoji Noyori et al., 1995).

When CO_2 is present in the gas stream, CO_3^- and a few O^- anions are expected to be produced by dissociative electron attachment to CO_2 molecules at low temperature (Price and Moruzzi, 1966).

In the case of NH_3 removal, the removed NH_3 was converted to needle-like bright crystal, which was observed inside the reactor and the gas line downstream. It is reported (Sugimitsu, 1998) that NH_3 does not react with O_3 to directly form NH_4NO_3. Instead the following consecutive reactions are mentioned:
$2\ NH_3 + 4O_3 = NH_4NO_2 + H_2O_2 + 4O_2$; $NH_4NO_2 + H_2O_2 = NH_4NO_3 + H_2O$. Our result is also consistent with published reports that NH_4NO_3 solid is produced by corona treatment of humid air containing NH_3 (Bityurin et al., 2000; Kanasawa et al., 1998; Urashima, Kim and Chang, 1999). The mechanism for NH_4NO_3 formation in the high temperature range is not clear but it may be considered that NH_3, H_2O and NO_x as well as N and H radicals could react to form NH_4NO_3.

5.3 Substantiation of ozone effect

When O_2 is present in N_2 or a gas mixture, it readily reacts with electrons of sufficient energy level. Electron attachment on O_2 has been reported in the literature (Morruzzi and Phelps, 1966; Massey, 1976; Rapp and Briglia, 1976; Chantry and Schulz, 1967)

$$O_2 + e^- \longrightarrow O_2^- \qquad \text{(a)}$$

$$O_2 + e^- \longrightarrow O + O^- \qquad \text{(b)}$$

Moruzzi and Phelps (1966) report that the reaction in Equation (a) occurs in the low electron energy range ($E/p < 1.5$ $V.m^{-1}.Pa^{-1}$). In contrast, the reaction in Equation (b) occurs in the higher electron energy range. Also in a corona - discharge reactor, the closer the electrons are to the cathode wire, the higher their energy level. When O_2 collides with a high - energy electron near the cathode wire in the corona-discharge reactor, production of O^- is expected as in Equation (b). Next O_3 is produced from the reaction of O^- with O_2 (Loiseau et al., 1994; Hadj-Zaine et al., 1992).

In short, not only O_2^- and O^- radicals but some ozone (O_3) is also produced. Since O_3 is very reactive, the ozonation reaction is used in some commercial devices for deodorization and sterilization. The same ozonation reaction as well as the oxidation reaction with O^- radicals is expected to contribute to the decomposition and removal of gas impurities in the present corona discharge reactor. The O^- radical is also expected to contribute to the formation of ionic clusters and removal of the gas impurities.

To substantiate the role of the ozonation, two identical reactors are connected serially. **Figure 5.1** shows the experimental setup used to confirm the O_3 effect. N_2 - O_2 mixture is supplied to the first reactor to produce O_3 by corona discharge. Then a gas impurity is mixed into the effluent stream from the first reactor, and the resulting mixture is introduced to the second reactor. No voltage is supplied to the second reactor, so there is no corona discharge in the second reactor, which only provides space for the reaction of ozone with the impurity. Then the change in the concentration of the impurity at the outlet of the second reactor is measured. The decrease in the outlet concentration from the second reactor gives the O_3 effect.

Chaichanawong (2003) shows that the formation of O_3 from N_2 - O_2 mixed gas (N_2 65 cc/min and O_2 5 cc/min). In the first reactor, N_2 - O_2 mixed gas is carried out at the discharge current 0.20 mA and the effluent stream is mixed with N_2 20 cc/min before feeding to the second reactor without discharge current. $[O_3]_{in}$ and $[O_3]_{out}$ of the second reactor are 700 ppm and 650 ppm, respectively. Next CH_3CHO (2000 ppm balanced with N_2) at 30 cc/min is mixed with N_2 70 cc/min before feeding in the second reactor. $[CH_3CHO]_{in}$ and $[CH_3CHO]_{out}$ are 600 ppm and 583 ppm, respectively. In contrast, when CH_3CHO (2000 ppm balanced with N_2) at 30 cc/min is mixed with the N_2 - O_2 effluent stream (N_2 65 cc/min and O_2 5 cc/min) from the first reactor at the discharge current 0.20 mA, the outlet concentration of CH_3CHO at the outlet of the second reactor is reduced from 600 ppm to 380 ppm. It can be confirmed that O_3 has an important role on CH_3CHO removal efficiency.

In addition, the effect of O_3 on the removal of $(CH_3)_3N$ was also investigated as shown in appendix K. The results were the same as in the case of CH_3CHO. In

the case of NH_3, O_3 also has an important role on the removal efficiency (Chaiyo, 2001).

5.4 Blank test for the investigation of the effect of temperature on acetaldehyde, ammonia and trimethyl amine removal

The experimental results in the Appendices D - K show the results of the blank test for the investigation of temperature effect on acetaldehyde, ammonia and trimethyl amine removal. Here the concentration of the target gases at the reactor outlet was measured at various temperatures in the absence of the discharge current. **Figure 5.2** shows the results of the blank test for investigation of temperature effect on acetaldehyde (CH_3CHO) in N_2 - O_2 - CO_2 mixture. There appeared a concentration drop at room temperature, which is considered to be due to physical adsorption inside the reactor. At moderate temperature, the effect of adsorption inside the reactor slightly increased as the reactor temperature increased. However, the outlet concentration of CH_3CHO again decreased at 300°C. The reverse effect at this highest temperature may be attributed to the thermal decomposition. **Figure 5.3** shows the results of the blank test for investigation of temperature effect on ammonia (NH_3) in N_2 - O_2 - CO_2 mixture. It is found that the outlet concentration of NH_3 slightly decreases at 300°C via the thermal decomposition. **Figure 5.4** shows the results of the blank test for the investigation of temperature effect on trimethylamine $(CH_3)_3N$ in N_2 - O_2 - CO_2 mixture. It is found that the outlet concentration of $(CH_3)_3N$ decreases above room temperature. Some extraneous peaks were observed in the gas chromatogram of the effluent stream which confirmed that thermal decomposition of $(CH_3)_3N$ may occur.

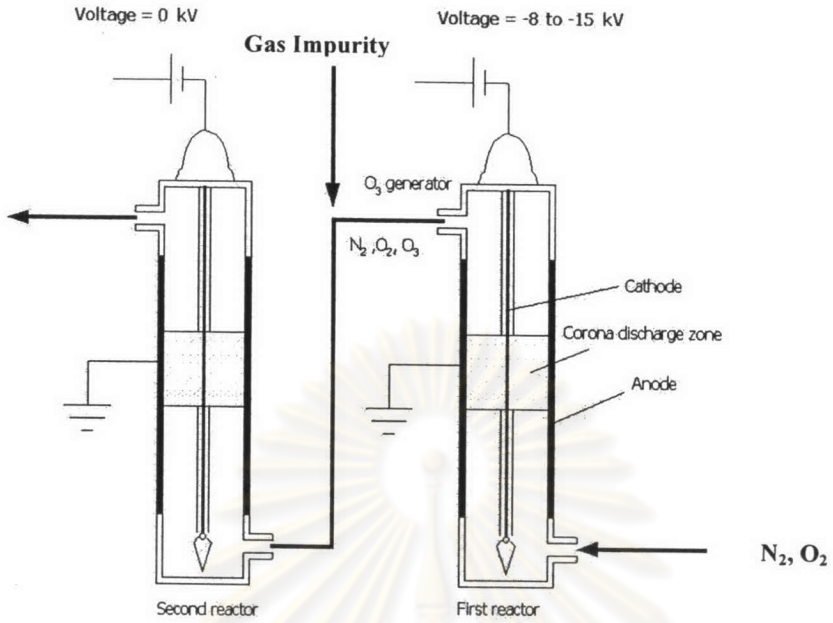

Figure 5.1 Apparatus to substantiate O_3 effect

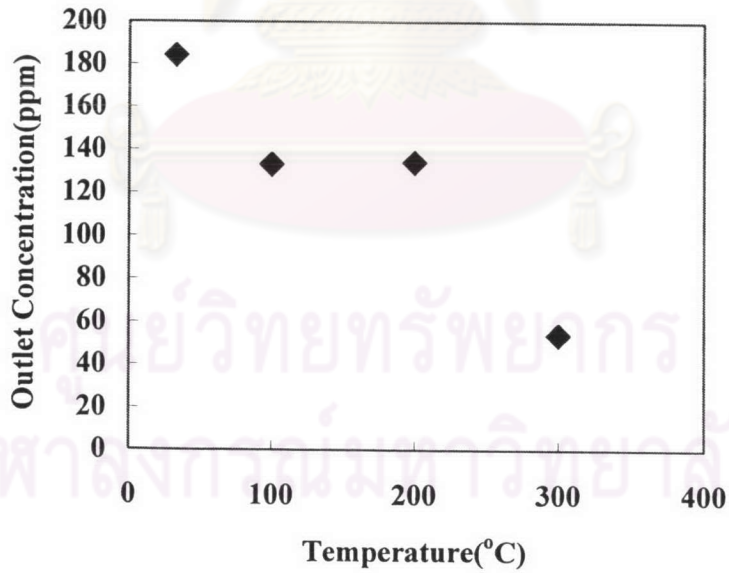

Figure 5.2 Blank tests for the removal of CH_3CHO 200 ppm from N_2 - O_2(10%) - CO_2(10%)

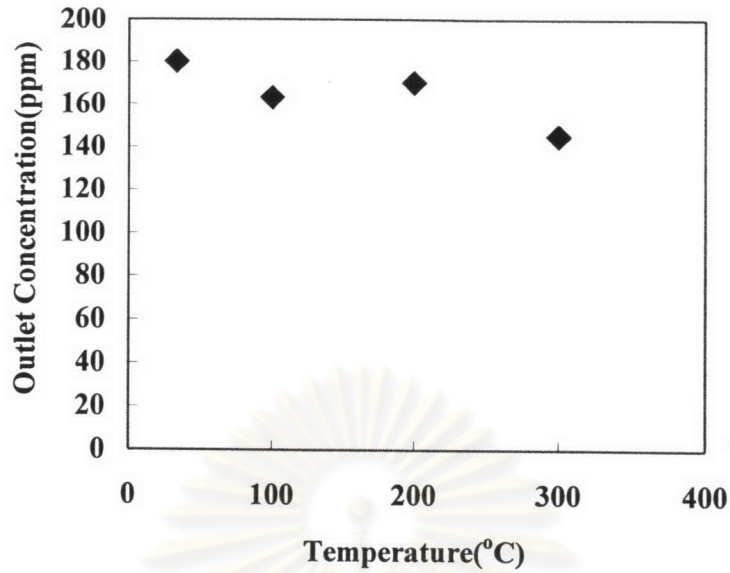

Figure 5.3 Blank tests for the removal of NH_3 200 ppm from N_2 - O_2(10%) - CO_2(10%)

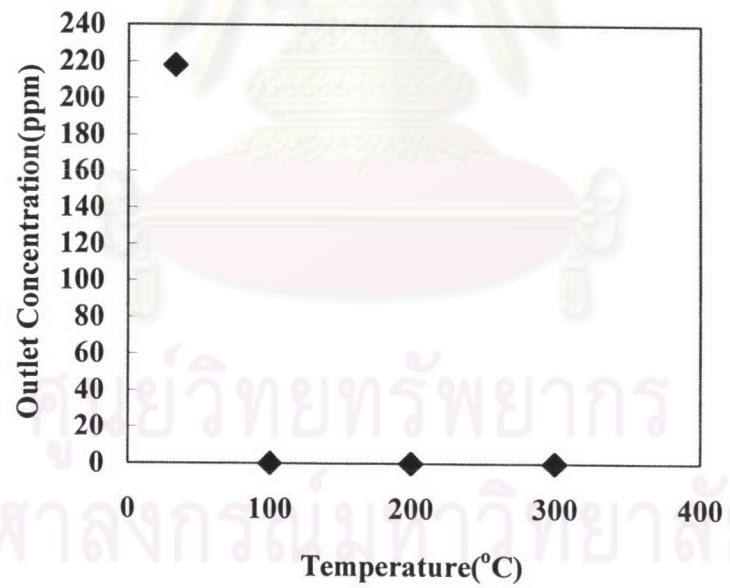

Figure 5.4 Blank tests for the removal of $(CH_3)_3N$ 200 ppm from N_2 - O_2(10%) - CO_2(10%)

ศูนย์วิทยทรัพยากร
จุฬาลงกรณ์มหาวิทยาลัย

5.5 Removal of acetaldehyde (CH_3CHO)

5.5.1 Effect of temperature and coexisting CO_2 on the removal of CH_3CHO from N_2

In most actual applications of gas purification, several kinds of gas components often coexist. Therefore, it is necessary to study the influence of common coexisting gases on the removal efficiency.

Figure 5.5 shows the removal efficiency ψ' of CH_3CHO versus temperature. From **Figure 5.5 (a),** we see that, as the temperature increases, the removal efficiency ψ' decrease from room temperature up to 200°C, then the tendency reverses up to 300°C because the effect of O^- anion and CO_3^- is strong at low temperature but the mean residence time of the gas mixture inside the reactor decreases as the reactor temperature rises. This phenomenon is attributable to the fact that the gas mixture flows upward more quickly as its volume expands. Obviously, the presence of CO_2 does significantly affect the removal efficiency. It is postulated that CO_2 is less electronegative than CH_3CHO but the bonding strength of CO_2 molecules with the anode surface is stronger than that of CH_3CHO. Thus, at low temperature when a smaller number of electrons are available at low discharge currents, most electrons attach onto CH_3CHO and deposit on the anode wall is composed of mostly CH_3CHO. At high temperature, there is an excess of electrons that can attach to CO_2. When the CO_2 ions deposit on the anode surface, they replace (drive off) some of the previously deposited CH_3CHO. The higher the CO_2 concentration, the higher the removal efficiency. Since CO_2 is a highly oxidized, thermodynamically stable compound, its utilization requires reaction with certain high - energy substances or electro reductive processes. Catalytic hydrogenation is one of the most promising approaches to CO_2 fixation. Recent research has shown that high catalytic efficiency, yield, and rate of reaction can be obtained from CO_2 with the use of optimum conditions and catalysts (Ryoji Noyori et al., 1995). **Figure 5.5 (b)** reveals that when the negative effect of reduced residence time is taken in account, the value of ψ'' increases with temperature up to 100°C.

At room temperature, 100, 200 and 300°C, ψ_{elec} of CH_3CHO at 200 ppm - CO_2 (10%, 20%) are 3.9, 3.5, 1.0, 1.3 and 4.5, 3.7, 1.3, 1.2, respectively. Interestingly, ψ_{elec} at 200°C of CO_2 (10%) become lower than 300°C, thus indicating the possible existence of an optimal temperature. The high values of ψ_{elec} at low temperature reveal that ion clusters may be produced. It has been reported that dissociate electron attachment of CH_3CHO may produce O^-, C_2O^-, HC_2O^-, CH_3CO^-, or CH_3^- (Dressler and Allan, 1985). The selectivity to produce these ions depends on the level of electron energy. However, at high temperatures, electron detachment would become significant so that the positive effect of these ions is negated. Moreover, at high temperatures, the rate of detachment of the attached CH_3CHO molecules on the reactor wall is sufficiently enhanced by the lowered adsorption equilibrium to overcome the effect of electrostatic attraction, thus significantly reducing the net rate of CH_3CHO deposition on the wall. However, ψ_{elec} at 200°C of CO_2 (20%) becomes higher than 300°C because of the effect of reduced residence time and removal efficiency in case of CO_2 (20%) is higher than CO_2 (10%). Obviously, the presence of CO_2 does significantly enhance the removal efficiency.

5.5.2 Effect of temperature and coexisting CO_2 and O_2 on the removal of CH_3CHO from N_2

Figure 5.6 shows the removal efficiency ψ' of CH_3CHO versus temperature. From **Figure 5.6 (a),** we see that, as the temperature increases, the removal efficiency ψ' remains nearly 100% from room temperature up to 300°C because of the effect of O_3, CO_3^- and O^- anion at low temperatures and various radicals at high temperatures. This can be attributed to the fact that O_3 is produced from O_2 by the corona discharge reaction and is quite stable at room temperature. At room to moderate temperatures, electron attachment reactions contribute to, and relevant ion cluster formation enhances, the removal of numerous electro - negative compounds (Sano et al., 1997; Bityurin; 2000). N radicals should also contribute to the removal of CH_3CHO from both N_2 and air at high temperatures. In addition, in the removal

from air, there should be the extra effect of O radicals produced by electron impact on O_2 and by O_3 decomposition (Peyrous, Pignolet and Held, 1989; Loiseau et al. 1994; Hadj - Ziane, 1990). Therefore, the CH_3CHO removal efficiency ψ' at high temperatures should be enhanced by O radicals although O_3 oxidation is not effective. And the presence of CO_2 does significantly affect the removal efficiency of CH_3CHO from N_2 - O_2. **Figure 5.6 (b)** reveals that when the negative effect of reduced residence time is taken in account, the value of ψ^{*} increases with temperature increases.

At room temperature, 100, 200 and 300°C, ψ_{elec} of CH_3CHO at 200 ppm-O_2 (10, 20%)-CO_2 (10%, 20%) are (3.9, 2.3, 1.8, 0.6), (3.9, 3.0, 2.7, 0.8), (4.0, 3.0, 2.7, 0.8), (3.3, 2.7, 2.1, 0.6) respectively. Interestingly, as the temperature increases, ψ_{elec} decreases, thus, indicating the possible existence of an optimal temperature. The high values of ψ_{elec} at low temperatures reveal that electron attachment reactions contribute to, and relevant ion cluster formation enhances, the removal of numerous electro-negative compounds (Sano et al., 1997; Bityurin; 2000). This can be attributed to the fact that O_3 is produced from O_2 by the corona discharge reaction and is quite stable at room temperature. N radicals should also contribute to the removal of CH_3CHO from both N_2 and air at high temperatures.

5.5.3 Effect of temperature and coexisting CO_2 and H_2O on the removal of CH_3CHO from N_2

Figure 5.7 shows the removal efficiency ψ' of CH_3CHO versus temperature. From **Figure 5.7 (a),** we see that, as the temperature increases, the removal efficiency ψ' decrease from room temperature up to 200°C, then the tendency reverses up to 300°C because the mean residence time of the gas mixture inside the reactor decreases as the reactor temperature rises. For the effect of H^-, OH^-, a few O^- anions and CO_3^- should contribute to the removal of CH_3CHO at low to moderate temperatures. At 200°C, the presence of H_2O and CO_2 slightly retards the removal efficiency of CH_3CHO because at low discharge currents, the relatively much

smaller number of electrons tends to attach mostly to H_2O and CO_2. In addition, N radicals are consumed by their reaction with H_2O at high temperatures. Obviously, the presence of CO_2 does significantly affect the removal efficiency. The higher the CO_2 concentration, the higher the removal efficiency. **Figure 5.7 (b)** reveals that when the negative effect of reduced residence time is taken in account, the value of $\psi^{"}$ increases with temperature up to 100°C.

At room temperature, 100, 200 and 300°C, ψ_{elec} of CH_3CHO at 200 ppm - H_2O (5250, 10500, 21800 ppm) - CO_2 (10%, 20%) are (3.2, 2.3, 0.6, 1.0), (3.8, 2.8, 1.3, 1.3), (3.5, 3.0, 1.4, 1.3), (3.7, 3.0, 1.5, 1.5), (4.1, 3.0, 1.4, 1.3), (4.1, 3.1 2.5, 1.5) respectively. Interestingly, as the temperature increases, ψ_{elec} decreases, thus, indicating the possible existence of an optimal temperature. The high values of ψ_{elec} at low temperature reveal that ion clusters may produce and these clusters increase when the inlet concentration increases. It has been reported that dissociative electron attachment of CH_3CHO may produce O^-, C_2O^-, HC_2O^-, CH_3CO^-, or CH_3^- (Dressler and Allan, 1985). The selectivity to produce these ions depends on the level of electron energy. However, at high temperatures, electron detachment would become significant so that the positive effect of these ions is negated. Moreover, at high temperatures, the rate of detachment of attached CH_3CHO molecules on the reactor wall is sufficiently enhanced by the lowered adsorption equilibrium to overcome the effect of electrostatic attraction, thus significantly reducing the net rate of CH_3CHO deposition on the wall. As mentioned earlier, the high values of ψ_{elec} at low temperature reveal that electron attachment reactions contribute to, and relevant ion cluster formation enhances, the removal of numerous electro-negative compounds (Sano et al., 1997; Bityurin; 2000).

5.5.4 Effect of temperature and coexisting CO_2, O_2 and H_2O on the removal of CH_3CHO from N_2

Figure 5.8 shows the removal efficiency ψ' of CH_3CHO versus temperature. From **Figure 5.8 (a),** we see that, as the temperature increases, the removal

efficiency ψ' remains nearly 100% from room temperature up to 300°C. This can be attributed to the fact that O_3 is produced from O_2 by the corona discharge reaction and is quite stable at room temperature. At room to moderate temperatures, electron attachment reactions contribute to, and relevant ion cluster formation enhances, the removal of numerous electro-negative compounds (Sano et al., 1997; Bityurin; 2000). N radicals should also contribute to the removal of CH_3CHO from both N_2 and air at high temperatures. In addition, in the removal from air, there should be the extra effect of O radicals produced by electron impact to O_2 and by O_3 decomposition (Peyrous, Pignolet and Held, 1989; Loiseau et al. 1994; Hadj - Ziane, 1990). CO_3^-, H^-, OH^- and a few O^- anions should contribute to the removal of CH_3CHO at low to moderate temperatures. At high temperatures, electron detachment would become significant so that radicals of O, H, and OH may play a more important role than their anionic counterparts. These radicals are also expected to contribute to the removal of the CH_3CHO. And the presence of CO_2 does significantly affect the removal efficiency of CH_3CHO from N_2 - O_2 - H_2O. **Figure 5.8 (b)** reveals that when the negative effect of reduced residence time is taken in account, the value of ψ'' increases with temperature increases.

The effects of coexisting CO_2, O_2 and H_2O are shown in Figure A and B. The influence of CO_2 concentration was examined and shown in cases A and B. The concentration CO_2 is varied from 10% to 20% with fixed concentration O_2 and H_2O. Similarly, the influence of concentration H_2O in the range of (5250 – 21800 ppm) at fixed concentrations of O_2 and CO_2 was examined and shown in cases C, G and K to evaluate the effect of H_2O. Here, we can not see the effects of both CO_2 and H_2O in this concentration range. This is because the concentration of O_2 is excessive for all runs. When O_2 concentration is excessive, ψ' can reach 100% although the concentrations of CO_2 and H_2O are changed.

The experimental results from the removal of NH_3 and $(CH_3)_3N$ from single, double and tertiary components could also be explained as mentioned above.

5.5.5 Preliminary summary

Generally, two other types of removal efficiency are reported for a corona-discharge system. The electron - based efficiency ψ_{elec} (-) is defined as the number of gas molecules removed by one discharged electron, and the energy-based efficiency ψ_{ener} (mol gas $.J^{-1}$) is defined as the mole of gas removed per energy consumption (J). At 33, 100, 200 and 300°C, the experimental values of ψ_{elec} and ψ_{ener} of the CH_3CHO 200 ppm removal are as follows:

N_2 - CO_2 (10%), (I=0.2 mA):

ψ_{elec} = 3.9, 3.5, 1.0, 1.3 $\psi_{ener} \times 10^{-9}$ = 4.8, 5.6, 2.6, 4.4

N_2 - O_2 (10%) - CO_2 (10%), (I=0.2 mA):

ψ_{elec} = 3.9, 2.3, 1.8, 0.6 $\psi_{ener} \times 10^{-9}$ = 4.5, 3.1, 3.0, 1.2

N_2 - H_2O (10500 ppm) - CO_2 (10%), (I=0.2 mA):

ψ_{elec} = 3.5, 3.0, 1.4, 1.3 $\psi_{ener} \times 10^{-9}$ = 4.1, 4.2, 2.9, 3.7

N_2 - O_2 (10%) - H_2O (10500 ppm) - CO_2 (10%), (I=0.2 mA):

ψ_{elec} = 4.1, 3.3, 2.6, 0.9 $\psi_{ener} \times 10^{-9}$ = 4.5, 4.4, 4.2, 2.0

Generally ψ_{elec} and ψ_{ener} tends to decrease as the gas temperature increases. This trend may be ascribed to the combined effect of reduced residence time and the shift in removal mechanism. Interestingly, in the case of N_2 - CO_2, ψ_{elec} and ψ_{ener} at 200°C become lower than at 300°C, thus indicating the possible existence of an optimal temperature.

In actual applications of gas purification, it is important to consider the energy-based efficiency ψ_{ener}. From the above results, it is recommended to operate from 100 to 200°C for minimizing the operating cost when air is purified because the values of ψ_{ener} are high.

5.5.6 Byproducts dected on the removal of acetaldehyde

Figure 5.9 shows the concentration of the main byproduct CO versus temperature in the presence of CO_2. In **Figure 5.9** as the temperature increases, the byproducts CO decrease starting from room temperature up to 200°C, then the tendency reverses up to 300°C because the mean residence time of the gas mixture inside the reactor decreases as the reactor temperature rises. It is known that CO can be produced by dissociative attachment reaction. This is also confirmed in our experiments.

Figure 5.10 shows the concentration of another byproduct NO_x versus temperature in the presence of CO_2. In **Figure 5.10** as the temperature increases, the byproducts NO_x increase. It is known that production of NO_x by the discharge process is favored at high temperature. This is also confirmed in our experiments. While, the outlet concentration of NO_x was negligible at room temperature, its concentration gradually increased with temperature rise.

Figure 5.11 shows the concentration of the byproduct CO versus temperature in the presence of O_2 and CO_2. In **Figure 5.11** as the temperature increases, the byproduct CO decreases as the temperature rises because at high temperatures O_3 is unstable.

Figure 5.12 shows the concentration of byproduct O_3 versus temperature in the presence of O_2 and CO_2. In **Figure 5.12** as the temperature increases, the byproduct O_3 decreases as the temperature rises. This is because O_3 is unstable at high temperature (Peyrous, Pignolet and Held, 1989; Devins, 1956).

Figure 5.13 shows the concentration of the byproduct NO_x versus temperature in the presence of O_2 and CO_2. In **Figure 5.13** as the temperature increases, the byproducts NO_x decrease starting from room temperature up 200°C, then the tendency reverses up to 300°C. As the temperature increases, the byproduct O_3 decreases with temperature rises and the mean residence time of the gas mixture inside the reactor decreases as the reactor temperature rises.

Figure 5.14 shows the concentration of the byproduct CO versus temperature in the presence of H_2O and CO_2. In **Figure 5.14** as the temperature increases, the byproducts CO increase. At low temperatures, the presence of CO_2 and H_2O in the

gas stream CO_3^-, H^-, OH^- and a few O^- anions are expected to be produced by dissociative electron attachment to CO_2 and H_2O molecules (Massey, 1976; Moruzzi and Phelps, 1966). At high temperature, electron detachment would become significant so that radicals of CO_3, O, H, and OH may play a more important role than their anionic counterparts.

Figure 5.15 shows the concentration of the byproduct NO_x versus temperature in the presence of H_2O and CO_2. In **Figure 5.15** as the temperature increases, the byproduct NO_x increases. It is known that production of NO_x by the discharge process is favored at high temperature. This is also confirmed in our experiments. While the outlet concentration of NO_x was negligible at room temperature, its concentration gradually increased with the temperature rise.

Figure 5.16 shows the concentration of the byproduct CO versus temperature in the presence of O_2, H_2O and CO_2. In **Figure 5.16** as the temperature increases, the byproduct CO decreases with the temperature rise. Since CO_2 and H_2O are present in the gas stream, CO_3^-, H^-, OH^- and a few O^- anions are expected to be produced by dissociative electron attachment to CO_2 and H_2O molecules at low temperature (Massey, 1976; Moruzzi and Phelps, 1966).

Figure 5.17 shows the concentration of the byproduct O_3 versus temperature in the presence of O_2, H_2O and CO_2. In **Figure 5.17** as the temperature increases, the byproduct O_3 decreases with the temperature rise because at high temperature, O_3 is unstable (Peyrous, Pignolet and Held, 1989; Devins, 1956).

Figure 5.18 shows the concentration of the byproduct NO_x versus temperature in the presence of O_2, H_2O and CO_2. In **Figure 5.18** as the temperature increases, the byproduct NO_x decreases starting from room temperature up 200°C, then the tendency reverses up to 300°C. As the temperature starts to increase, the byproduct O_3 decreases. At high temperatures, electron detachment would become significant so that radicals of CO_3, O, H, and OH may play a more important role than their anionic counterparts. However, the mean residence time of the gas mixture inside the reactor decreases as the reactor temperature rises.

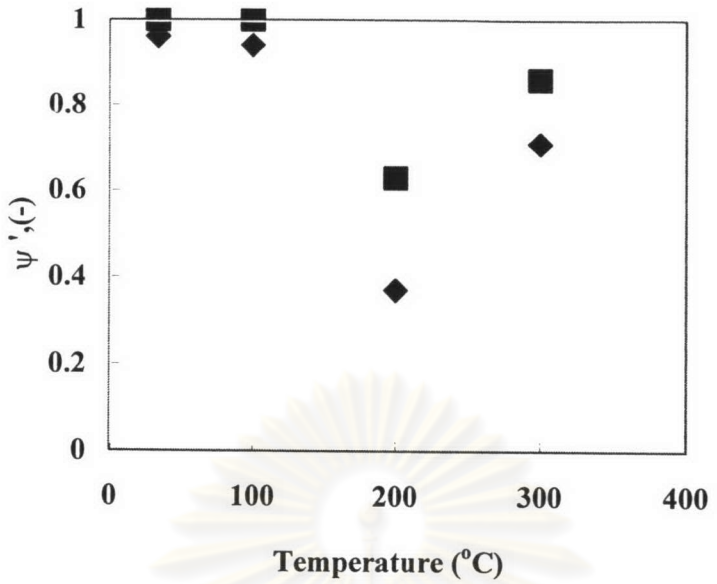

(a)

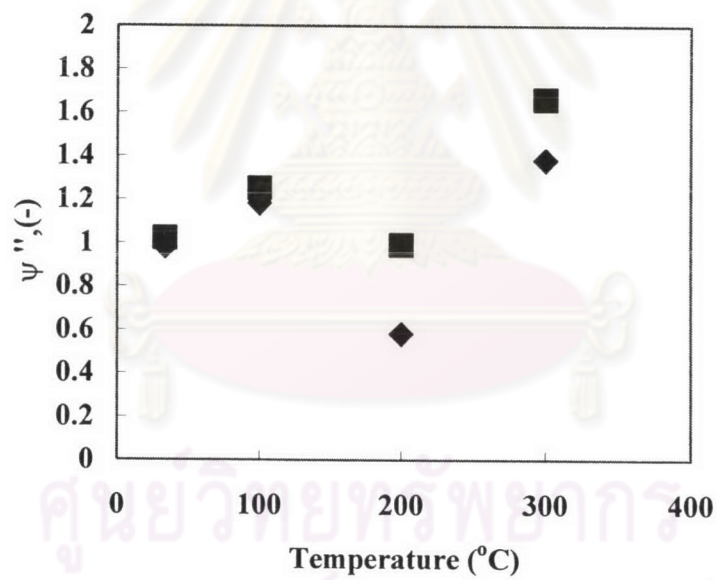

(b)

Figure 5.5 Effect of CO_2 on the removal of CH_3CHO from N_2; $C_{in,\ acetaldehyde}$=200ppm, I=0.2mA, SV=55.8 hr^{-1} at room temperature: ◆ CO_2 (10%), ■ CO_2 (20%)

ศูนย์วิทยทรัพยากร
จุฬาลงกรณ์มหาวิทยาลัย

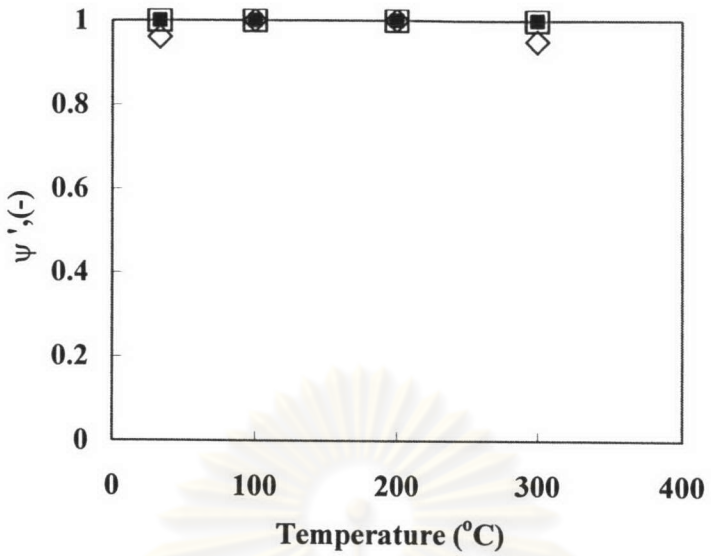

(a)

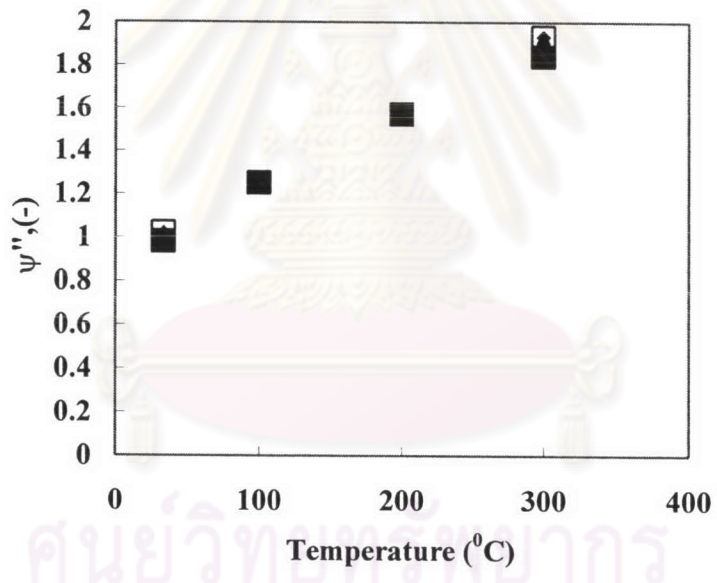

(b)

Figure 5.6 Effect of coexisting O_2-CO_2 on the removal of CH_3CHO from N_2; $C_{in,\ acetaldehyde}$=200ppm, I=0.2mA, SV=55.8 hr^{-1} at room temperature:
◆ CO_2 (10%) - O_2 (10%),
◇ CO_2 (20%) - O_2 (10%),
■ CO_2 (10%) - O_2 (20%),
□ CO_2 (20%) - O_2 (20%)

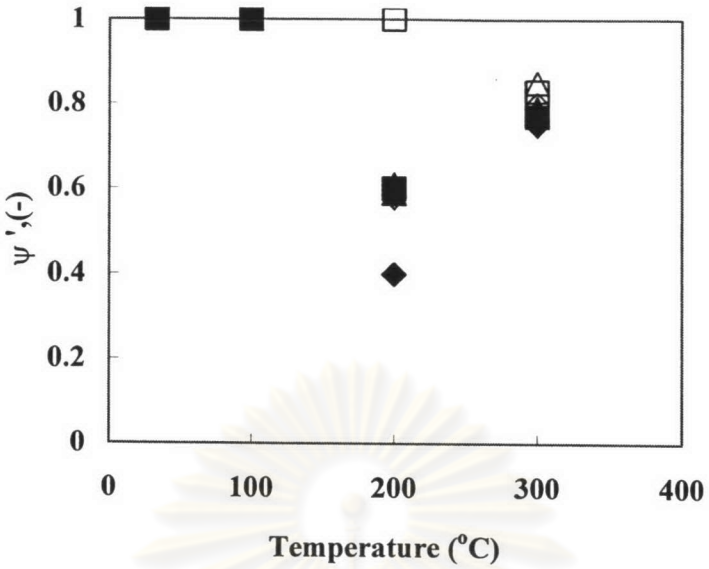

(a)

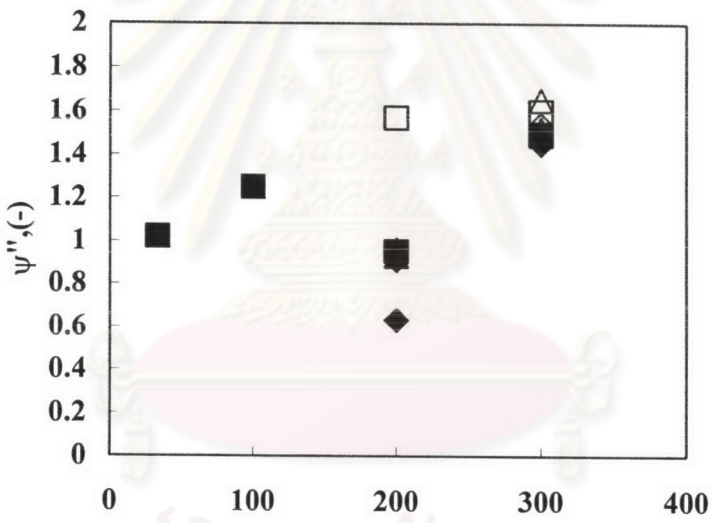

(b)

Figure 5.7 Effect of coexisting H_2O-CO_2 on the removal of CH_3CHO from N_2; $C_{in,\ acetaldehyde}$=200ppm, I=0.2mA, SV=55.8 hr^{-1} at room temperature:
- ◆ CO_2 (10%) - H_2O (5250ppm),
- ◇ CO_2 (20%) - H_2O (5250ppm),
- ▲ CO_2 (10%) - H_2O (10500ppm),
- △ CO_2 (20%) - H_2O (10500ppm),
- ■ CO_2 (10%) - H_2O (21800ppm),
- □ CO_2 (20%) - H_2O (21800ppm)

ศูนย์วิทยทรัพยากร
จุฬาลงกรณ์มหาวิทยาลัย

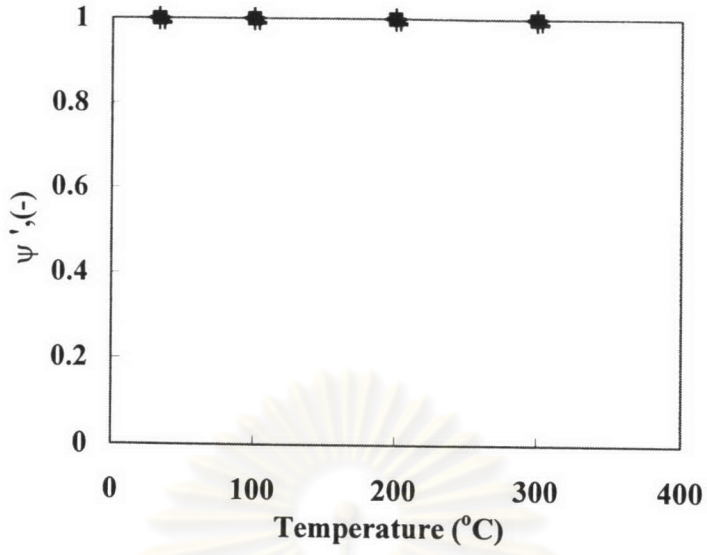

(a)

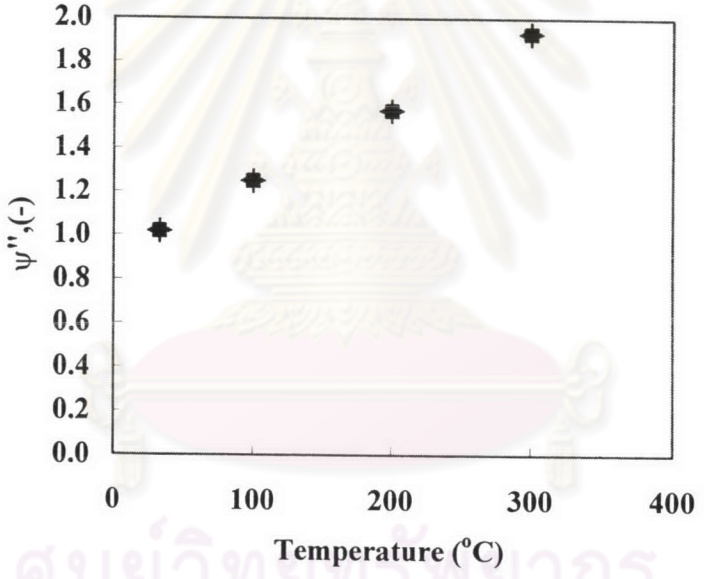

(b)

Figure 5.8 Effect of coexisting O_2-H_2O-CO_2 on the removal of CH_3CHO from N_2; $C_{in,\ acetaldehyde}$=200ppm, I=0.2mA, SV=55.8 hr^{-1} at room temperature:

A ◆ CO_2 (10%)-O_2 (10%)-H_2O (5250ppm), ◇ CO_2 (20%)-O_2 (10%)-H_2O (5250ppm), **B**
C ▲ CO_2 (10%)-O_2 (20%)-H_2O (5250ppm), △ CO_2 (20%)-O_2 (20%)-H_2O (5250ppm), **D**
E ■ CO_2 (10%)-O_2 (10%)-H_2O (10500ppm), □ CO_2 (20%)-O_2 (10%)-H_2O (10500ppm), **F**
G ● CO_2 (10%)-O_2 (20%)-H_2O (10500ppm), ○ CO_2 (20%)-O_2 (20%)-H_2O (10500ppm), **H**
I ⁎ CO_2 (10%)-O_2 (10%)-H_2O (21800ppm), × CO_2 (20%)-O_2 (10%)-H_2O (21800ppm), **J**
K + CO_2 (10%)-O_2 (20%)-H_2O (21800ppm), ━ CO_2 (20%)-O_2 (20%)-H_2O (21800ppm) **L**

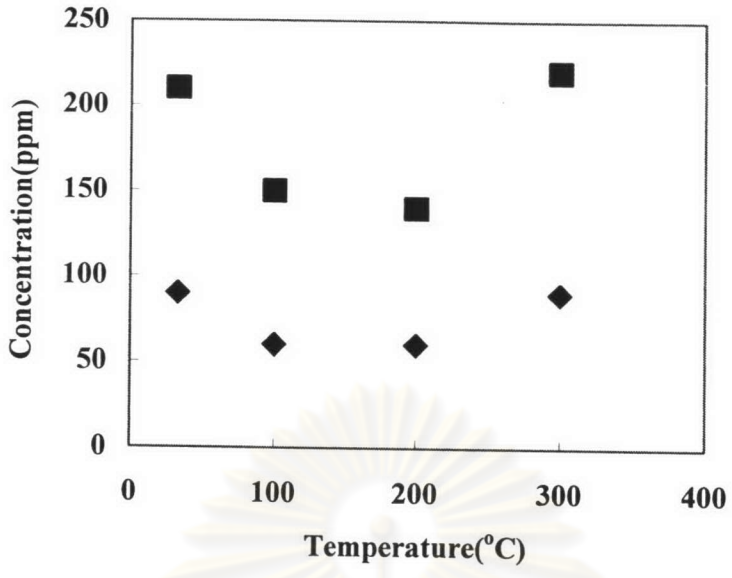

Figure 5.9 Byproduct (CO) on the removal of CH_3CHO from N_2-CO_2: ◆ CO_2 (10%), ■ CO_2 (20%)

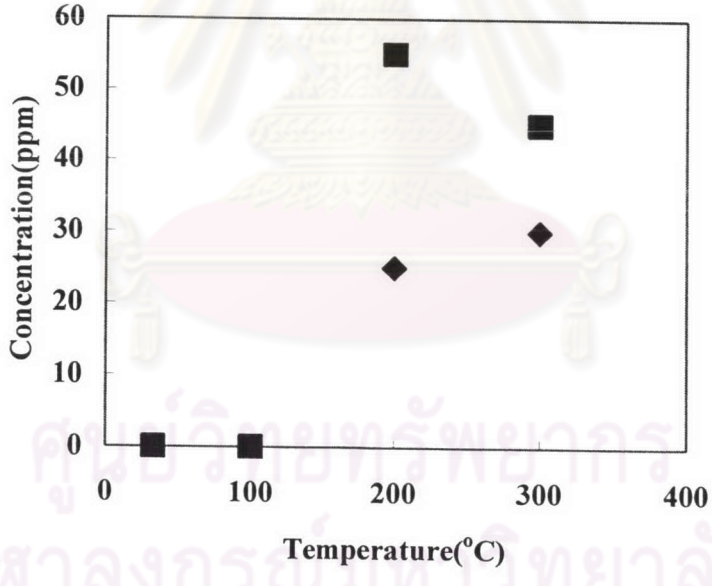

Figure 5.10 Byproduct (NO_x) on the removal of CH_3CHO from N_2-CO_2: ◆ CO_2 (10%), ■ CO_2 (20%)

ศูนย์วิทยทรัพยากร
จุฬาลงกรณ์มหาวิทยาลัย

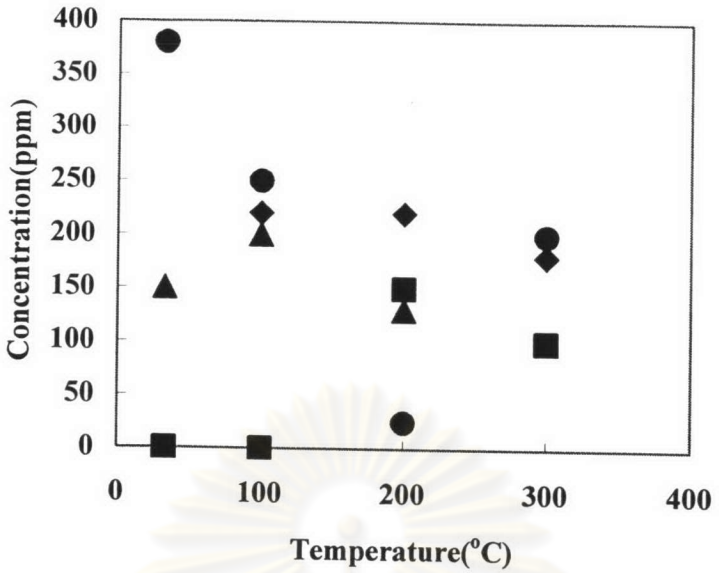

Figure 5.11 Byproduct (CO) on the removal of CH_3CHO from N_2-O_2-CO_2:
◆ CO_2 (10%) - O_2 (10%),
▲ CO_2 (20%) - O_2 (10%),
■ CO_2 (10%) - O_2 (20%),
● CO_2 (20%) - O_2 (20%)

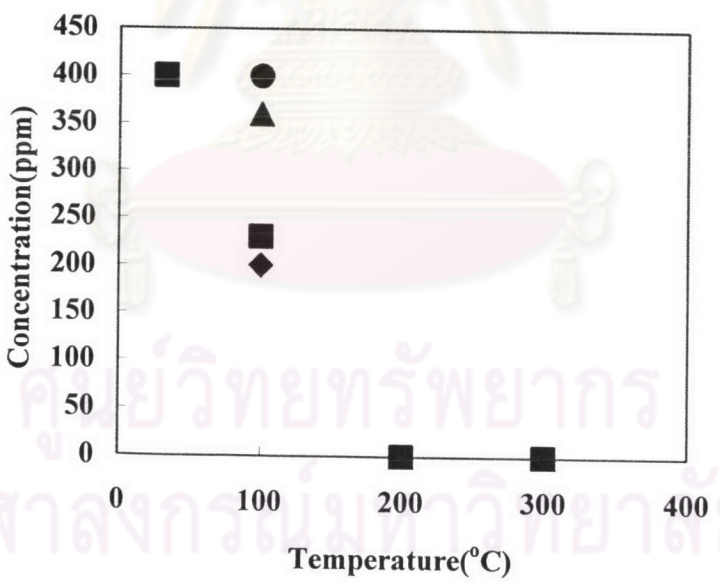

Figure 5.12 Byproduct (O_3) on the removal of CH_3CHO from N_2-O_2-CO_2:
◆ CO_2 (10%) - O_2 (10%),
▲ CO_2 (20%) - O_2 (10%),
■ CO_2 (10%) - O_2 (20%),
● CO_2 (20%) - O_2 (20%)

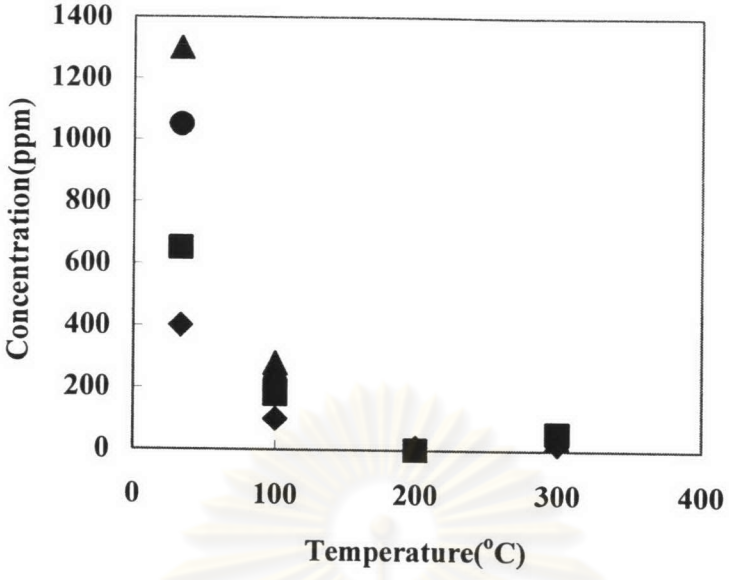

Figure 5.13 Byproduct (NO_x) on the removal of CH_3CHO from N_2-O_2-CO_2:
- ◆ CO_2 (10%) - O_2 (10%),
- ▲ CO_2 (20%) - O_2 (10%),
- ■ CO_2 (10%) - O_2 (20%),
- ● CO_2 (20%) - O_2 (20%)

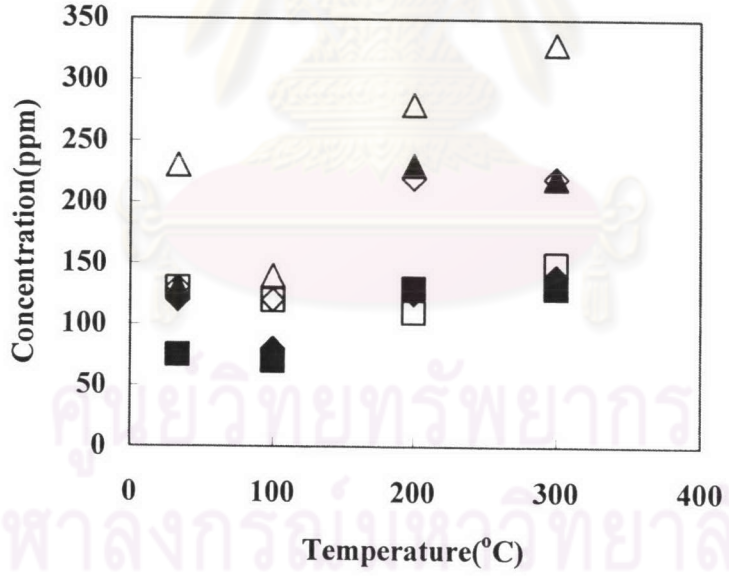

Figure 5.14 Byproduct (CO) on the removal of CH_3CHO from N_2-H_2O-CO_2:
- ◆ CO_2 (10%) - H_2O (5250ppm),
- ◇ CO_2 (20%) - H_2O (5250ppm),
- ▲ CO_2 (10%) - H_2O (10500ppm),
- △ CO_2 (20%) - H_2O (10500ppm),
- ■ CO_2 (10%) - H_2O (21800ppm),
- □ CO_2 (20%) - H_2O (21800ppm)

ศูนย์วิทยทรัพยากร
จุฬาลงกรณ์มหาวิทยาลัย

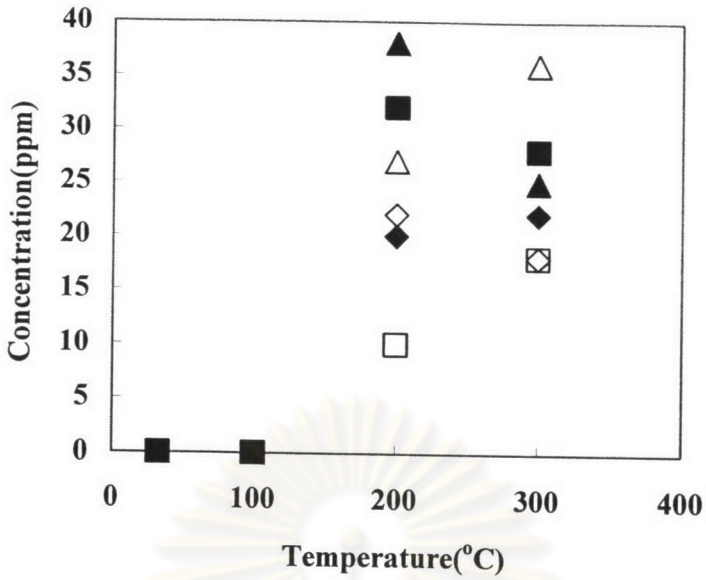

Figure 5.15 Byproduct (NO_x) on the removal of CH_3CHO from N_2-H_2O-CO_2:
◆ CO_2 (10%) - H_2O (5250ppm),
◇ CO_2 (20%) - H_2O (5250ppm),
▲ CO_2 (10%) - H_2O (10500ppm),
△ CO_2 (20%) - H_2O (10500ppm),
■ CO_2 (10%) - H_2O (21800ppm),
□ CO_2 (20%) - H_2O (21800ppm)

ศูนย์วิทยทรัพยากร
จุฬาลงกรณ์มหาวิทยาลัย

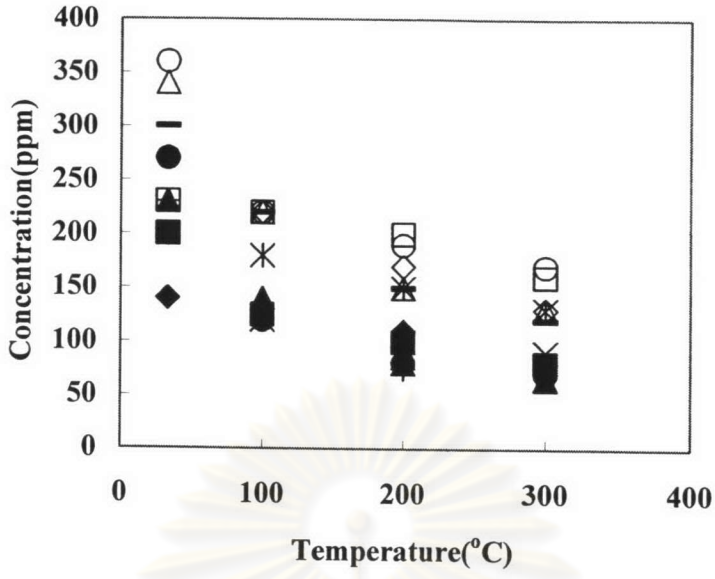

Figure 5.16 Byproduct (CO) on the removal of CH_3CHO from N_2-O_2-H_2O-CO_2:
- ◆ CO_2 (10%) - O_2 (10%) - H_2O (5250ppm),
- ◇ CO_2 (20%) - O_2 (10%) - H_2O (5250ppm),
- ▲ CO_2 (10%) - O_2 (20%) - H_2O (5250ppm),
- △ CO_2 (20%) - O_2 (20%) - H_2O (5250ppm),
- ■ CO_2 (10%) - O_2 (10%) - H_2O (10500ppm),
- □ CO_2 (20%) - O_2 (10%) - H_2O (10500ppm),
- ● CO_2 (10%) - O_2 (20%) - H_2O (10500ppm),
- ○ CO_2 (20%) - O_2 (20%) - H_2O (10500ppm),
- * CO_2 (10%) - O_2 (10%) - H_2O (21800ppm),
- × CO_2 (20%) - O_2 (10%) - H_2O (21800ppm),
- + CO_2 (10%) - O_2 (20%) - H_2O (21800ppm),
- – CO_2 (20%) - O_2 (20%) - H_2O (21800ppm)

ศูนย์วิทยทรัพยากร
จุฬาลงกรณ์มหาวิทยาลัย

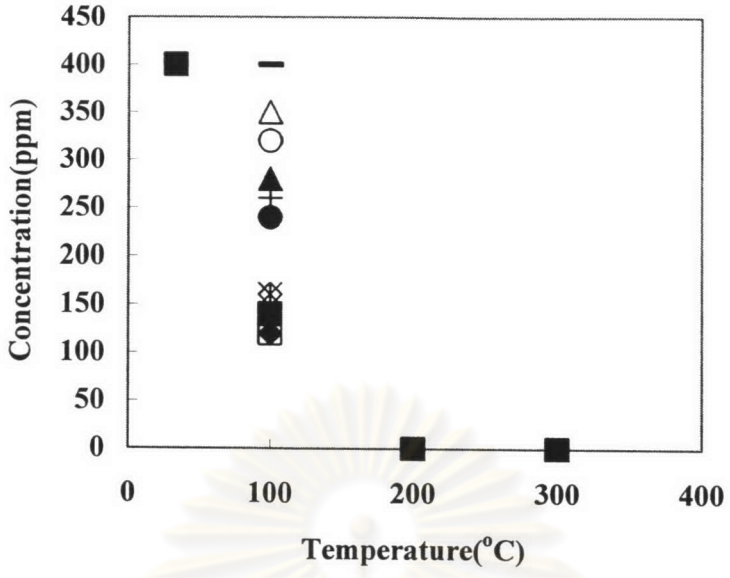

Figure 5.17 Byproduct (O_3) on the removal of CH_3CHO from N_2-O_2-H_2O-CO_2:
◆ CO_2 (10%) - O_2 (10%) - H_2O (5250ppm),
◇ CO_2 (20%) - O_2 (10%) - H_2O (5250ppm),
▲ CO_2 (10%) - O_2 (20%) - H_2O (5250ppm),
△ CO_2 (20%) - O_2 (20%) - H_2O (5250ppm),
■ CO_2 (10%) - O_2 (10%) - H_2O (10500ppm),
□ CO_2 (20%) - O_2 (10%) - H_2O (10500ppm),
● CO_2 (10%) - O_2 (20%) - H_2O (10500ppm),
○ CO_2 (20%) - O_2 (20%) - H_2O (10500ppm),
* CO_2 (10%) - O_2 (10%) - H_2O (21800ppm),
× CO_2 (20%) - O_2 (10%) - H_2O (21800ppm),
+ CO_2 (10%) - O_2 (20%) - H_2O (21800ppm),
– CO_2 (20%) - O_2 (20%) - H_2O (21800ppm)

ศูนย์วิทยทรัพยากร
จุฬาลงกรณ์มหาวิทยาลัย

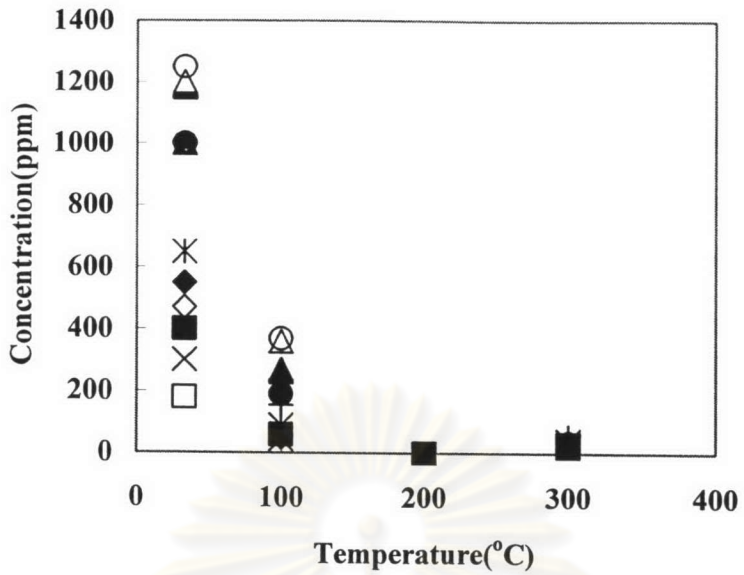

Figure 5.18 Byproduct (NO_x) on the removal of CH_3CHO from N_2-O_2-H_2O-CO_2:
◆ CO_2 (10%) - O_2 (10%) - H_2O (5250ppm),
◇ CO_2 (20%) - O_2 (10%) - H_2O (5250ppm),
▲ CO_2 (10%) - O_2 (20%) - H_2O (5250ppm),
△ CO_2 (20%) - O_2 (20%) - H_2O (5250ppm),
■ CO_2 (10%) - O_2 (10%) - H_2O (10500ppm),
□ CO_2 (20%) - O_2 (10%) - H_2O (10500ppm),
● CO_2 (10%) - O_2 (20%) - H_2O (10500ppm),
○ CO_2 (20%) - O_2 (20%) - H_2O (10500ppm),
* CO_2 (10%) - O_2 (10%) - H_2O (21800ppm),
× CO_2 (20%) - O_2 (10%) - H_2O (21800ppm),
+ CO_2 (10%) - O_2 (20%) - H_2O (21800ppm),
– CO_2 (20%) - O_2 (20%) - H_2O (21800ppm)

ศูนย์วิทยทรัพยากร
จุฬาลงกรณ์มหาวิทยาลัย

5.6 Removal of ammonia (NH_3)

5.6.1 Effect of temperature and coexisting CO_2 on the removal of NH_3 from N_2

Figure 5.19 shows the removal efficiency ψ' of NH_3 versus temperature. From **Figure 5.19 (a),** we see that, as the temperature increases, the removal efficiency ψ' increases monotonically from room temperature to 300°C because of the effect of CO_3^- and O^- anion at low temperatures whereas at high temperatures, N radical is consumed by their reaction wuth CO_2. Obviously, the presence of CO_2 positively affects the removal efficiency. The higher the CO_2 concentration, the higher the removal efficiency. Since CO_2 is a highly oxidized, thermodynamically stable compound, its utilization requires reaction with certain high-energy substances or electro reductive processes. Recent research has shown that high catalytic efficiency, yield, and rate of reaction can be obtained from CO_2 with the use of optimum conditions and catalysts (Ryoji Noyori et al., 1995). **Figure 5.19(b)** reveals that when the negative effect of reduced residence time is taken in account, the value of ψ'' still increases as the temperature increases.

At room temperature, 100, 200 and 300°C, ψ_{elec} of NH_3 at 200 ppm-CO_2 (10%, 20%) are 0.2, 0.5, 0.7, 0.6 and 1.1, 0.8, 0.6, 0.7, respectively. Interestingly, at CO_2 10%, as the temperature increases, ψ_{elec} increases from room temperature up to 200°C, above which the tendency reverses however, at CO_2 20%, high temperatures has adverse effect because the mean residence time of the gas mixture inside the reactor decreases as the reactor temperature increases.

ศูนย์วิทยทรัพยากร

5.6.2 Effect of temperature and coexisting CO_2 and O_2 on the removal of NH_3 from N_2

จุฬาลงกรณ์มหาวิทยาลัย

Figure 5.20 shows the removal efficiency ψ' of NH_3 versus temperature. From **Figure 5.20 (a),** we see that, as the temperature increases, the removal efficiency ψ' remains nearly 100% from room temperature to 300°C. As mentioned previously, this is due to the effect of O_3, CO_3^- and O^- anion at low temperatures but

various radicals at high temperatures. This can partly be attributed to the fact that O_3 is produced from O_2 by the corona discharge reaction and is quite stable at room temperature. At room to moderate temperatures, electron attachment reactions contribute to, and relevant ion cluster formation enhances, the removal of numerous electro - negative compounds (Sano et al., 1997; Bityurin; 2000). N radicals should also contribute to the removal of NH_3 from both N_2 and air at high temperatures. In addition, in the case of removal from air, there should be the extra effect of O radicals produced by electron impact to O_2 and by O_3 decomposition (Peyrous, Pignolet and Held, 1989; Loiseau et al. 1994; Hadj-Ziane, 1990). Therefore, the NH_3 removal efficiency ψ' at high temperatures should be enhanced by O radicals though O_3 oxidation is not effective. **Figure 5.20 (b)** reveals that when the negative effect of reduced residence time is taken in account, the value of ψ'' increases as the temperature increases.

At room temperature, 100, 200 and 300°C, ψ_{elec} of NH_3 at 200 ppm - O_2 (10%, 20%) - CO_2 (10%, 20%) are (3.8, 2.9, 2.4, 1.7), (3.9, 3.0, 2.3, 1.6), (3.2, 2.7, 2.1, 1.3), (3.8, 2.8, 2.2, 1.2) respectively. Interestingly, as mentioned in the previous section, as the temperature increases, ψ_{elec} decreases, thus indicating the possible existence of an optimal temperature. The high values of ψ_{elec} at low temperatures reveal that electron attachment reactions contribute to, and relevant ion cluster formation enhances, the removal of numerous electro - negative compounds (Sano et al., 1997; Bityurin; 2000). On the other hand, N radicals should contribute to the removal of NH_3 from both N_2 and air at high temperatures.

ศูนย์วิทยทรัพยากร
จุฬาลงกรณ์มหาวิทยาลัย

5.6.3 Effect of temperature and coexisting CO_2 and H_2O on the removal of NH_3 from N_2

Figure 5.21 shows the removal efficiency ψ' of NH_3 versus temperature. From **Figure 5.21 (a),** we see that, as the temperature increases, the removal efficiency ψ' increases from room temperature up to 200°C. Then the tendency reverses up to 300°C. As mentioned above, the effect of H^-, OH^-, a few O^- anions and CO_3^- should contribute to the removal of NH_3 at low to moderate temperatures. At high temperature, the tendency reverses because the mean residence time decreases. **Figure 5.21(b)** reveals that, if the negative effect of reduced residence time is taken in account, the value of ψ'' continued to increase as the temperature increases.

At room temperature, 100, 200 and 300°C, ψ_{elec} of NH_3 at 200 ppm - H_2O (5250, 10500, 21800 ppm) - CO_2 (10%, 20%) are (0.8, 0.9, 1.0, 1.0), (1.0, 1.0, 0.8, 0.9), (1.0, 0.7, 0.7, 0.6), (0.7, 0.8, 1.0, 0.6), (0.3, 0.6, 0.4, 0.1) and (0.1, 0.2, 0.1, 0.1) respectively. Interestingly, as the temperature increases, ψ_{elec} increases from room temperature to a moderate temperature above which the ψ_{elec} tend to significantly decrease again because the mean residence time of the gas mixture inside the reactor decreases as the reactor temperature rises.

5.6.4 Effect of temperature and coexisting CO_2, O_2 and H_2O on the removal of NH_3 from N_2

Figure 5.22 shows the removal efficiency ψ' of NH_3 versus temperature. From **Figure 5.22 (a),** we see that, as the temperature increases, the removal efficiency ψ' remains nearly 100% from room temperature to 300°C. As mentioned previously, this is due to the effect of O_3, H^-, OH^-, CO_3^- and O^- anion at low to moderate temperatures but that of various radicals generated from CO_2, O_2 and H_2O at high temperatures. This can be attributed to the fact that O_3 is produced from O_2 by the corona discharge reaction and is quite stable at room temperature. At room to

moderate temperatures, electron attachment reactions contribute to, and relevant ion cluster formation enhances, the removal of numerous electro - negative compounds (Sano et al., 1997; Bityurin; 2000). N radicals should also contribute to the removal of NH_3 from both N_2 and air at high temperatures. In addition, in the case of removal from air, there should be the extra effect of O radicals produced by electron impact to O_2 and by O_3 decomposition (Peyrous, Pignolet and Held, 1989; Loiseau et al. 1994; Hadj - Ziane, 1990). At high temperatures, electron detachment would become significant so that radicals of CO_3, O, H, and OH may play a more important role than their anionic counterparts. These radicals are expected to contribute to the removal of the NH_3. **Figure 5.22 (b)** reveals that, if the negative effect of the reduced residence time is taken in account, the value of ψ'' increases as the temperature increases.

5.6.5 Preliminary summary

Generally, two other types of removal efficiency are reported for a corona-discharge system: the electron - based efficiency ψ_{elec} (-) and the energy - based efficiency ψ_{ener} (mol gas .J^{-1}). At 33, 100, 200 and 300°C, the experimental values of ψ_{elec} and ψ_{ener} of the NH_3 200 ppm removal are as follows:

N_2 - CO_2 (10%), (I=0.2 mA):

ψ_{elec} = 0.2, 0.5, 0.7, 0.6 $\psi_{ener} \times 10^{-9}$ = 0.32, 1.0, 2.1, 2.2

N_2 - O_2 (10%) - CO_2 (10%), (I=0.2 mA):

ψ_{elec} = 3.8, 2.9, 2.4, 1.7 $\psi_{ener} \times 10^{-9}$ = 4.6, 3.9, 3.8, 3.7

N_2 - H_2O (10500 ppm) - CO_2 (10%), (I=0.2 mA):

ψ_{elec} = 1.0, 0.7, 0.7, 0.6 $\psi_{ener} \times 10^{-9}$ = 1.6, 1.4, 1.8, 1.8

N_2 - O_2 (10%) - H_2O (10500 ppm) - CO_2 (10%), (I=0.2 mA):

ψ_{elec} = 3.8, 2.9, 2.3, 1.7 $\psi_{ener} \times 10^{-9}$ = 4.7, 4.1, 3.9, 3.9

Generally, ψ_{elec} and ψ_{ener} tend to decrease as the gas temperature increases. This trend may be ascribed to the combined effect of the reduced residence time and the shift in removal mechanism. Interestingly, in the case of N_2 - CO_2, ψ_{elec} and ψ_{ener} tend to increase as the gas temperature increases, thus indicating the possible existence of an optimal temperature.

In actual applications of gas purification, it is important to consider the energy-based efficiency ψ_{ener}. From the above results, it is recommended to operate in the range from 100°C to 200°C so as to minimize the operating cost when air is purified, Compared to the case of the removal of CH_3CHO from N_2 - CO_2, ψ_{ener} of NH_3 at 200°C is approximately 20% lower than that in the case of CH_3CHO, thus indicating the operating cost of the removal of NH_3 from N_2 - CO_2 are lower than that of CH_3CHO.

ศูนย์วิทยทรัพยากร
จุฬาลงกรณ์มหาวิทยาลัย

5.6.6 Byproducts dected on the removal of ammonia

Figure 5.23 shows the concentration of the byproduct CO versus temperature in the presence of CO_2. In **Figure 5.23** as the temperature increases, the byproduct CO increases because of the effect of O^- anion and CO_3^- at low temperature. At high temperatures, electron detachment would become significant so that radicals of N, H, O, CO_3 and OH may play a more important role than their anionic counterparts. As mentioned previously, production of CO by dissociative attachment reaction is known.

Figure 5.24 shows the concentration of the byproduct NO_x versus temperature in the presence of CO_2. In **Figure 5.24** as the temperature increases, the byproduct NO_x increases. As mentioned previously, it is known that production of NO_x take place by the discharge process of NH_3 and N_2 at high temperatures. This is also confirmed in our experiments. Though the outlet concentration of NO_x was negligible at room temperature, NO_x concentration gradually increases as the temperature rise.

Figure 5.25 shows the concentration of the byproduct CO versus temperature in the presence of O_2 and CO_2. In **Figure 5.25** as the temperature increases, the byproduct CO decreases as the temperature rises because O_3 is unstable at high temperature.

Figure 5.26 shows the concentration of the byproduct O_3 versus temperature in the presence of O_2 and CO_2. In **Figure 5.26** as the temperature increases, the byproduct O_3 decreases. This is because O_3 is unstable at high temperature (Peyrous, Pignolet and Held, 1989; Devins, 1956).

Figure 5.27 shows the concentration of the byproduct NO_x versus temperature in the presence of O_2 and CO_2. In **Figure 5.27** as the temperature increases, the byproduct NO_x decrease from room temperature up 200°C, then the tendency reverses up to 300°C.

Figure 5.28 shows the concentration of the byproduct CO versus temperature in the presence of H_2O and CO_2. In **Figure 5.28** as the temperature increases, the byproduct CO increases from room temperature up 100°C. Above 100°C the CO concentration tends to decrease because at high temperatures, H_2O is unstable and

the mean residence time of the gas mixture inside the reactor decreases as the reactor temperature increases.

Figure 5.29 shows the concentration of the byproduct NO_x versus temperature in the presence of H_2O and CO_2. In **Figure 5.29** as the temperature increases, the byproduct NO_x increases. It is known that production of NO_x by the discharge process is favored at high temperatures. This fact is also confirmed in our experiments. While, the outlet concentration of NO_x was negligible at room temperature, its concentration gradually increased as the temperature rises.

Figure 5.30 shows the concentration of the byproduct CO versus temperature in the presence of O_2, H_2O and CO_2. In **Figure 5.30** as the temperature increases, the byproduct CO increases from room temperature up 200°C, then the tendency reverses up to 300°C. At low temperatures, H_2O is present in the gas stream, CO_3^-, H^-, OH^- and O^- anions are expected to be produced by dissociative electron attachment to CO_2 and H_2O molecules (Massey, 1976; Moruzzi and Phelps, 1966). At high temperatures CO_2, O_3 and H_2O become unstable as the temperature rises. On the other hand, the mean residence time of the gas mixture inside the reactor decreases as the reactor temperature rises.

Figure 5.31 shows the concentration of the byproduct O_3 versus temperature in the presence of O_2, H_2O and CO_2. In **Figure 5.31** as the temperature increases, the byproduct O_3 decreases because at high temperatures, O_3 is unstable (Peyrous, Pignolet and Held, 1989; Devins, 1956).

Figure 5.32 shows the concentration of the byproduct NO_x versus temperature in the presence of O_2, H_2O and CO_2. In **Figure 5.32** as the temperature increases, the byproduct NO_x decrease from room temperature up 200°C, then the tendency reverses up to 300°C.

ศูนย์วิทยทรัพยากร
จุฬาลงกรณ์มหาวิทยาลัย

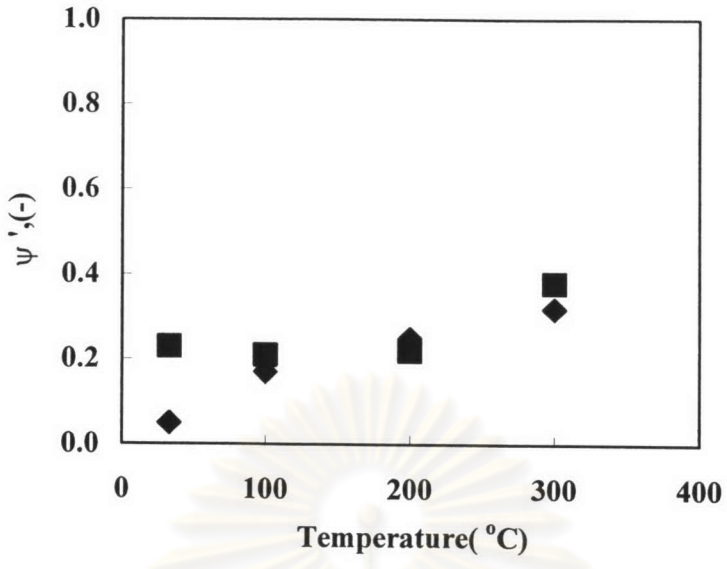

(a)

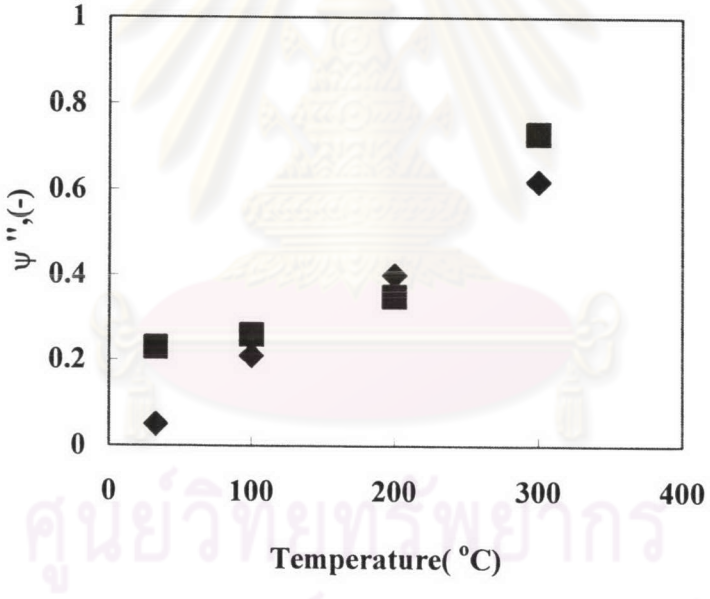

(b)

Figure 5.19 Effect of coexisting CO_2 on the removal of NH_3 from N_2; $C_{in,ammonia}$=200ppm, I=0.2mA, SV=55.8 hr^{-1} at room temperature : ◆ CO_2 (10%), ■ CO_2 (20%)

ศูนย์วิทยทรัพยากร
จุฬาลงกรณ์มหาวิทยาลัย

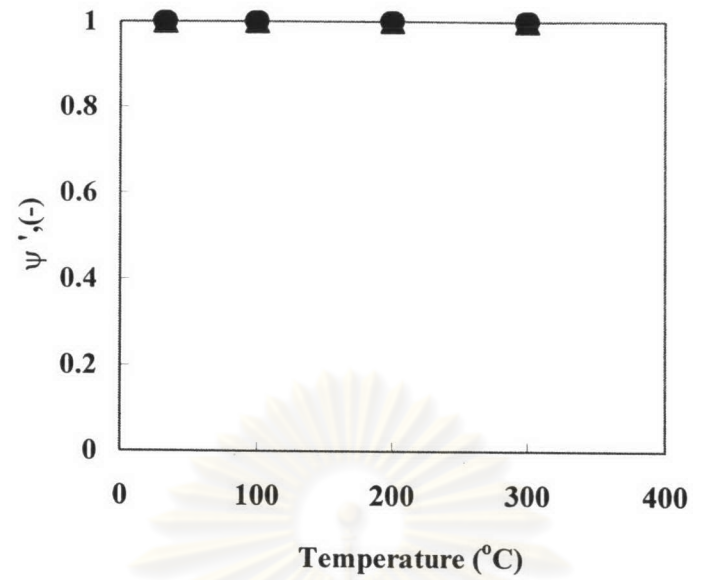

(a)

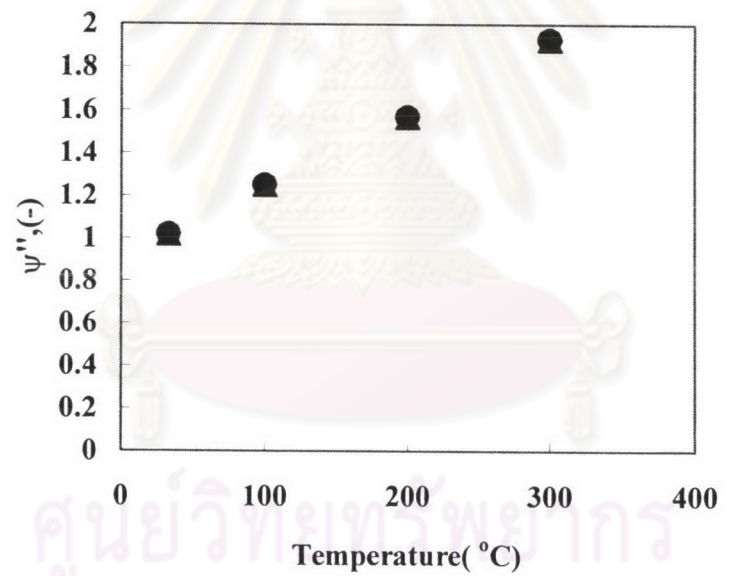

(b)

Figure 5.20 Effect of coexisting O_2-CO_2 on the removal of NH_3 from N_2; $C_{in,ammonia}$=200ppm, I=0.2mA, SV=55.8 hr^{-1} at room temperature :
◆ CO_2 (10%) - O_2 (10%),
▲ CO_2 (20%) - O_2 (10%),
■ CO_2 (10%) - O_2 (20%),
● CO_2 (20%) - O_2 (20%)

ศูนย์วิทยทรัพยากร
จุฬาลงกรณ์มหาวิทยาลัย

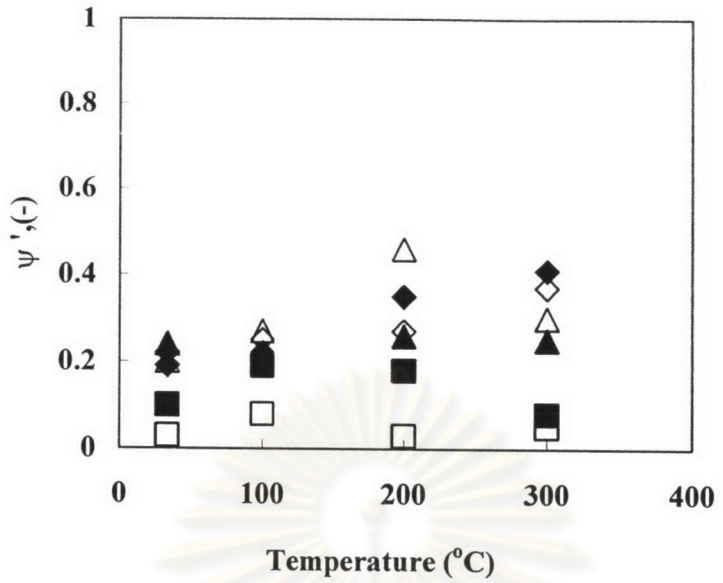

(a)

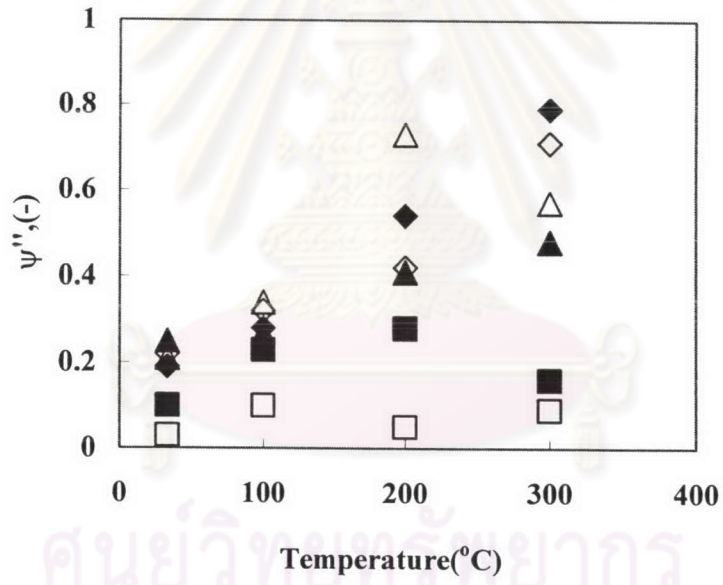

(b)

Figure 5.21 Effect of coexisting H_2O-CO_2 on the removal of NH_3 from N_2; $C_{in,ammonia}$=200ppm, I=0.2mA, SV=55.8 hr^{-1} at room temperature :

- ◆ CO_2 (10%) - H_2O (5250ppm),
- ◇ CO_2 (20%) - H_2O (5250ppm),
- ▲ CO_2 (10%) - H_2O (10500ppm),
- △ CO_2 (20%) - H_2O (10500ppm),
- ■ CO_2 (10%) - H_2O (21800ppm),
- □ CO_2 (20%) - H_2O (21800ppm)

ศูนย์วิทยทรัพยากร
จุฬาลงกรณ์มหาวิทยาลัย

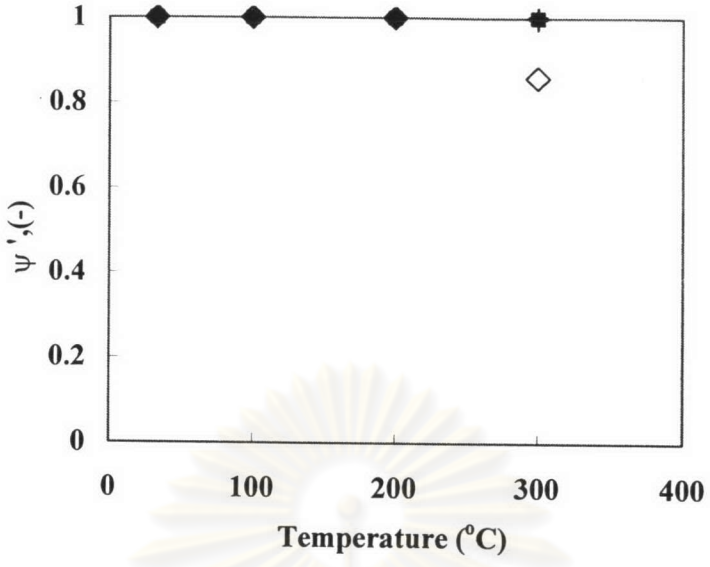

(a)

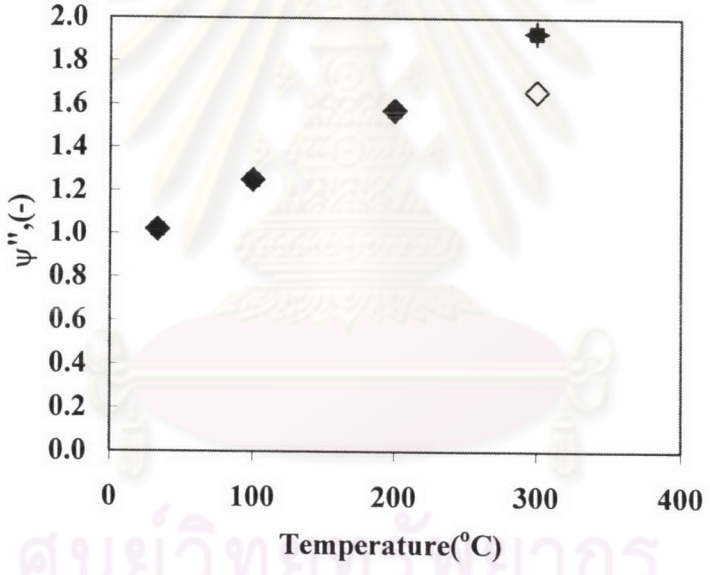

(b)

Figure 5.22 Effect of coexisting O_2-H_2O-CO_2 on the removal of NH_3 from N_2; $C_{in,ammonia}$=200ppm, I=0.2mA, SV=55.8 hr^{-1} at room temperature :

◆ CO_2 (10%)-O_2 (10%)-H_2O (5250ppm), ◇ CO_2 (20%)-O_2 (10%)-H_2O (5250ppm),
▲ CO_2 (10%)-O_2 (20%)-H_2O (5250ppm), △ CO_2 (20%)-O_2 (20%)-H_2O (5250ppm),
■ CO_2 (10%)-O_2 (10%)-H_2O (10500ppm), □ CO_2 (20%)-O_2 (10%)-H_2O (10500ppm),
● CO_2 (10%)-O_2 (20%)-H_2O (10500ppm), ○ CO_2 (20%)-O_2 (20%)-H_2O (10500ppm),
* CO_2 (10%)-O_2 (10%)-H_2O (21800ppm), × CO_2 (20%)-O_2 (10%)-H_2O (21800ppm),
+ CO_2 (10%)-O_2 (20%)-H_2O (21800ppm), ━ CO_2 (20%)-O_2 (20%)-H_2O (21800ppm)

ศูนย์วิทยทรัพยากร
จุฬาลงกรณ์มหาวิทยาลัย

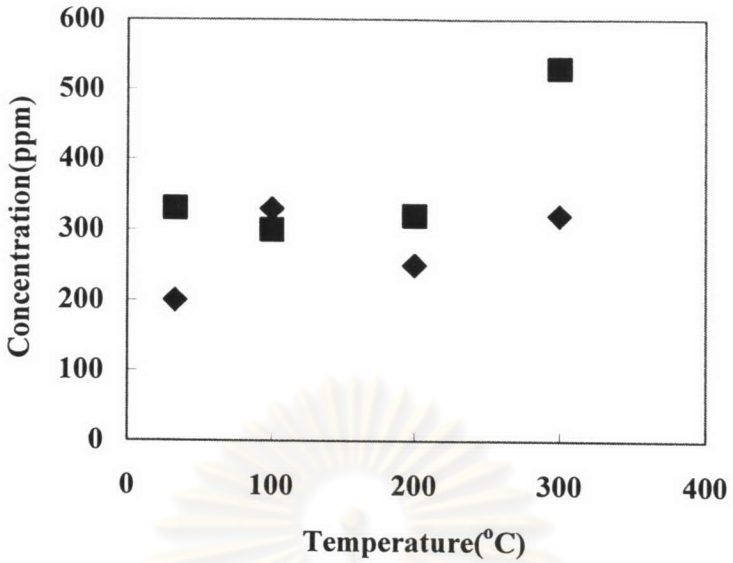

Figure 5.23 Byproduct (CO) on the removal of NH_3 from N_2-CO_2:
◆ CO_2 (10%), ■ CO_2 (20%)

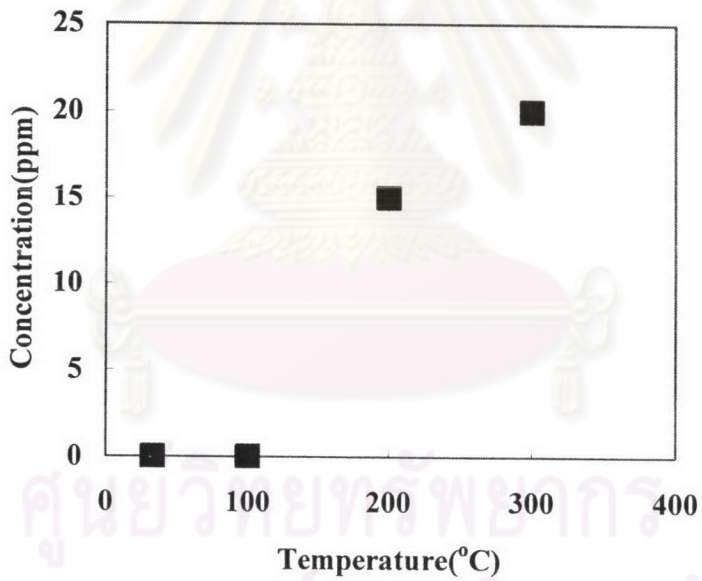

Figure 5.24 Byproduct (NO_x) on the removal of NH_3 from N_2-CO_2:
◆ CO_2 (10%), ■ CO_2 (20%)

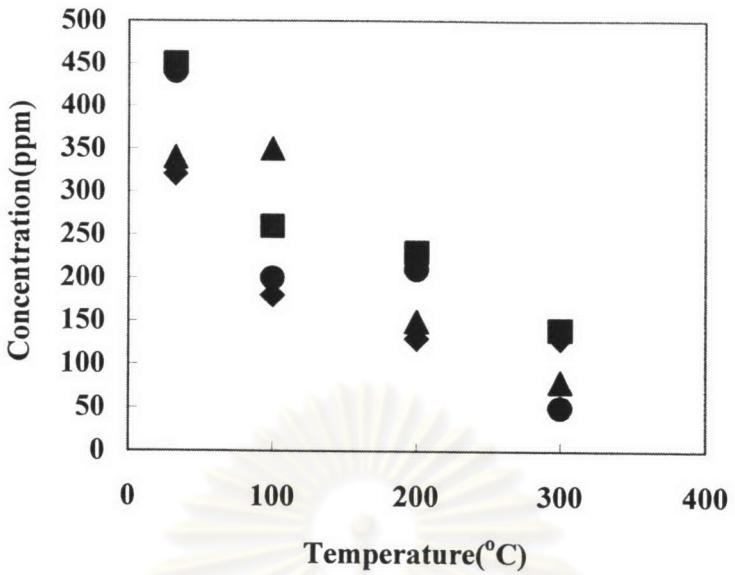

Figure 5.25 Byproduct (CO) on the removal of NH_3 from N_2-O_2-CO_2:
◆ CO_2 (10%) - O_2 (10%),
▲ CO_2 (20%) - O_2 (10%),
■ CO_2 (10%) - O_2 (20%),
● CO_2 (20%) - O_2 (20%)

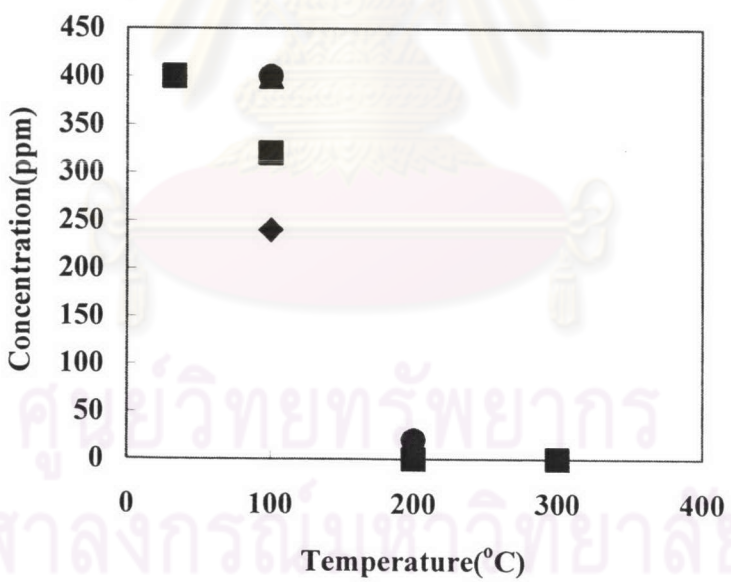

Figure 5.26 Byproduct (O_3) on the removal of NH_3 from N_2-O_2-CO_2:
◆ CO_2 (10%) - O_2 (10%),
▲ CO_2 (20%) - O_2 (10%),
■ CO_2 (10%) - O_2 (20%),
● CO_2 (20%) - O_2 (20%)

ศูนย์วิทยทรัพยากร
จุฬาลงกรณ์มหาวิทยาลัย

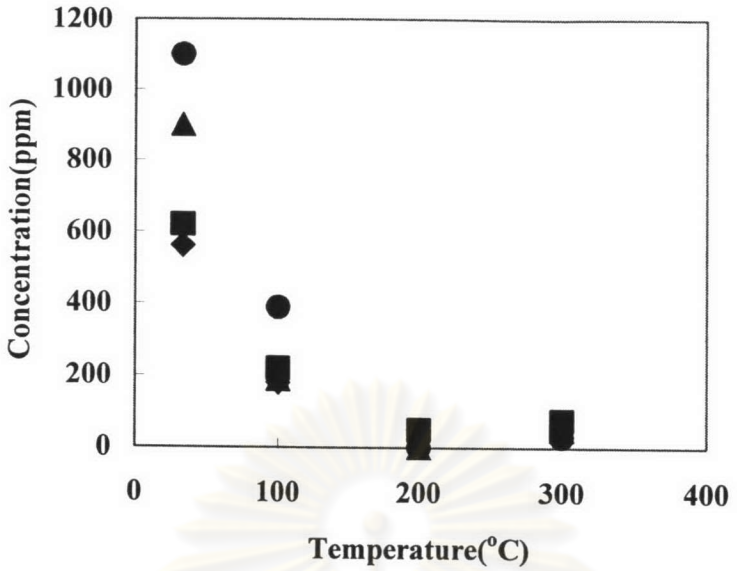

Figure 5.27 Byproduct (NO_x) on the removal of NH_3 from N_2-O_2-CO_2:
- ◆ CO_2 (10%) - O_2 (10%),
- ▲ CO_2 (20%) - O_2 (10%),
- ■ CO_2 (10%) - O_2 (20%),
- ● CO_2 (20%) - O_2 (20%)

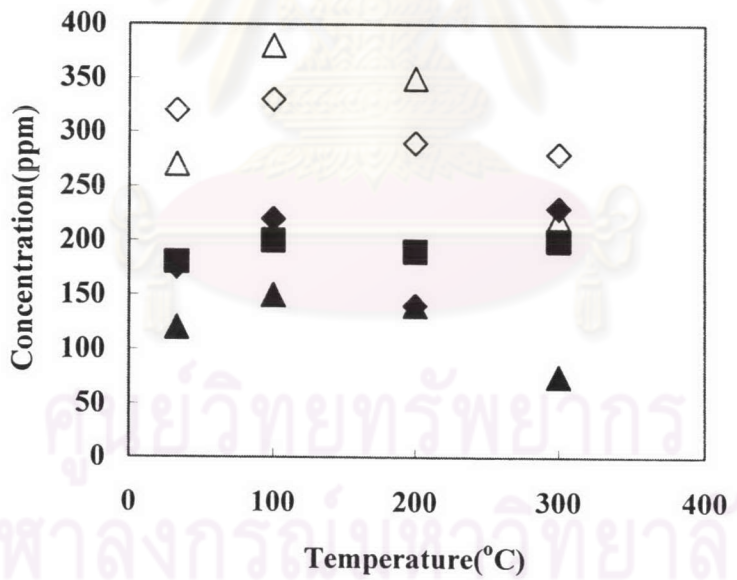

Figure 5.28 Byproduct (CO) on the removal of NH_3 from N_2-H_2O-CO_2:
- ◆ CO_2 (10%) - H_2O (5250ppm),
- ◇ CO_2 (20%) - H_2O (5250ppm),
- ▲ CO_2 (10%) - H_2O (10500ppm),
- △ CO_2 (20%) - H_2O (10500ppm),
- ■ CO_2 (10%) - H_2O (21800ppm),
- □ CO_2 (20%) - H_2O (21800ppm)

ศูนย์วิทยทรัพยากร
จุฬาลงกรณ์มหาวิทยาลัย

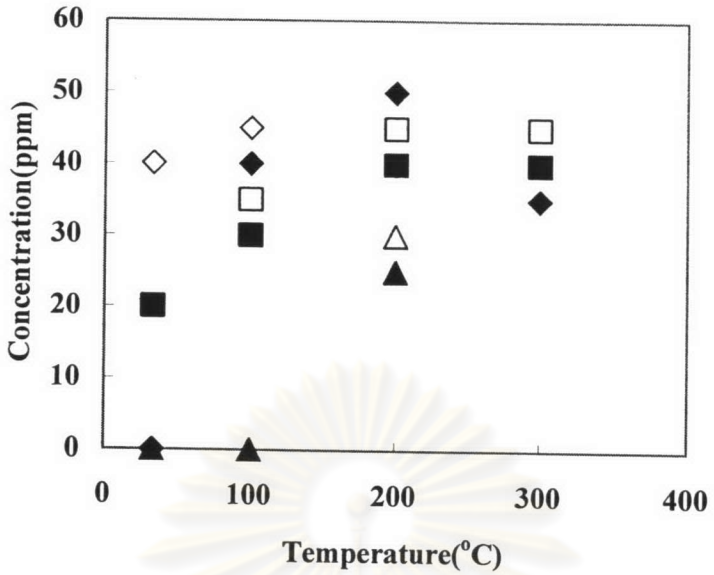

Figure 5.29 Byproduct (NO_x) on the removal of NH_3 from N_2-H_2O-CO_2:
◆ CO_2 (10%) - H_2O (5250ppm),
◇ CO_2 (20%) - H_2O (5250ppm),
▲ CO_2 (10%) - H_2O (10500ppm),
△ CO_2 (20%) - H_2O (10500ppm),
■ CO_2 (10%) - H_2O (21800ppm),
□ CO_2 (20%) - H_2O (21800ppm)

ศูนย์วิทยทรัพยากร
จุฬาลงกรณ์มหาวิทยาลัย

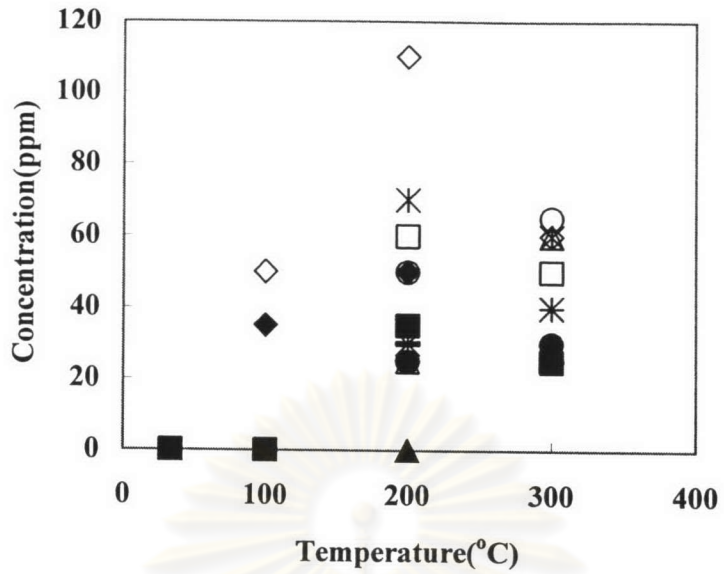

Figure 5.30 Byproduct (CO) on the removal of NH_3 from N_2-O_2-H_2O-CO_2:
◆ CO_2 (10%) - O_2 (10%) - H_2O (5250ppm),
◇ CO_2 (20%) - O_2 (10%) - H_2O (5250ppm),
▲ CO_2 (10%) - O_2 (20%) - H_2O (5250ppm),
△ CO_2 (20%) - O_2 (20%) - H_2O (5250ppm),
■ CO_2 (10%) - O_2 (10%) - H_2O (10500ppm),
□ CO_2 (20%) - O_2 (10%) - H_2O (10500ppm),
● CO_2 (10%) - O_2 (20%) - H_2O (10500ppm),
○ CO_2 (20%) - O_2 (20%) - H_2O (10500ppm),
* CO_2 (10%) - O_2 (10%) - H_2O (21800ppm),
× CO_2 (20%) - O_2 (10%) - H_2O (21800ppm),
+ CO_2 (10%) - O_2 (20%) - H_2O (21800ppm),
– CO_2 (20%) - O_2 (20%) - H_2O (21800ppm)

ศูนย์วิทยทรัพยากร
จุฬาลงกรณ์มหาวิทยาลัย

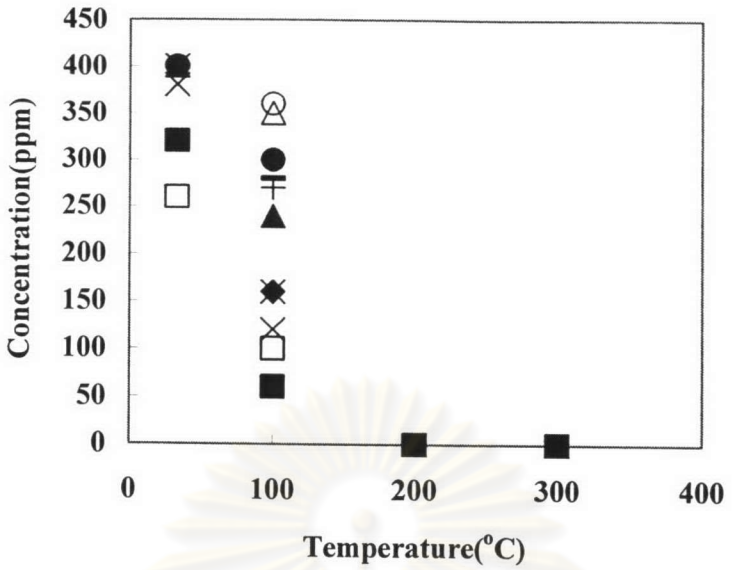

Figure 5.31 Byproduct (O_3) on the removal of NH_3 from N_2-O_2-H_2O-CO_2:
◆ CO_2 (10%) - O_2 (10%) - H_2O (5250ppm),
◇ CO_2 (20%) - O_2 (10%) - H_2O (5250ppm),
▲ CO_2 (10%) - O_2 (20%) - H_2O (5250ppm),
△ CO_2 (20%) - O_2 (20%) - H_2O (5250ppm),
■ CO_2 (10%) - O_2 (10%) - H_2O (10500ppm),
□ CO_2 (20%) - O_2 (10%) - H_2O (10500ppm),
● CO_2 (10%) - O_2 (20%) - H_2O (10500ppm),
○ CO_2 (20%) - O_2 (20%) - H_2O (10500ppm),
* CO_2 (10%) - O_2 (10%) - H_2O (21800ppm),
× CO_2 (20%) - O_2 (10%) - H_2O (21800ppm),
+ CO_2 (10%) - O_2 (20%) - H_2O (21800ppm),
– CO_2 (20%) - O_2 (20%) - H_2O (21800ppm)

ศูนย์วิทยทรัพยากร
จุฬาลงกรณ์มหาวิทยาลัย

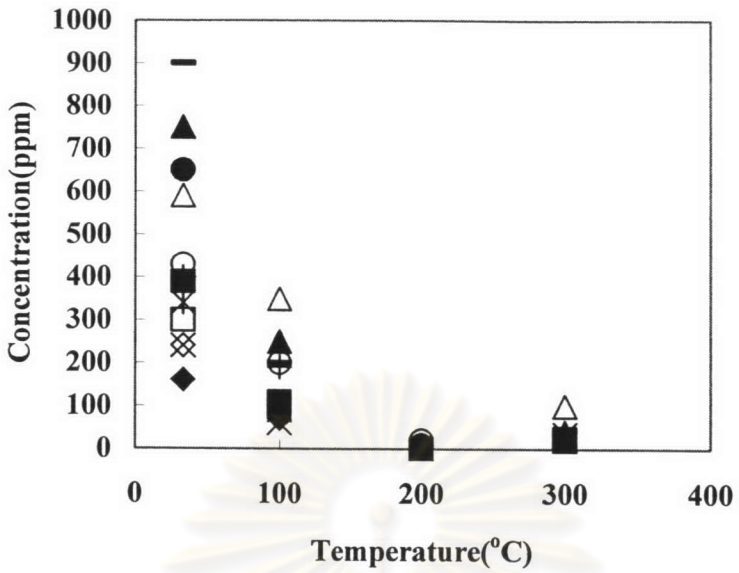

Figure 5.32 Byproduct (NO_x) on the removal of NH_3 from N_2-O_2-H_2O-CO_2:
◆ CO_2 (10%) - O_2 (10%) - H_2O (5250ppm),
◇ CO_2 (20%) - O_2 (10%) - H_2O (5250ppm),
▲ CO_2 (10%) - O_2 (20%) - H_2O (5250ppm),
△ CO_2 (20%) - O_2 (20%) - H_2O (5250ppm),
■ CO_2 (10%) - O_2 (10%) - H_2O (10500ppm),
□ CO_2 (20%) - O_2 (10%) - H_2O (10500ppm),
● CO_2 (10%) - O_2 (20%) - H_2O (10500ppm),
○ CO_2 (20%) - O_2 (20%) - H_2O (10500ppm),
* CO_2 (10%) - O_2 (10%) - H_2O (21800ppm),
× CO_2 (20%) - O_2 (10%) - H_2O (21800ppm),
+ CO_2 (10%) - O_2 (20%) - H_2O (21800ppm),
– CO_2 (20%) - O_2 (20%) - H_2O (21800ppm)

ศูนย์วิทยทรัพยากร
จุฬาลงกรณ์มหาวิทยาลัย

5.7 Removal of trimethyl amine $(CH_3)_3N$

5.7.1 Effect of temperature and coexisting CO_2 on the removal of $(CH_3)_3N$ from N_2

Figure 5.33 shows the removal efficiency ψ' of $(CH_3)_3N$ versus temperature. From **Figure 5.33 (a),** we see that, as the temperature increases, the removal efficiency ψ' remains nearly 100% from room temperature up to 200°C. In addition, the reduction of $(CH_3)_3N$ concentration via the thermal decomposition at 300°C may contribute to the enhancement of the removal efficiency of $(CH_3)_3N$. Obviously, the presence of CO_2 does significantly affect the removal efficiency. The higher the CO_2 concentration, the higher the removal efficiency. Since CO_2 is a highly oxidized, thermodynamically stable compound, its utilization requires reaction with certain high - energy substances or electro reductive processes. **Figure 5.33(b)** reveals that when the negative effect of reduced residence time is taken in account, the value of ψ'' continues to increase as the temperature increases.

5.7.2 Effect of temperature and coexisting CO_2 and O_2 on the removal of $(CH_3)_3N$ from N_2

Figure 5.34 shows the two kinds of removal efficiency of $(CH_3)_3N$ versus temperature. It is found that, as the temperature increases, the removal efficiency ψ' and ψ'' equal to 100% even in blank tests without corona discharge at 100°C to 300°C. This means that the thermal decomposition of $(CH_3)_3N$ contributes to complete removal efficiency of $(CH_3)_3N$. To distinguish the perfect effect of thermal decomposition, the removal efficiency ψ' *and* ψ'' are arbitrarily shown as zero. As mentioned previously, the improved removal efficiency for $(CH_3)_3N$ can be attributed to effect of CO_3^-, O_3 and O^- anion at low temperatures and various radicals at high temperatures. Obviously, the presence of O_2 does significantly enhance the removal efficiency of $(CH_3)_3N$.

5.7.3 Effect of temperature and coexisting CO_2 and H_2O on the removal of $(CH_3)_3N$ from N_2

Figure 5.35 shows the two kinds of removal efficiency of $(CH_3)_3N$ versus temperature. It is found that, as the temperature increases, the removal efficiency ψ' and ψ'' equal to 100% even in blank tests without corona discharge at 100°C to 300°C. As in 5.72 the thermal decomposition of $(CH_3)_3N$ concentration contributes to the complete removal efficiency of $(CH_3)_3N$ above 100°C. As mentioned previously, H^-, OH^-, CO_3^- and O^- anions should contribute to the removal of $(CH_3)_3N$ at low to moderate temperatures. Obviously, the presence of H_2O does significantly enhance the removal efficiency of $(CH_3)_3N$.

5.74 Effect of temperature and coexisting CO_2, O_2 and H_2O on the removal of $(CH_3)_3N$ from N_2

Figure 5.36 shows the two kinds of removal efficiency of $(CH_3)_3N$ versus temperature. It is again found that, as the temperature increases, the removal efficiency ψ' and ψ'' equal to 100% even in blank test without corona discharge at 100°C to 300°C. As mentioned previously, CO_3^-, H^-, OH^-, O_3 and O^- anions should contribute to the removal of $(CH_3)_3N$ at low to moderate temperatures. Obviously, the presence of O_2 and H_2O significantly enhance the removal efficiency of $(CH_3)_3N$.

5.75 Preliminary summary

Generally, two more types of removal efficiency are often reported for a corona-discharge system: the electron-based efficiency ψ_{elec} (-) and the energy - based efficiency ψ_{ener} (mol gas $.J^{-1}$). At 33, 100, 200 and 300°C, the experimental values of ψ_{elec} and ψ_{ener} of the $(CH_3)_3N$ 200 ppm removal are as follows:

N_2 - CO_2 (10%), (I=0.2 mA):

ψ_{elec} = 4.5, 3.9, 3.0, 0.0 $\quad$ $\psi_{ener} \times 10^{-9}$ = 6.1, 5.9, 5.9, 0.0

N_2 - O_2 (10%) - CO_2 (10%), (I=0.2 mA):

ψ_{elec} = 3.8, -0.6, -0.1, 0.0 $\psi_{ener} \times 10^{-9}$ = 4.4, -8.8, -8.7, 0.0

N_2 - H_2O (10500 ppm) - CO_2 (10%), (I=0.2 mA):

ψ_{elec} = 3.9, -0.1, 0.0, 0.0 $\psi_{ener} \times 10^{-9}$ = 5.3, -0.13, 0.0, 0.0

N_2 - O_2 (10%) - H_2O (10500 ppm) - CO_2 (10%), (I=0.2 mA):

ψ_{elec} = 2.9, -0.5, 0.0, 0.0 $\psi_{ener} \times 10^{-9}$ = 3.3, -0.7, -0.07, 0.0

Typically, ψ_{elec} and ψ_{ener} tend to decrease as the gas temperature increases. This trend may be ascribed to the combined effect of the reduced residence time and the shift in removal mechanism. Interestingly, in some cases ψ_{elec} and ψ_{ener} are negative because $(CH_3)_3N$ is thermally decomposed even without corona discharge but the corona discharge resulted in the detection of $(CH_3)_3N$, thus indicating a high electron energy level could affect the reaction mechanism.

In actual applications of gas purification, it is important to maximaze the energy - based efficiency ψ_{ener}. From the above results, it is recommended to operate at 300°C when air is purified. Compared to the case of the removal of CH_3CHO and NH_3 from N_2 - CO_2, the average value ψ_{ener} of $(CH_3)_3N$ is lower than that the case of CH_3CHO by approximately 10% but higher than that the case of NH_3 by approximately 70%. This indicates that the operating costs of the removal of $(CH_3)_3N$ from N_2 - CO_2 are lower than that of CH_3CHO but higher than that of NH_3.

ศูนย์วิทยทรัพยากร
จุฬาลงกรณ์มหาวิทยาลัย

5.76 Byproducts dected on the removal of trimethyl amine

Figure 5.37 shows the concentration of the byproduct CO versus temperature in the presence of CO_2. In **Figure 5.37,** as the temperature increases, the byproduct CO increases due to CO_3^- and O^- anion at low temperature. At high temperatures, electron detachment would become significant so that radicals of O, H, and N may play a more important role than their anionic counterparts. As mentioned previously, production of CO is caused by dissociative attachment reaction.

Figure 5.38 shows the concentration of the byproduct NO_x versus temperature in the presence of CO_2. In **Figure 5.38,** as the temperature increases, the byproduct NO_x increases. As mentioned previously, it is well known that production of NO_x take place by the discharge process is favored at high temperatures. This phenomenon is also confirmed in our experiments. While the outlet concentration of NO_x was negligible at room temperature, NO_x concentration gradually increase as the with temperature rise.

Figure 5.39 shows the concentration of byproduct CO versus temperature in the presence of O_2 and CO_2. In **Figure 5.39**, as the temperature increases, the byproduct CO decreases because at high temperatures, O_3 is unstable.

Figure 5.40 shows the concentration of the byproduct O_3 versus temperature in the presence of O_2 and CO_2. In **Figure 5.40,** as the temperature increases, the byproduct O_3 decreases because O_3 is unstable at high temperatures (Peyrous, Pignolet and Held, 1989; Devins, 1956).

Figure 5.41 shows the concentration of the byproduct NO_x versus temperature in the presence of O_2 and CO_2. In **Figure 5.41,** as the temperature increases from room temperature up 200°C, the byproduct NO_x decreases then the tendency reverses from 200°C to 300°C.

Figure 5.42 shows the concentration of the byproduct CO versus temperature in the presence of H_2O and CO_2. In **Figure 5.42,** as the temperature increases, the byproduct CO increases from room temperature to 100°C, then the tendency reverses up to 200°C and increases again at 300°C. At low temperatures, since CO_2 and H_2O are present in the gas stream, CO_3^-, H^-, OH^- and O^- anions are produced by dissociative electron attachment (Massey, 1976; Moruzzi and Phelps, 1966). At

200°C, the presence of CO_2 and H_2O slightly retards the production of CO because at a low discharge current, the relatively much smaller number of electrons tends to attach mostly to CO_2 and H_2O. At high temperatures, electron detachment would become significant so that radicals of CO_3, O, H, N, and OH may play a more important role than their anionic counterparts. The mean residence time of the gas mixture inside the reactor decreases as the reactor temperature increases.

Figure 5.43 shows the concentration of the byproduct NO_x versus temperature in the presence of H_2O and CO_2. In **Figure 5.43,** as the temperature increases, the byproduct NO_x increases. It is known that production of NO_x by the discharge process is favored at high temperatures. This fact is also confirmed in our experiments. While the outlet concentration of NO_x was negligible at room temperature, its concentration gradually increased as the temperature rises.

Figure 5.44 shows the concentration of the byproduct CO versus temperature in the presence of O_2, H_2O and CO_2. In **Figure 5.44** as the temperature increases, the byproduct CO increases from room temperature to 100°C, then the tendency reverses up to 200°C but increases again at 300°C. The reason was given in relation to Figure 5.42

Figure 5.45 shows the concentration of the byproduct O_3 versus temperature in the presence of O_2, H_2O and CO_2. In **Figure 5.45** as the temperature increases, the byproduct O_3 decreases with temperature rise because O_3 is unstable at high temperature.

Figure 5.46 shows the concentration of the byproduct NO_x versus temperature in the presence of O_2, H_2O and CO_2. In **Figure 5.46** as the temperature increases, the byproduct NO_x decreases from room temperature up to 200°C, then the tendency reverses up to 300°C. The reasons were given previously in relation Figure 5.38.

ศูนย์วิทยทรัพยากร
จุฬาลงกรณ์มหาวิทยาลัย

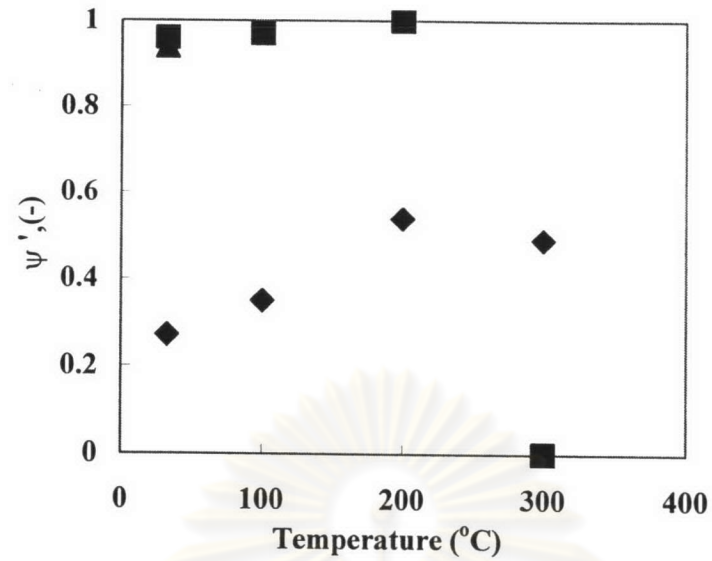

(a)

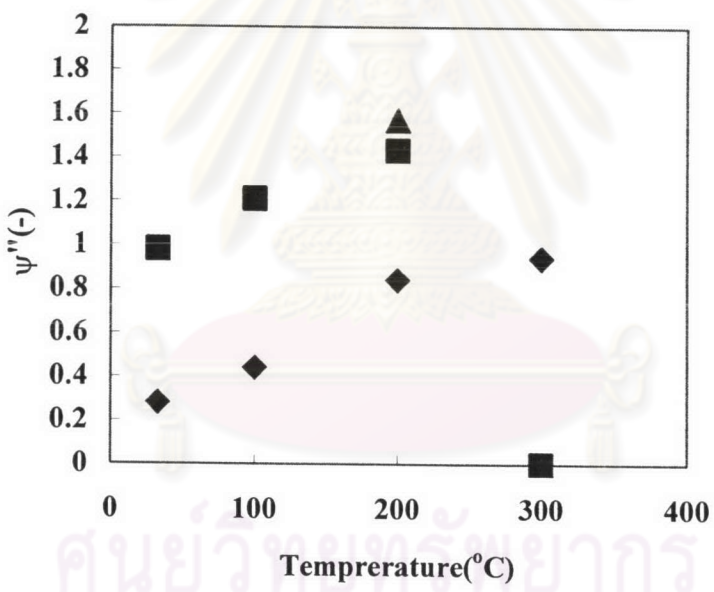

(b)

ศูนย์วิทยทรัพยากร
จุฬาลงกรณ์มหาวิทยาลัย

Figure 5.33 Effect of coexisting CO_2 on the removal of $(CH_3)_3N$ from N_2; $C_{in,trimethylamine}$=200ppm, I=0.2mA, SV=55.8 hr^{-1} at room temperature : ◆ CO_2 (0%) ▲ CO_2 (10%) ■ CO_2 (20%)

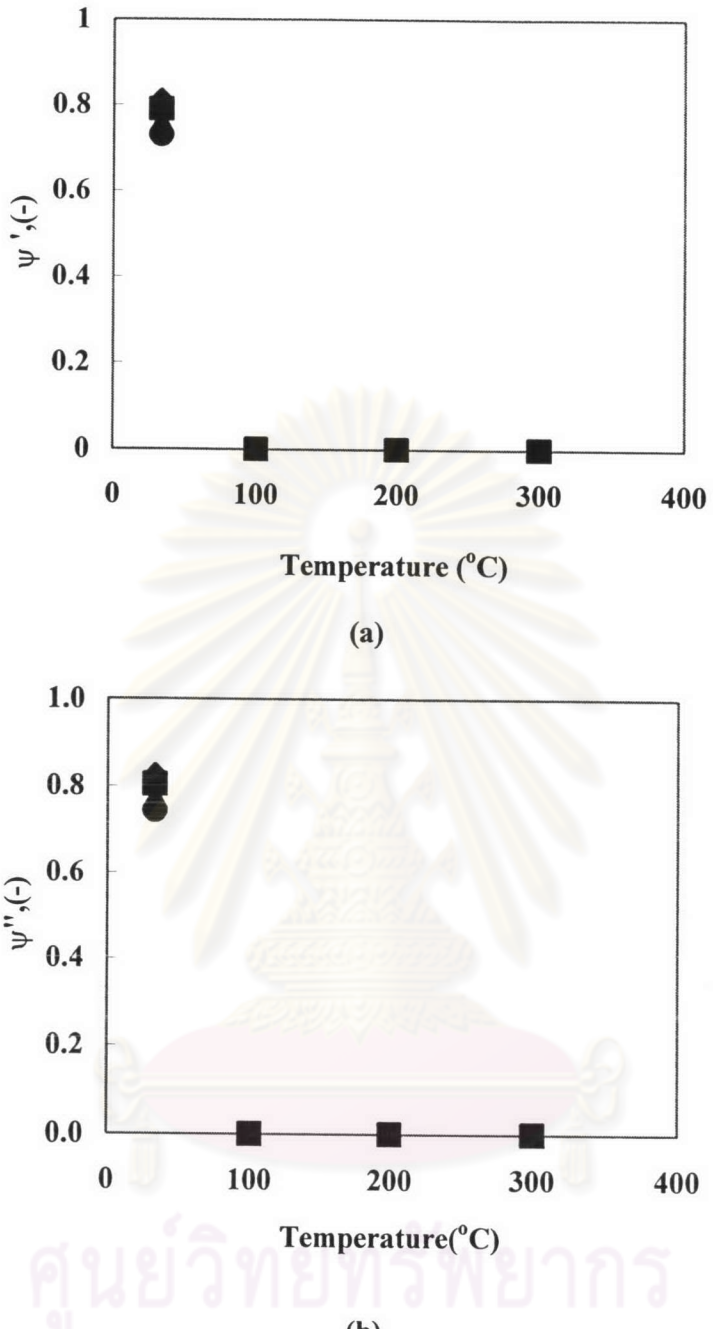

Figure 5.34 Effect of coexisting O_2-CO_2 on the removal of $(CH_3)_3N$ from N_2; $C_{in,trimethylamine}$=200ppm, I=0.2mA, SV=55.8 hr^{-1} at room temperature :
◆ CO_2 (10%) - O_2 (10%),
▲ CO_2 (20%) - O_2 (10%),
■ CO_2 (10%) - O_2 (20%),
● CO_2 (20%) - O_2 (20%)

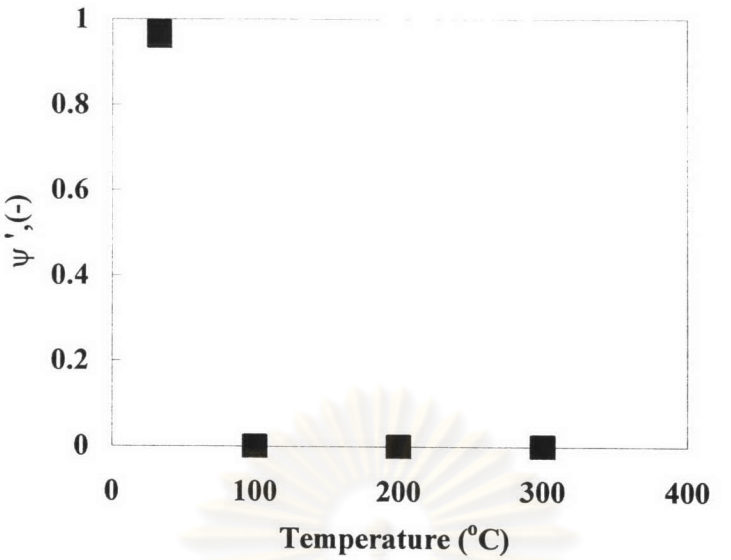

(a)

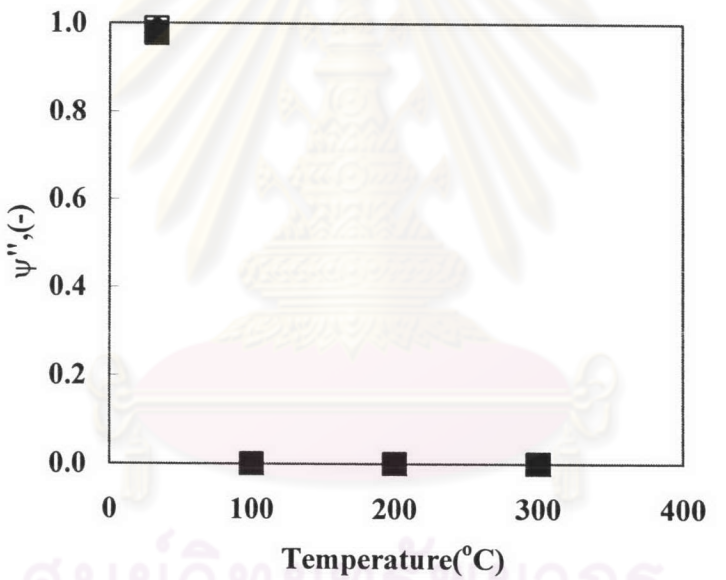

(b)

Figure 5.35 Effect of coexisting H_2O-CO_2 on the removal of $(CH_3)_3N$ from N_2; $C_{in,trimethylamine}$=200ppm, I=0.2mA, SV=55.8 hr^{-1} at room temperature :

- ◆ CO_2 (10%) - H_2O (5250ppm),
- ◇ CO_2 (20%) - H_2O (5250ppm),
- ▲ CO_2 (10%) - H_2O (10500ppm),
- △ CO_2 (20%) - H_2O (10500ppm),
- ■ CO_2 (10%) - H_2O (21800ppm),
- □ CO_2 (20%) - H_2O (21800ppm)

ศูนย์วิทยทรัพยากร
จุฬาลงกรณ์มหาวิทยาลัย

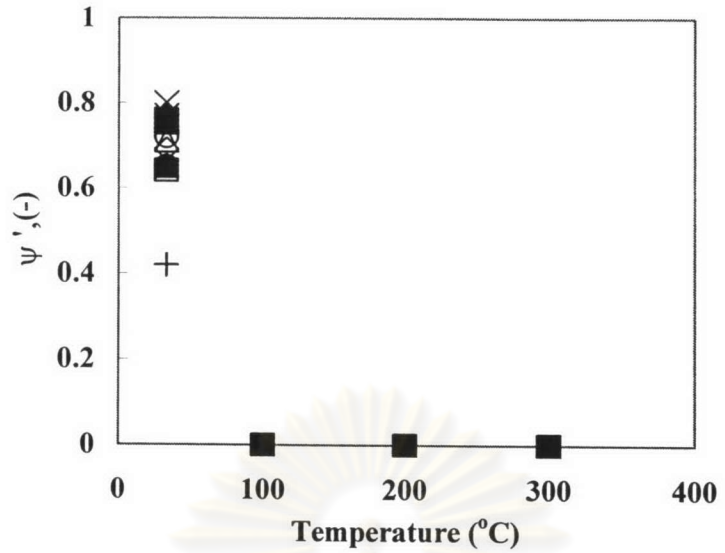

(a)

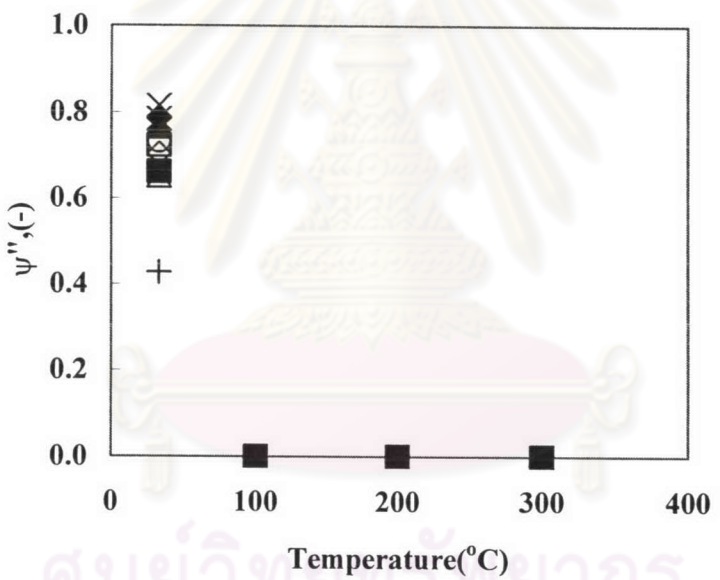

(b)

Figure 5.36 Effect of coexisting O_2-H_2O-CO_2 on the removal of $(CH_3)_3N$ from N_2; $C_{in,trimethylamine}$=200ppm, I=0.2mA, SV=55.8 hr^{-1} at room temperature :

◆ CO_2 (10%)-O_2 (10%)-H_2O (5250ppm), ◇ CO_2 (20%)-O_2 (10%)-H_2O (5250ppm),
▲ CO_2 (10%)-O_2 (20%)-H_2O (5250ppm), △ CO_2 (20%)-O_2 (20%)-H_2O (5250ppm),
■ CO_2 (10%)-O_2 (10%)-H_2O (10500ppm), □ CO_2 (20%)-O_2 (10%)-H_2O (10500ppm),
● CO_2 (10%)-O_2 (20%)-H_2O (10500ppm), ○ CO_2 (20%)-O_2 (20%)-H_2O (10500ppm),
* CO_2 (10%)-O_2 (10%)-H_2O (21800ppm), × CO_2 (20%)-O_2 (10%)-H_2O (21800ppm),
+ CO_2 (10%)-O_2 (20%)-H_2O (21800ppm), − CO_2 (20%)-O_2 (20%)-H_2O (21800ppm)

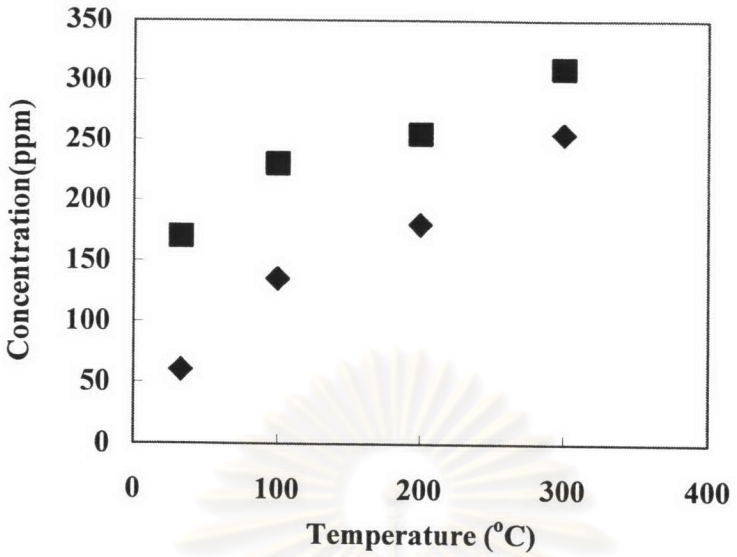

Figure 5.37 Byproduct (CO) on the removal of $(CH_3)_3N$ from N_2-CO_2: ◆ CO_2 (10%), ■ CO_2 (20%)

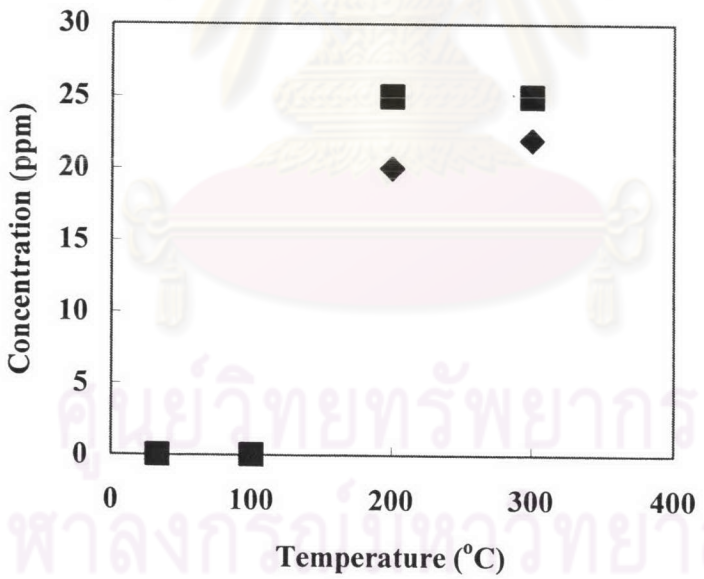

Figure 5.38 Byproduct (NO_x) on the removal of $(CH_3)_3N$ from N_2-CO_2: ◆ CO_2 (10%), ■ (CO_2 20%)

ศูนย์วิทยทรัพยากร
จุฬาลงกรณ์มหาวิทยาลัย

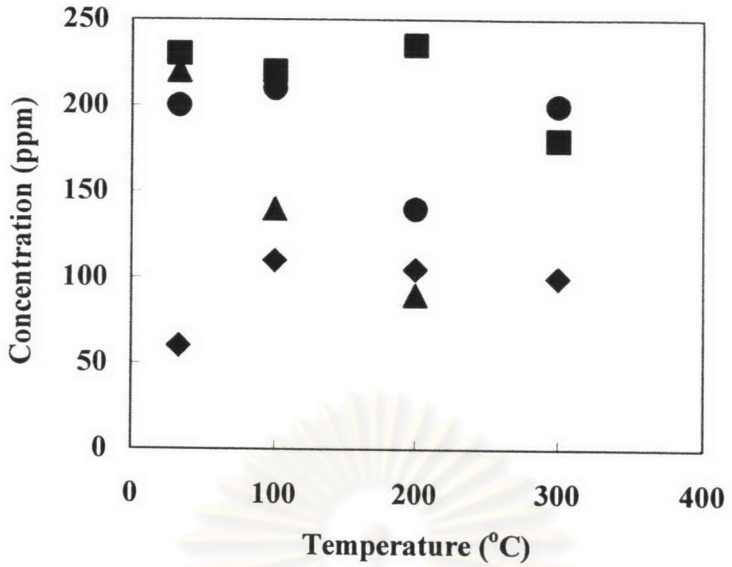

Figure 5.39 Byproduct (CO) on the removal of $(CH_3)_3N$ from N_2-O_2-CO_2:
◆ CO_2 (10%) - O_2 (10%),
▲ CO_2 (20%) - O_2 (10%),
■ CO_2 (10%) - O_2 (20%),
● CO_2 (20%) - O_2 (20%)

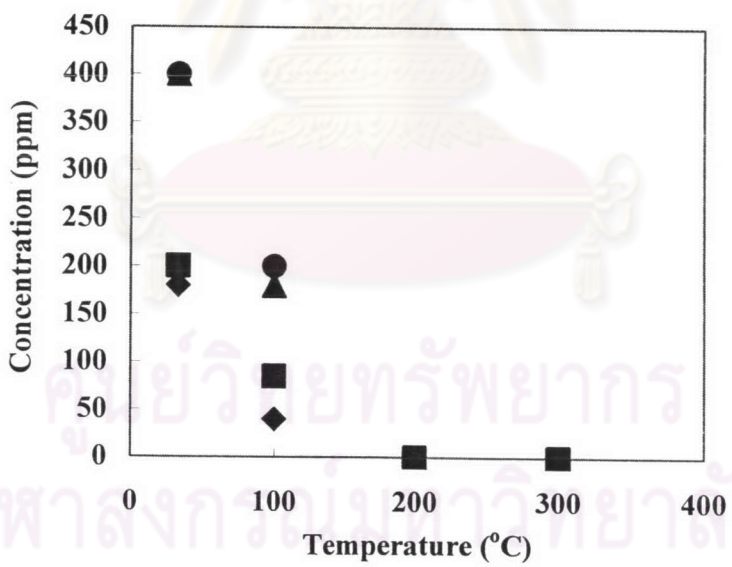

Figure 5.40 Byproduct (O_3) on the removal of $(CH_3)_3N$ from N_2-O_2-CO_2:
◆ CO_2 (10%) - O_2 (10%),
▲ CO_2 (20%) - O_2 (10%),
■ CO_2 (10%) - O_2 (20%),
● CO_2 (20%) - O_2 (20%)

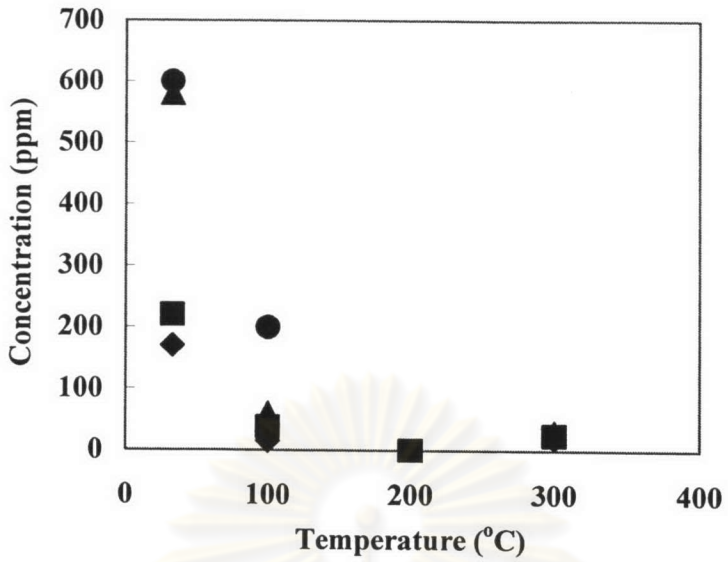

Figure 5.41 Byproduct (NO_x) on the removal of $(CH_3)_3N$ from N_2-O_2-CO_2:
◆ CO_2 (10%) - O_2 (10%),
▲ CO_2 (20%) - O_2 (10%),
■ CO_2 (10%) - O_2 (20%),
● CO_2 (20%) - O_2 (20%)

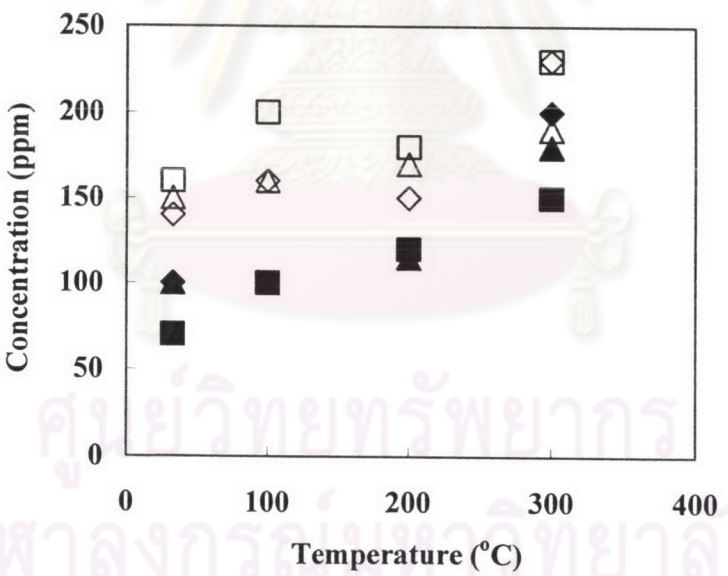

Figure 5.42 Byproduct (CO) on the removal of $(CH_3)_3N$ from N_2-H_2O-CO_2:
◆ CO_2 (10%) - H_2O (5250ppm),
◇ CO_2 (20%) - H_2O (5250ppm),
▲ CO_2 (10%) - H_2O (10500ppm),
△ CO_2 (20%) - H_2O (10500ppm),
■ CO_2 (10%) - H_2O (21800ppm),
□ CO_2 (20%) - H_2O (21800ppm)

ศูนย์วิทยทรัพยากร
จุฬาลงกรณ์มหาวิทยาลัย

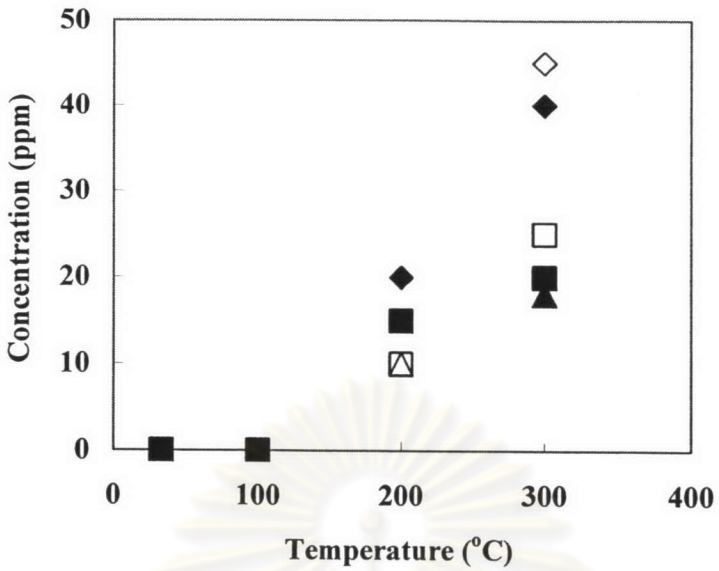

Figure 5.43 Byproduct (NO_x) on the removal of $(CH_3)_3N$ from N_2-H_2O-CO_2:
◆ CO_2 (10%) - H_2O (5250ppm),
◇ CO_2 (20%) - H_2O (5250ppm),
▲ CO_2 (10%) - H_2O (10500ppm),
△ CO_2 (20%) - H_2O (10500ppm),
■ CO_2 (10%) - H_2O (21800ppm),
□ CO_2 (20%) - H_2O (21800ppm)

ศูนย์วิทยทรัพยากร
จุฬาลงกรณ์มหาวิทยาลัย

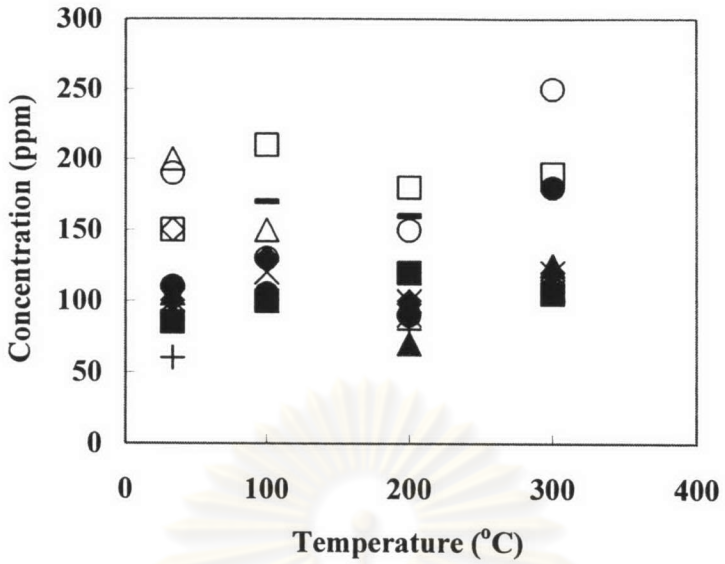

Figure 5.44 Byproduct (CO) on the removal of $(CH_3)_3N$ from N_2-O_2-H_2O-CO_2:
◆ CO_2 (10%) - O_2 (10%) - H_2O (5250ppm),
◇ CO_2 (20%) - O_2 (10%) - H_2O (5250ppm),
▲ CO_2 (10%) - O_2 (20%) - H_2O (5250ppm),
△ CO_2 (20%) - O_2 (20%) - H_2O (5250ppm),
■ CO_2 (10%) - O_2 (10%) - H_2O (10500ppm),
□ CO_2 (20%) - O_2 (10%) - H_2O (10500ppm),
● CO_2 (10%) - O_2 (20%) - H_2O (10500ppm),
○ CO_2 (20%) - O_2 (20%) - H_2O (10500ppm),
* CO_2 (10%) - O_2 (10%) - H_2O (21800ppm),
× CO_2 (20%) - O_2 (10%) - H_2O (21800ppm),
+ CO_2 (10%) - O_2 (20%) - H_2O (21800ppm),
– CO_2 (20%) - O_2 (20%) - H_2O (21800ppm)

ศูนย์วิทยทรัพยากร
จุฬาลงกรณ์มหาวิทยาลัย

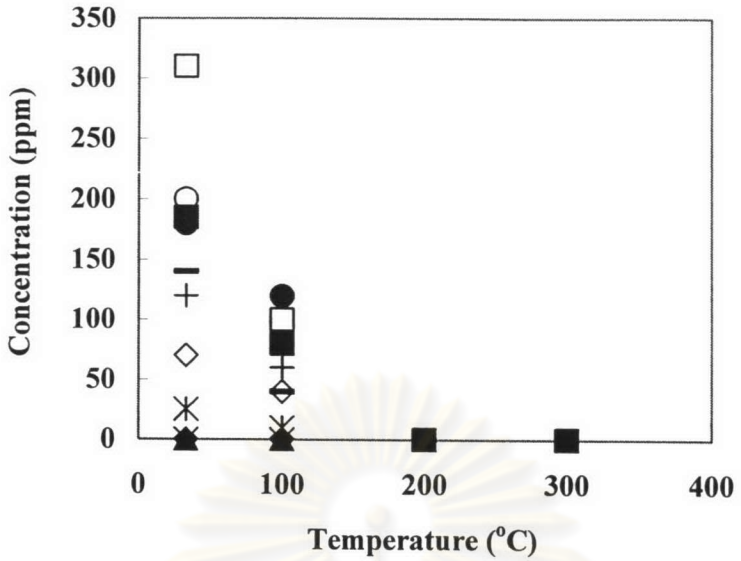

Figure 5.45 Byproduct (O_3) on the removal of $(CH_3)_3N$ from N_2-O_2-H_2O-CO_2:
◆ CO_2 (10%) - O_2 (10%) - H_2O (5250ppm),
◇ CO_2 (20%) - O_2 (10%) - H_2O (5250ppm),
▲ CO_2 (10%) - O_2 (20%) - H_2O (5250ppm),
△ CO_2 (20%) - O_2 (20%) - H_2O (5250ppm),
■ CO_2 (10%) - O_2 (10%) - H_2O (10500ppm),
□ CO_2 (20%) - O_2 (10%) - H_2O (10500ppm),
● CO_2 (10%) - O_2 (20%) - H_2O (10500ppm),
○ CO_2 (20%) - O_2 (20%) - H_2O (10500ppm),
* CO_2 (10%) - O_2 (10%) - H_2O (21800ppm),
× CO_2 (20%) - O_2 (10%) - H_2O (21800ppm),
+ CO_2 (10%) - O_2 (20%) - H_2O (21800ppm),
– CO_2 (20%) - O_2 (20%) - H_2O (21800ppm)

ศูนย์วิทยทรัพยากร
จุฬาลงกรณ์มหาวิทยาลัย

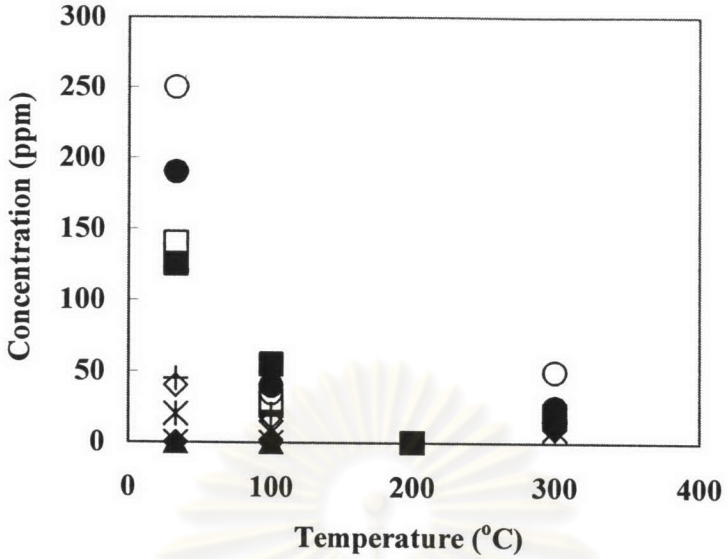

Figure 5.46 Byproduct (NO_x) on the removal of $(CH_3)_3N$ from N_2-O_2-H_2O-CO_2:
◆ CO_2 (10%) - O_2 (10%) - H_2O (5250ppm),
◇ CO_2 (20%) - O_2 (10%) - H_2O (5250ppm),
▲ CO_2 (10%) - O_2 (20%) - H_2O (5250ppm),
△ CO_2 (20%) - O_2 (20%) - H_2O (5250ppm),
■ CO_2 (10%) - O_2 (10%) - H_2O (10500ppm),
□ CO_2 (20%) - O_2 (10%) - H_2O (10500ppm),
● CO_2 (10%) - O_2 (20%) - H_2O (10500ppm),
○ CO_2 (20%) - O_2 (20%) - H_2O (10500ppm),
* CO_2 (10%) - O_2 (10%) - H_2O (21800ppm),
× CO_2 (20%) - O_2 (10%) - H_2O (21800ppm),
+ CO_2 (10%) - O_2 (20%) - H_2O (21800ppm),
– CO_2 (20%) - O_2 (20%) - H_2O (21800ppm)

ศูนย์วิทยทรัพยากร
จุฬาลงกรณ์มหาวิทยาลัย

5.8 Simultaneous removal of acetaldehyde and ammonia

5.8.1 Effect of temperature and coexisting CO_2 on the simultaneous removal of CH_3CHO and NH_3 from N_2

Figure 5.47 shows the effect of CO_2 on the simultaneous removal efficiency of CH_3CHO and NH_3 from N_2. The inlet concentrations of CH_3CHO and NH_3 are 150 ppm and 1,000 ppm, respectively, while the discharge current is 0.3 mA. It is found that the presence of CO_2 has a significant enhancement effect on the simultaneous CH_3CHO removal efficiency ψ' in **Figure 5.47(a)**. As the temperature increases from room temperature up to 200°C, the removal efficiency ψ' decreases then the tendency reverses up to 300°C because of the effect of O^- anion and CO_3^- at low temperatures and the reduced mean residence time of the gas mixture inside the reactor. As mentioned previously, it is postulated that CO_2 is less electronegative than CH_3CHO but the bonding strength CO_2 molecules with the anode surface is stronger than that of CH_3CHO. At low temperatures when a small number of electrons are available at a low discharge current, most electrons attach onto CH_3CHO, and the deposit on the anode wall is composed of mostly CH_3CHO. At high temperatures, there is an excess of electrons that can attach to CO_2. When the CO_2 ions deposit on the anode surface, they replace (drive off) some of the previously deposited CH_3CHO. Similarly, in **Figure 5.47(b)**, as the temperature increases, the removal efficiency ψ' of NH_3 decreases from room temperature up to 200°C, and then the tendency reverses up to 300°C. As expected, the presence of CO_2 has a significant enhancement effect on the simultaneous removal efficiency of NH_3.

ศูนย์วิทยทรัพยากร
จุฬาลงกรณ์มหาวิทยาลัย

5.8.2 Effect of temperature and coexisting CO_2 and O_2 on the simultaneous removal of CH_3CHO and NH_3 from N_2

Figure 5.48 shows the effect of CO_2 and O_2 on the simultaneous removal efficiency of CH_3CHO and NH_3 from N_2. The inlet concentrations of CH_3CHO and NH_3 are 150 ppm and 1,000 ppm, respectively, while the current is 0.3 mA. In **Figure 5.48(a)**, as the temperature increases, the removal efficiency ψ' of CH_3CHO decrease from room temperature up to 300°C because of lesser O_3 generated from O_2 and reduced mean residence time of the gas mixture inside the reactor at high temperatures. Similarly, in **Figure 5.48(b)**, as the temperature increases, the removal efficiency ψ' of NH_3 decreases from room temperature up to 300°C. The presence of CO_2 does significantly enhance the removal efficiency of CH_3CHO and NH_3 from N_2 - O_2.

5.8.3 Effect of temperature and coexisting CO_2 and H_2O on the simultaneous removal of CH_3CHO and NH_3 from N_2

Figure 5.49 shows the effect of CO_2 and H_2O on the simultaneous removal efficiency of CH_3CHO and NH_3 from N_2. The inlet concentrations of CH_3CHO and NH_3 are 150 ppm and 1,000 ppm, respectively, while the current is 0.3 mA. It is found that the presence of CO_2 has a significant enhancement effect on the simultaneous CH_3CHO removal efficiency ψ' in **Figure 5.49(a)**, as the temperature increases from room temperature up to 200°C, the removal efficiency ψ' of CH_3CHO decreases, then the tendency reverses up to 300°C because of the reduced mean residence time of the gas mixture inside the reactor decreases as the reactor temperature rises. As mentioned previously, H^-, OH^-, O^- anions and CO_3^- should contribute to the removal of CH_3CHO at low to moderate temperatures. At 200°C, the presence of H_2O and CO_2 slightly retards the removal efficiency of CH_3CHO because at low discharge current, the relatively much smaller number of electrons tends to attach mostly to H_2O and CO_2 In addition, N radicals are consumed by their

reaction with CO_2 and H_2O at high temperatures. In **Figure 5.49(b)**, as the temperature increases, the removal efficiency ψ' of NH_3 decreases from room temperature up to 200°C, then the tendency reverses up to 300°C because this condition, the synthesis occurs of NH_3 again. On the other hand, the mean residence time of the gas mixture inside the reactor decreases as the reactor temperature rises. Obviously, the presence of CO_2 does significantly enhance the removal efficiency.

5.84 Effect of temperature and coexisting CO_2, O_2 and H_2O on the simultaneous removal of CH_3CHO and NH_3 from N_2

Figure 5.50 shows the effect of CO_2 and H_2O on the simultaneous removal efficiency of CH_3CHO and NH_3 from N_2. The inlet concentrations of CH_3CHO and NH_3 are 150 ppm and 1,000 ppm, respectively, while the discharge current is 0.3 mA. It is found that the presence of CO_2 has a significant enhancement effect on the simultaneous CH_3CHO removal efficiency ψ' in **Figure 5.50(a)**. As the temperature increases from room temperature up to 300°C, the removal efficiency ψ' decreases. As mentioned previously, CO_3^-, H^-, OH^-, O_3 and O^- anions should contribute to the removal of CH_3CHO at low to moderate temperatures but at high temperatures CO_2, O_3 and H_2O unstable. Similarity in **Figure 5.50(b)**, as temperature increases, the removal efficiency ψ' decreases from room temperature up to 300°C. The presence of CO_2 does significantly enhance the removal efficiency of NH_3 from N_2 - O_2 - H_2O.

ศูนย์วิทยทรัพยากร
จุฬาลงกรณ์มหาวิทยาลัย

5.85 Byproducts from the simultaneous removal of acetaldehyde and ammonia

Figure 5.51 shows the concentration of byproduct CO versus temperature. In **Figure 5.51** as the temperature increases, the byproduct CO decreases from room temperature to 100°C, above which the tendency reverses up to 300°C because of the effect of O^- anion and CO_3^- at low temperature. At high temperatures, the mean residence time of the gas mixture inside the reactor decreases.

Figure 5.52 shows the concentration of byproduct O_3 versus temperature. In **Figure 5.52** as the temperature increases, the byproduct O_3 decreases because O_3 is unstable at high temperatures.

Figure 5.53 shows the concentration of byproduct NO_x versus temperature. In **Figure 5.53** as the temperature increases, the byproduct NO_x decreases from room temperature up 200°C, then the tendency reverses up to 300°C because the byproduct O_3 decreases with the temperature rise and so does the mean residence time of the gas mixture inside the reactor.

ศูนย์วิทยทรัพยากร
จุฬาลงกรณ์มหาวิทยาลัย

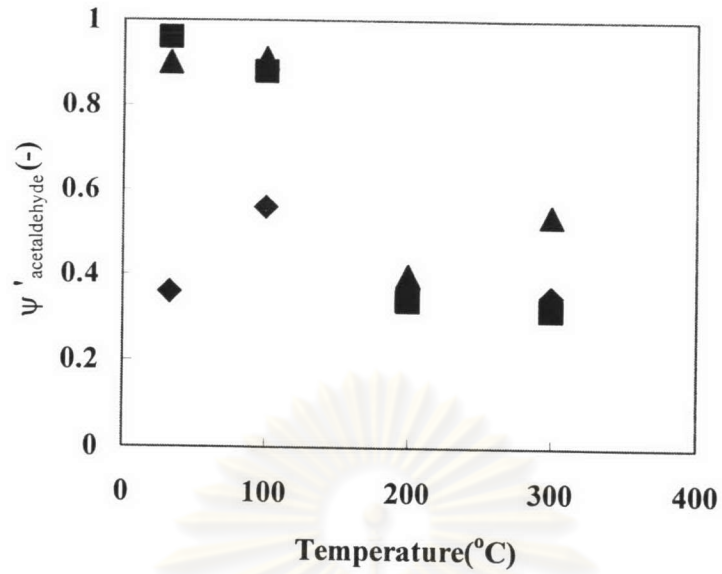

(a)

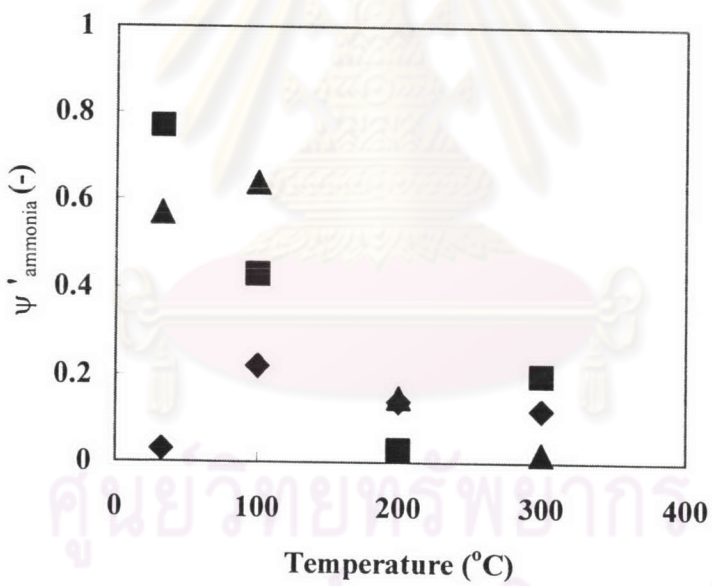

(b)

Figure 5.47 Effect of coexisting CO_2 on the simultaneous removal of CH_3CHO and NH_3 from N_2; $C_{in,\ acetaldehyde}$=150ppm, $C_{in,ammonia}$=1000ppm, I=0.3mA, SV=55.8 hr^{-1} at room temperature :
◆ CO_2 (0%), ■ CO_2 10%), ▲ CO_2 (20%)

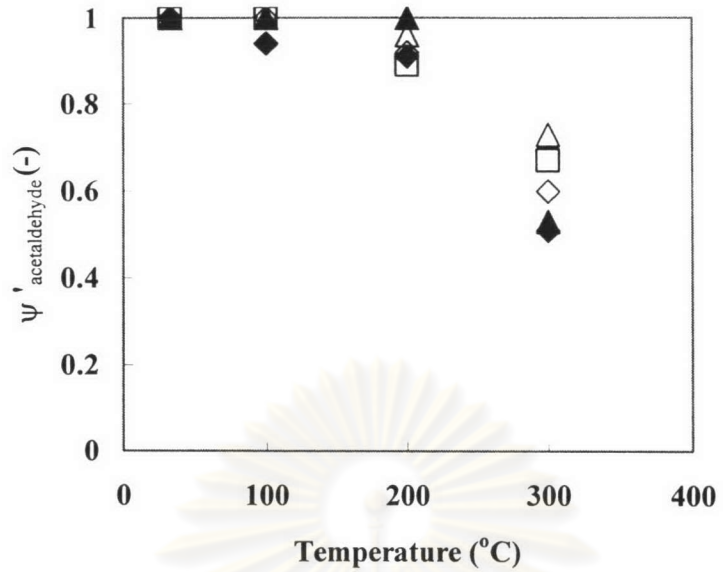

(a)

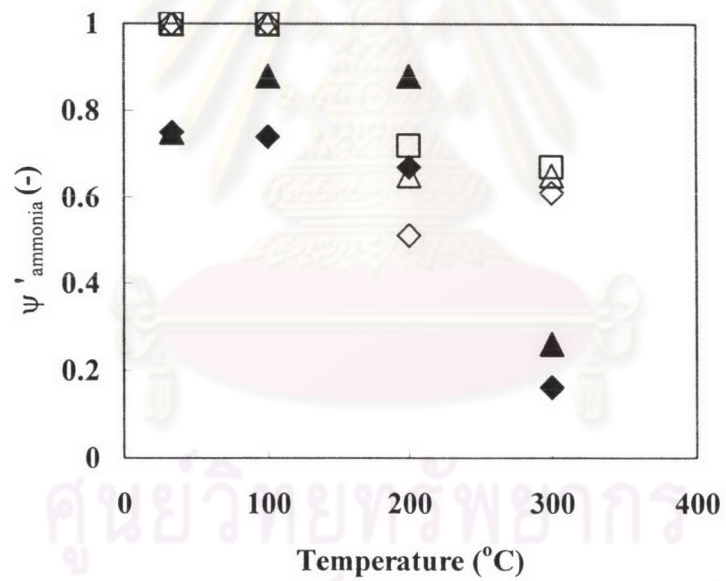

(b)

Figure 5.48 Effect of coexisting O_2-CO_2 on the simultaneous removal of CH_3CHO and NH_3 from N_2; $C_{in,\ acetaldehyde}$=150ppm, $C_{in,ammonia}$=1000ppm, I=0.3mA, SV=55.8 hr^{-1} at room temperature :

- ◆ CO_2 (0%) - O_2 (10%),
- ◇ CO_2 (10%) - O_2 (10%),
- □ CO_2 (20%) - O_2 (10%),
- ▲ CO_2 (0%) - O_2 (20%),
- △ CO_2 (10%) - O_2 (20%)

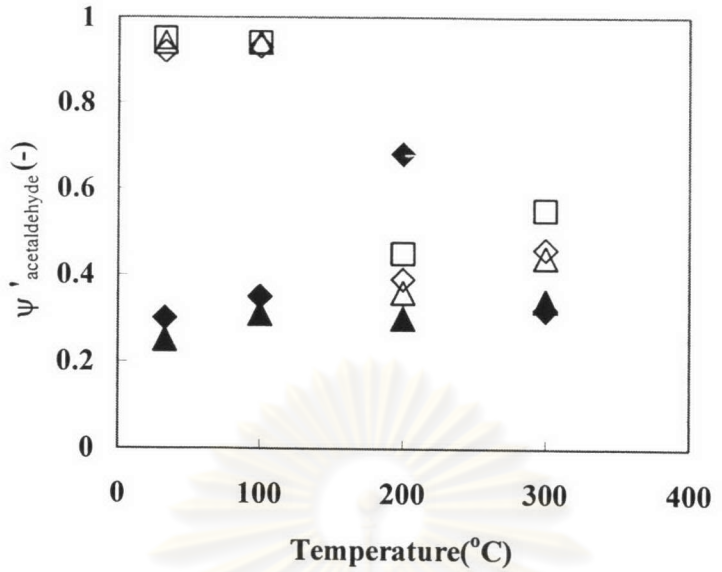

(a)

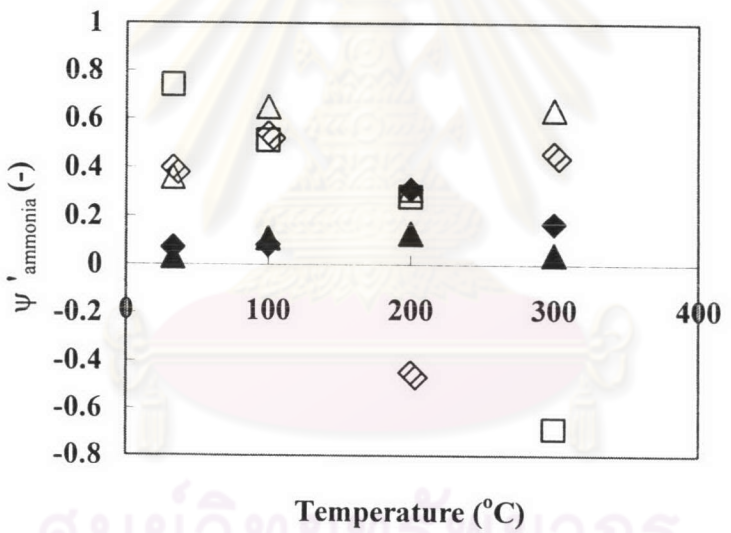

(b)

Figure 5.49 Effect of coexisting H_2O-CO_2 on the simultaneous removal of CH_3CHO and NH_3 from N_2; $C_{in,\ acetaldehyde}$=150ppm, $C_{in,ammonia}$=1000ppm, I=0.3mA, SV=55.8 hr^{-1} at room temperature :
◆ CO_2 (0%) - H_2O (5250ppm),
◇ CO_2 (10%) - H_2O (5250ppm),
□ CO_2 (20%) - H_2O (5250ppm),
▲ CO_2 (0%) - H_2O (10500ppm),
△ CO_2 (10%) - H_2O (10500ppm)

ศูนย์วิทยทรัพยากร
จุฬาลงกรณ์มหาวิทยาลัย

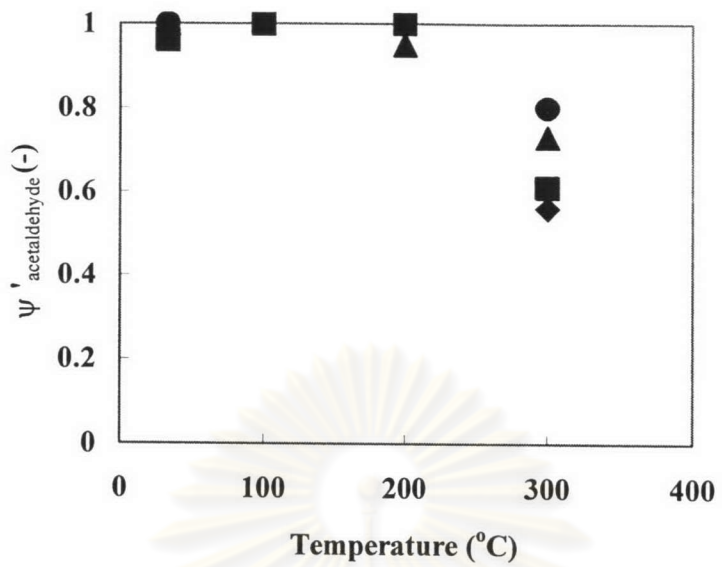

(a)

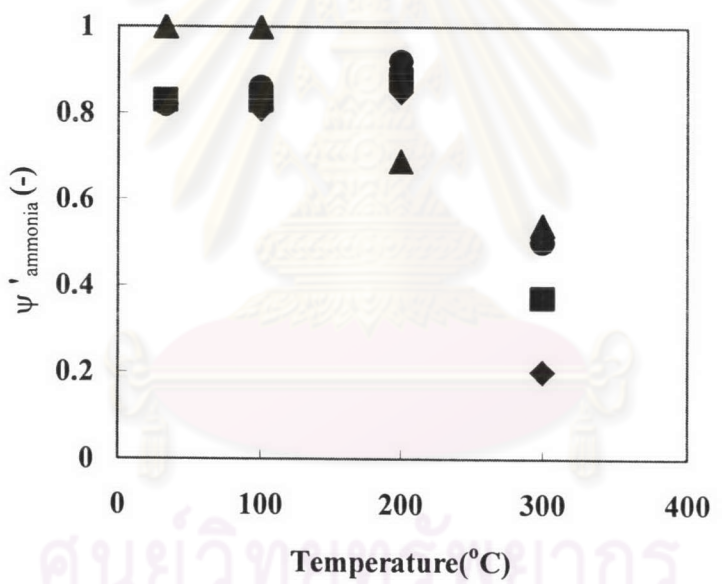

(b)

Figure 5.50 Effect of coexisting O_2-H_2O-CO_2 on the simultaneous removal of CH_3CHO and NH_3 from N_2; $C_{in,\ acetaldehyde}$=150ppm, $C_{in,ammonia}$=1000ppm, I=0.3mA, SV=55.8 hr^{-1} at room temperature :
◆ CO_2 (0%) - O_2 (10%) - H_2O (5250ppm),
■ CO_2 (0%) - O_2 (10%) - H_2O (10500ppm),
▲ CO_2 (10%) - O_2 (10%) - H_2O (5250ppm),
● CO_2 (0%) - O_2 (20%) - H_2O (5250ppm),

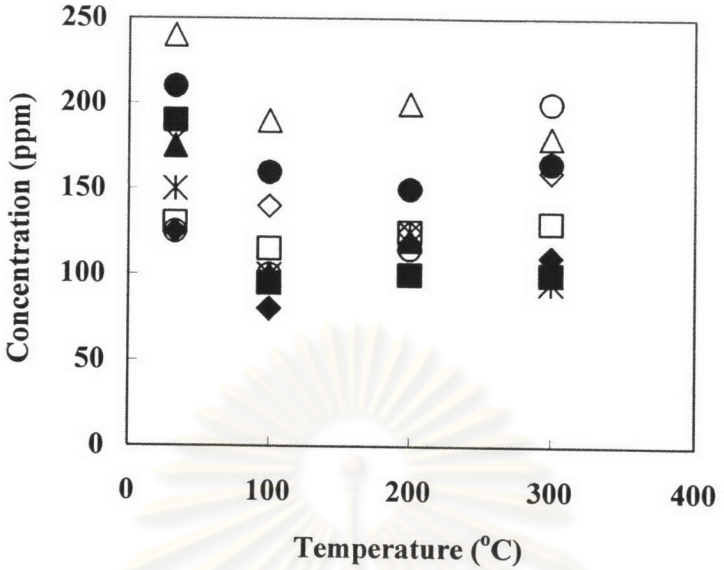

Figure 5.51 Byproduct (CO) on the simultaneous removal of CH_3CHO and NH_3:

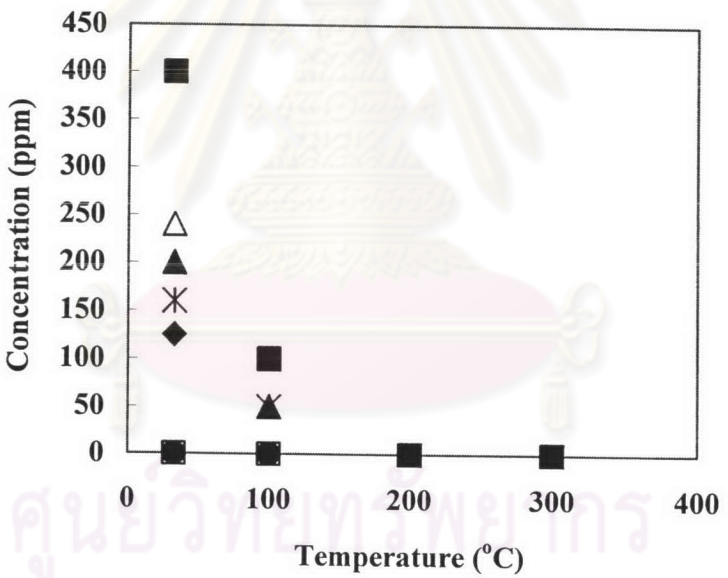

Figure 5.52 Byproduct (O_3) on the simultaneous removal of CH_3CHO and NH_3:

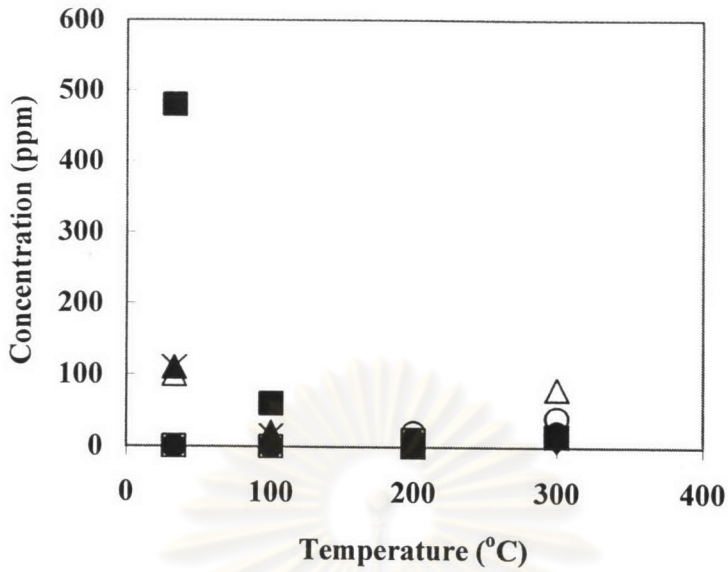

Figure 5.53 Byproduct (NO_x) on the simultaneous removal of CH_3CHO and NH_3:

ศูนย์วิทยทรัพยากร
จุฬาลงกรณ์มหาวิทยาลัย

5.9 Simultaneous removal of acetaldehyde and trimethylamine

5.91 Effect of temperature and coexisting CO_2 on the simultaneous removal of CH_3CHO and $(CH_3)_3N$ from N_2

Figure 5.54 shows the effect of CO_2 on the simultaneous removal efficiency of CH_3CHO and $(CH_3)_3N$ from N_2. The inlet concentrations of CH_3CHO and $(CH_3)_3N$ are 150 ppm and 100 ppm, respectively, while the discharge current is 0.3 mA. It is found that the presence of CO_2 has a significant enhancement effect on the simultaneous CH_3CHO removal efficiency ψ' in **Figure 5.54(a)**, as the temperature increases, the CH_3CHO removal efficiency ψ' increases from room temperature up to 100°C, above which the CH_3CHO removal efficiency tends to significantly decreases because effect of O^- anion and CO_3^- at low temperatures and CO_2 is unstable at high temperatures. Similarity in **Figure 5.54(b)**, as the temperature increases, the $(CH_3)_3N$ removal efficiency ψ' increase from room temperature up to 100°C, above which the $(CH_3)_3N$ removal efficiency tends to significantly decreases because effect of O^- anion and CO_3^- at low temperatures and the reduced mean residence time of the gas mixture inside the reactor decreases as the reactor temperature rises, and some case equal to 100% even in blank tests without corona discharge. The higher the CO_2 concentration, the higher the removal efficiency becomes.

5.92 Effect of temperature and coexisting CO_2 and O_2 on the simultaneous removal of CH_3CHO and $(CH_3)_3N$ from N_2

Figure 5.55 shows the effect of CO_2 and O_2 on the simultaneous removal efficiency of CH_3CHO and $(CH_3)_3N$ from N_2. The inlet concentrations of CH_3CHO and $(CH_3)_3N$ are 150 ppm and 100 ppm, respectively, while the discharge current is 0.3 mA. It is found that the presence of CO_2 has a significant enhancement effect on the simultaneous CH_3CHO removal efficiency ψ' in **Figure 5.55(a),** as the temperature increases, the CH_3CHO removal efficiency ψ' decrease from room

temperature up to 300°C because O_3 and CO_2 are unstable at high temperatures. Similarity, in **Figure 5.55(b)**, as the temperature increases, the $(CH_3)_3N$ removal efficiency ψ' increases from room temperature up to 300°C, and some case equal to 100% even in blank tests without corona discharge.

5.93 Effect of temperature and coexisting CO_2 and H_2O on the simultaneous removal of CH_3CHO and $(CH_3)_3N$ from N_2

Figure 5.56 shows the effect of CO_2 and H_2O on the simultaneous removal efficiency of CH_3CHO and $(CH_3)_3N$ from N_2. The inlet concentrations of CH_3CHO and $(CH_3)_3N$ are 150 ppm and 100 ppm, respectively, while the discharge current is 0.3 mA. It is found that the presence of CO_2 has a significant enhancement effect on the simultaneous CH_3CHO removal efficiency ψ' in **Figure 5.56(a),** as the temperature increases, the CH_3CHO removal efficiency ψ' decreases from room temperature up to 200°C, and then the tendency reverses up to 300°C. As mentioned previously, H^-, OH^-, CO_3^- and O^- anions should contribute to the removal of CH_3CHO at low temperatures. At 200°C, the presence of H_2O and CO_2 slightly retards the removal efficiency of CH_3CHO because at low discharge current, the relatively much smaller number of electrons tends to attach mostly to H_2O and CO_2. In **Figure 5.56(b)**, Compared to the case of only coexisting H_2O, the simultaneous removal efficiency of $(CH_3)_3N$ is enhance by the presence of CO_2. Obviously, the presence of CO_2 positively affects the removal efficiency. The higher the CO_2 concentration, the higher the removal efficiency becomes and some case equal to 100% even in blank tests without corona discharge.

ศูนย์วิทยทรัพยากร
จุฬาลงกรณ์มหาวิทยาลัย

5.94 Effect of temperature and coexisting CO_2, O_2 and H_2O on the simultaneous removal of CH_3CHO and $(CH_3)_3N$ from N_2

Figure 5.57 shows the effect of CO_2, O_2 and H_2O on the simultaneous removal efficiency of CH_3CHO and $(CH_3)_3N$ from N_2. The inlet concentrations of CH_3CHO and $(CH_3)_3N$ are 150 ppm and 100 ppm, respectively, while the discharge current is 0.3 mA. It is found that the presence of CO_2 has a significant enhancement effect on the simultaneous CH_3CHO removal efficiency ψ' in **Figure 5.57(a)**, as the temperature increases, the CH_3CHO removal efficiency ψ' remains equal 100% from room temperature up to 300°C because effect of O_3, CO_3^-, H^-, OH^- and O^- anion at low temperatures and various radicals at high temperatures. And some case equal to 100% even in blank tests without corona discharge. In **Figure 5.57(b)**, as the temperature increases, the $(CH_3)_3N$ removal efficiency ψ' remains equal 100% at room temperature and 100°C some case, at 100°C to 300°C equal to 100% even in blank tests without corona discharge.

ศูนย์วิทยทรัพยากร
จุฬาลงกรณ์มหาวิทยาลัย

5.95 Byproduct from the simultaneous removal of acetaldehyde and trimethyl amine

Figure 5.58 shows the concentration of byproduct CO versus temperature in the presence of CO_2. In **Figure 5.58** as the temperature increases, the byproduct CO increases from room temperature to 100°C, then the tendency reverses up at 200°C above which the byproducts (CO) increase again at 300°C because effect of CO_3^- and O^- anion at low temperatures. At 200°C, the presence of CO_2 slightly retards the removal efficiency of CH_3CHO and $(CH_3)_3N$ because at low discharge current, the relatively much smaller number of electrons tends to attach mostly to CO_2. In addition, N radicals are consumed by their reaction with CO_2 at high temperatures. As mentioned previously, it is knowns that production of CO by dissociative attachment reaction.

Figure 5.59 shows the concentration of byproduct NO_x versus temperature in the presence of CO_2. In **Figure 5.59** as the temperature increases, the byproduct NO_x increase. As mentioned previously, it is well known that production of NO_x by the discharge process is favored at high temperatures. This phenomenon is also confirmed in our experiments. While the outlet concentration of NO_x was negligible at room temperature, its concentration gradually increased as the temperature rise.

Figure 5.60 shows the concentration of byproduct CO versus temperature in the presence of O_2 and CO_2. In **Figure 5.60** as the temperature increases, the byproduct CO decreases from room temperature to 100°C, then the tendency reverses up at 200°C above which the byproduct CO decreases again at 300°C. As mentioned previously, effect of O_3 and O^- anion at low temperatures and at high temperatures, O_3 is unstable.

Figure 5.61 shows the concentration of byproduct O_3 versus temperature in the presence of O_2 and CO_2. In **Figure 5.61** as the temperature increases, the byproduct O_3 decreases from room temperature to 300°C. This is because O_3 is unstable at high temperatures.

Figure 5.62 shows the concentration of byproduct NO_x versus temperature in the presence of O_2 and CO_2. In **Figure 5.62** as the temperature increases, the

byproduct NO_x decreases from room temperature up 200°C, then the tendency reverses up to 300°C.

Figure 5.63 shows the concentration of byproduct CO versus temperature in the presence of H_2O and CO_2. In **Figure 5.63** as the temperature increases, the byproduct CO increases from room temperature to 300°C because at low temperature, the presence of CO_2 and H_2O in the gas stream, CO_3^-, H^-, OH^- and a few O^- anions are expected to be produced by dissociative electron attachment to CO_2 and H_2O molecules (Massey, 1976; Moruzzi and Phelps, 1966).

Figure 5.64 shows the concentration of byproduct NO_x versus temperature in the presence of H_2O and CO_2. In **Figure 5.64** as the temperature increases, the byproduct NO_x increases. As mentioned previously, it is known that production of NO_x by the discharge process is favored at high temperatures. This fact is also confirmed in our experiments. While the outlet concentration of NO_x was negligible at room temperature, its concentration gradually increased as the temperature rise.

Figure 5.65 shows the concentration of byproduct CO versus temperature in the presence of O_2 and H_2O and CO_2. In **Figure 5.65** as the temperature increases, the byproduct CO increases from room temperature up 200°C, then the tendency reverses up to 300°C because at low temperatures, CO_2 and H_2O are present in the gas stream, CO_3^-, H^-, OH^- and a few O^- anions are expected to be produced by dissociative electron attachment to CO_2 and H_2O molecules (Massey, 1976; Moruzzi and Phelps, 1966). At high temperatures, CO_2, O_3 and H_2O are unstable.

Figure 5.66 shows the concentration of byproduct O_3 versus temperature in the presence of O_2 and H_2O and CO_2. In **Figure 5.66** as the temperature increases, the byproduct (O_3) decreases with temperature rise because O_3 is unstable at high temperatures.

Figure 5.67 shows the concentration of byproduct NO_x versus temperature in the presence of O_2 and H_2O and CO_2. From **Figure 5.67** as the temperature increases, the byproduct NO_x decreases starting from room temperature up 200°C, then the tendency reverses up to 300°C. The reasons were given previously in relation to Figure 5.38.

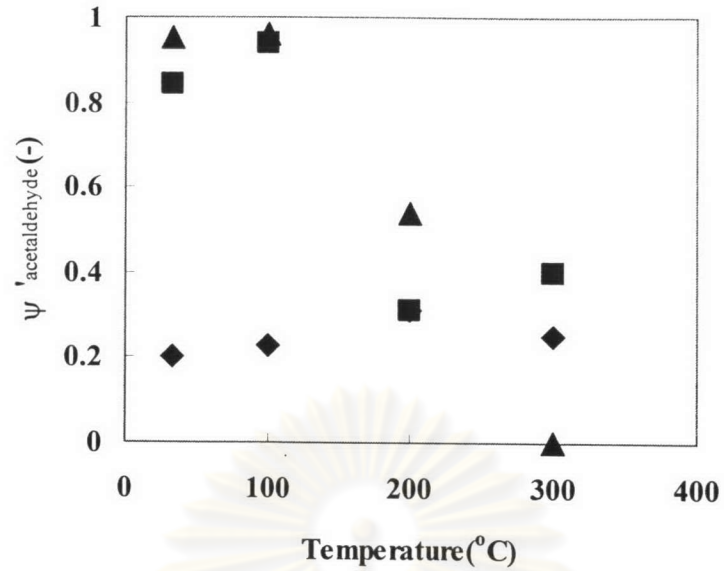

(a)

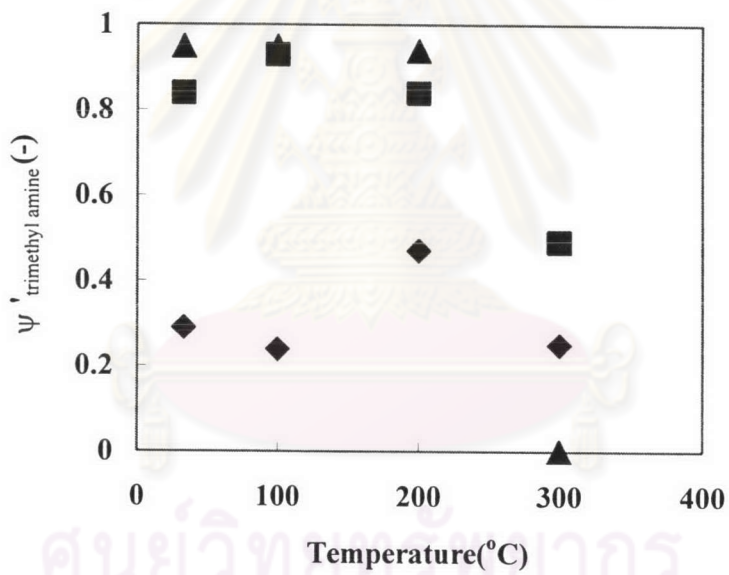

(b)

Figure 5.54 Effect of coexisting CO_2 on the simultaneous removal of CH_3CHO and $(CH_3)_3N$ from N_2; $C_{in,\ acetaldehyde}$=150ppm, $C_{in,trimethylamine}$=100ppm, I=0.3mA, SV=55.8 hr^{-1} at room temperature :
◆ CO_2 (0%), ■ CO_2 (10%), ▲ CO_2 (20%)

ศูนย์วิทยทรัพยากร
จุฬาลงกรณ์มหาวิทยาลัย

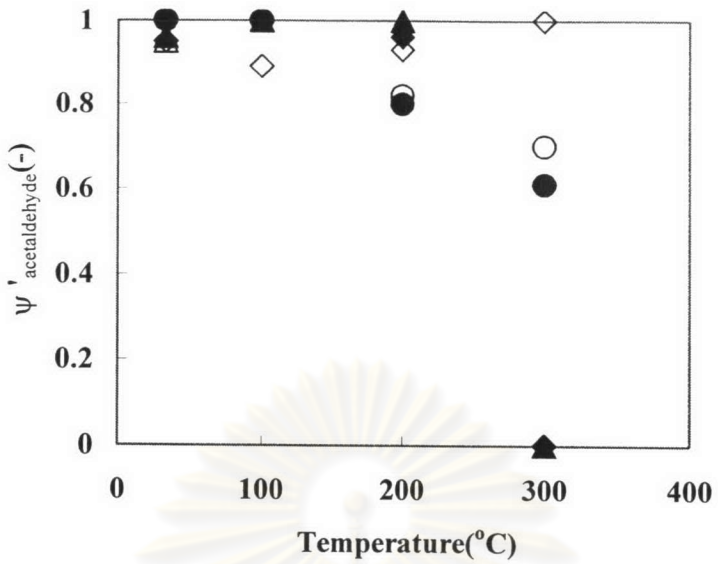

(a)

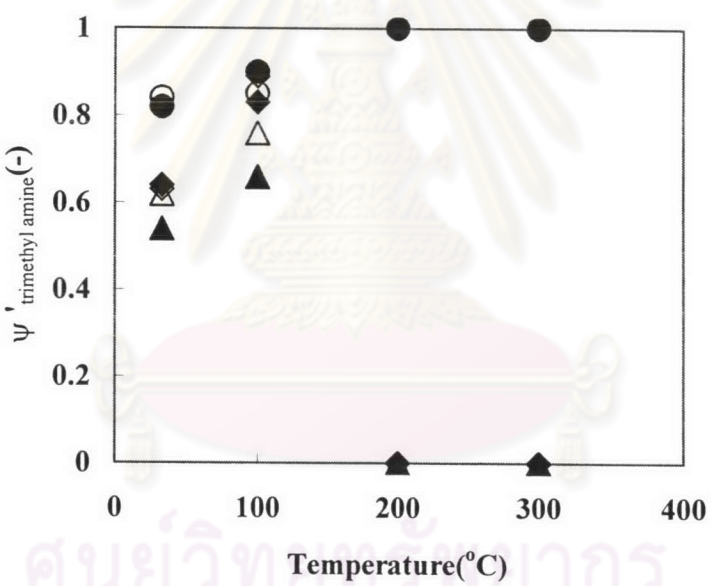

(b)

Figure 5.55 Effect of coexisting O_2-CO_2 on the simultaneous removal of CH_3CHO and $(CH_3)_3N$ from N_2; $C_{in,\ acetaldehyde}$=150ppm, $C_{in,trimethylamine}$=100ppm, I=0.3mA, SV=55.8 hr^{-1} at room temperature :

- ● CO_2 (0%) - O_2 (10%),
- ▲ CO_2 (10%) - O_2 (10%),
- ◆ CO_2 (20%) - O_2 (10%),
- ○ CO_2 (0%) - O_2 (20%),
- △ CO_2 (10%) - O_2 (20%)
- ◇ CO_2 (20%) - O_2 (20%)

ศูนย์วิทยทรัพยากร
จุฬาลงกรณ์มหาวิทยาลัย

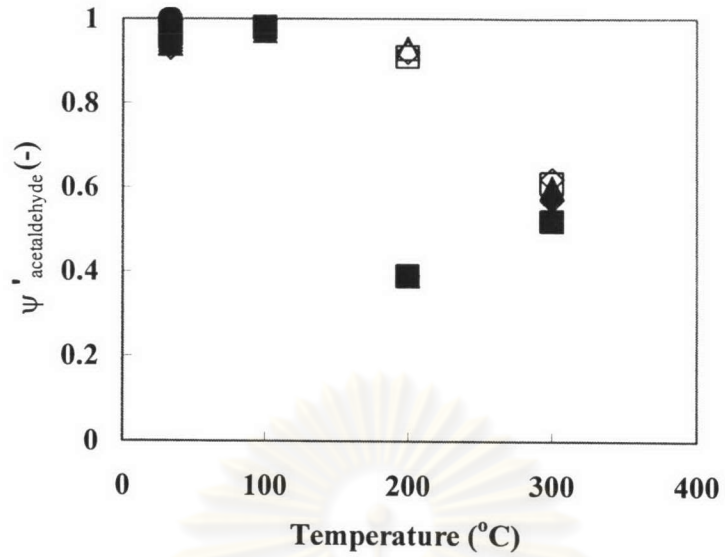

(a)

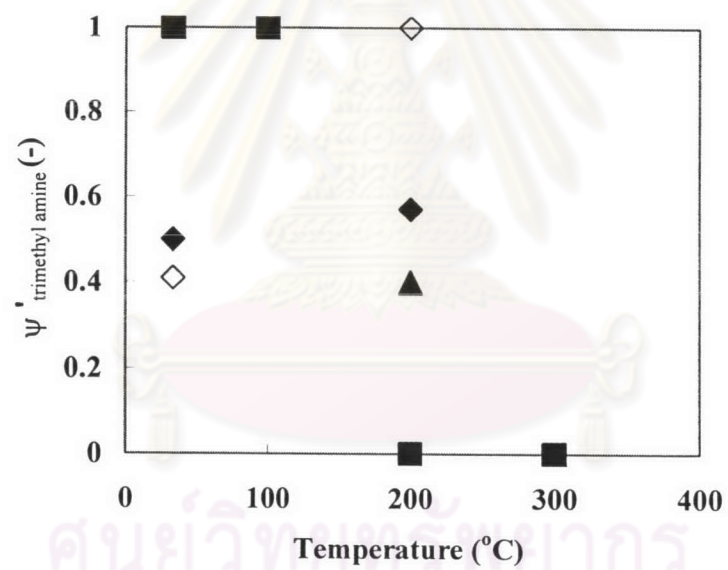

(b)

Figure 5.56 Effect of coexisting H_2O-CO_2 on the simultaneous removal of CH_3CHO and $(CH_3)_3N$ from N_2; $C_{in,\ acetaldehyde}$=150ppm, $C_{in,trimethylamine}$=100ppm, I=0.3mA, SV=55.8 hr^{-1} at room temperature :

- ◆ CO_2 (10%) - H_2O (5250ppm),
- ◇ CO_2 (20%) - H_2O (5250ppm),
- ■ CO_2 (10%) - H_2O (10500ppm),
- □ CO_2 (20%) - H_2O (10500ppm),
- ▲ CO_2 (10%) - H_2O (21800ppm),
- △ CO_2 (20%) - H_2O (21800ppm)

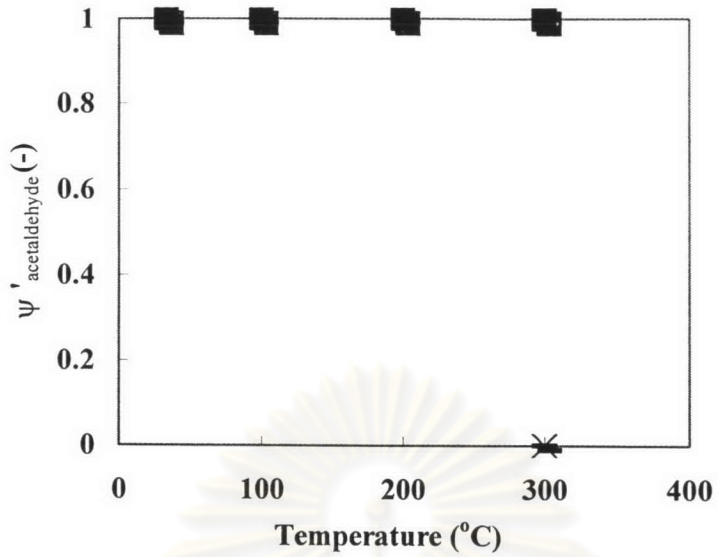

(a)

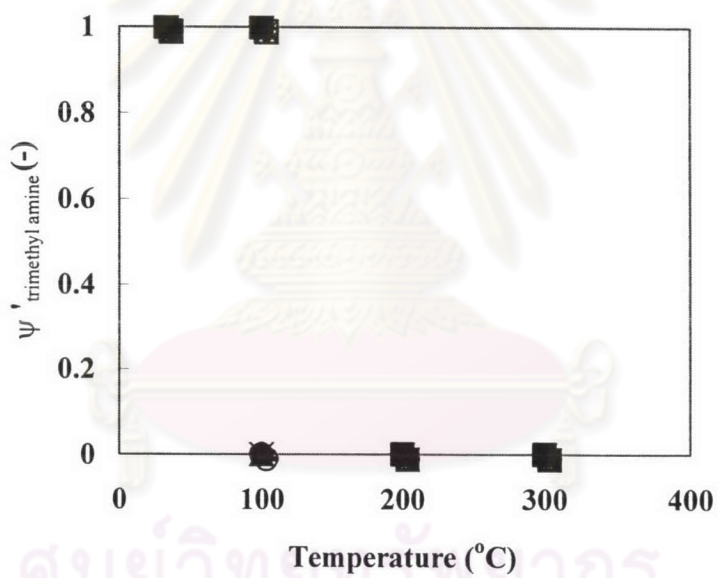

(b)

Figure 5.57 Effect of coexisting O_2-H_2O-CO_2 on the simultaneous removal of CH_3CHO and $(CH_3)_3N$ from N_2; $C_{in,\ acetaldehyde}$=150ppm, $C_{in,trimethylamine}$=100ppm, I=0.3mA, SV=55.8 hr^{-1} at room temperature :

◆ CO_2 (10%)-O_2 (10%)-H_2O (5250ppm), ◇ CO_2 (20%)-O_2 (10%)-H_2O (5250ppm),
▲ CO_2 (10%)-O_2 (20%)-H_2O (5250ppm), △ CO_2 (20%)-O_2 (20%)-H_2O (5250ppm),
■ CO_2 (10%)-O_2 (10%)-H_2O (10500ppm), □ CO_2 (20%)-O_2 (10%)-H_2O (10500ppm),
● CO_2 (10%)-O_2 (20%)-H_2O (10500ppm), ○ CO_2 (20%)-O_2 (20%)-H_2O (10500ppm),
* CO_2 (10%)-O_2 (10%)-H_2O (21800ppm), × CO_2 (20%)-O_2 (10%)-H_2O (21800ppm),
+ CO_2 (10%)-O_2 (20%)-H_2O (21800ppm), ━ CO_2 (20%)-O_2 (20%)-H_2O (21800ppm)

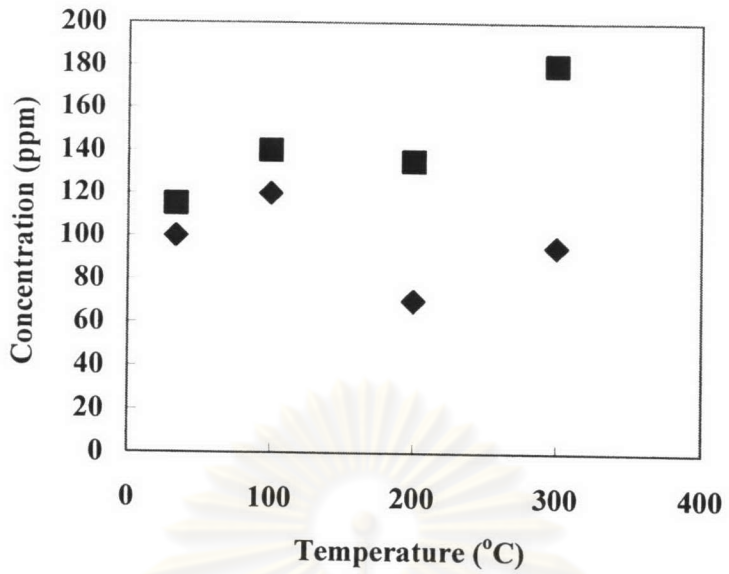

Figure 5.58 Byproduct (CO) on the simultaneous removal of CH_3CHO and $(CH_3)_3N$ from N_2-CO_2:
◆ CO_2 (10%), ■ CO_2 (20%)

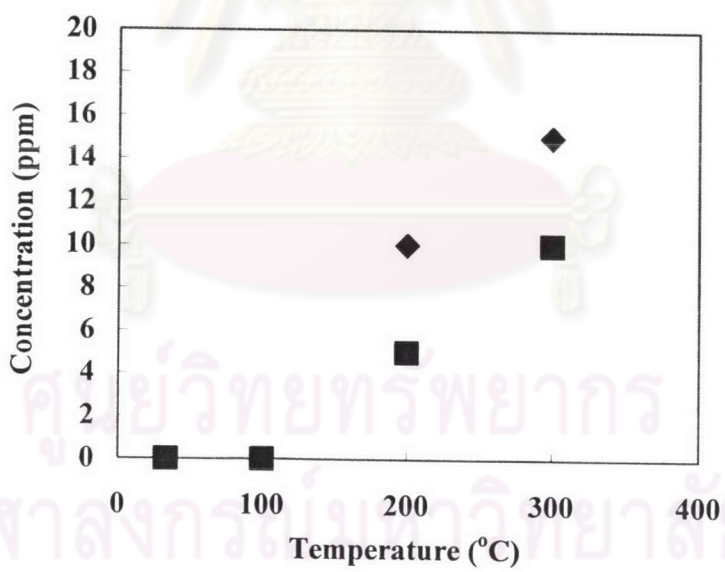

Figure 5.59 Byproduct (NO_x) on the simultaneous removal of CH_3CHO and $(CH_3)_3N$ from N_2-CO_2:
◆ CO_2 (10%), ■ CO_2 (20%)

ศูนย์วิทยทรัพยากร
จุฬาลงกรณ์มหาวิทยาลัย

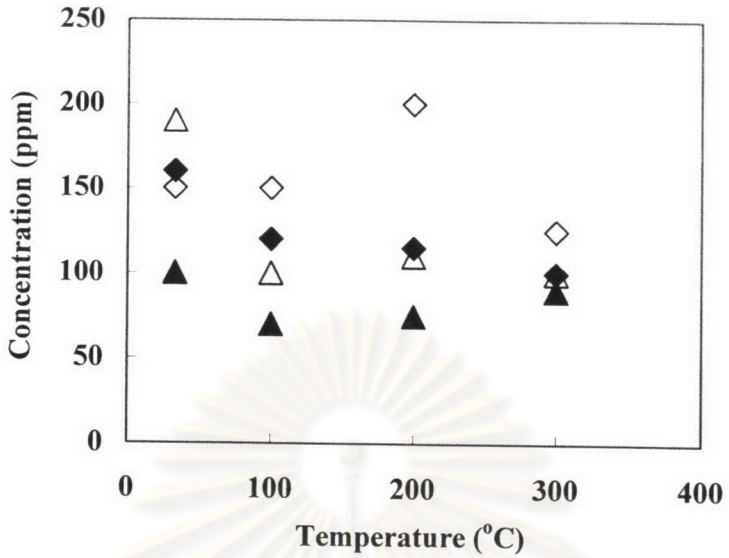

Figure 5.60 Byproduct (CO) on the simultaneous removal of CH_3CHO and $(CH_3)_3N$ from N_2-O_2-CO_2:
◆ CO_2 (10%) - O_2 (10%),
◇ CO_2 (20%) - O_2 (10%),
▲ CO_2 (10%) - O_2 (20%),
△ CO_2 (20%) - O_2 (20%)

ศูนย์วิทยทรัพยากร
จุฬาลงกรณ์มหาวิทยาลัย

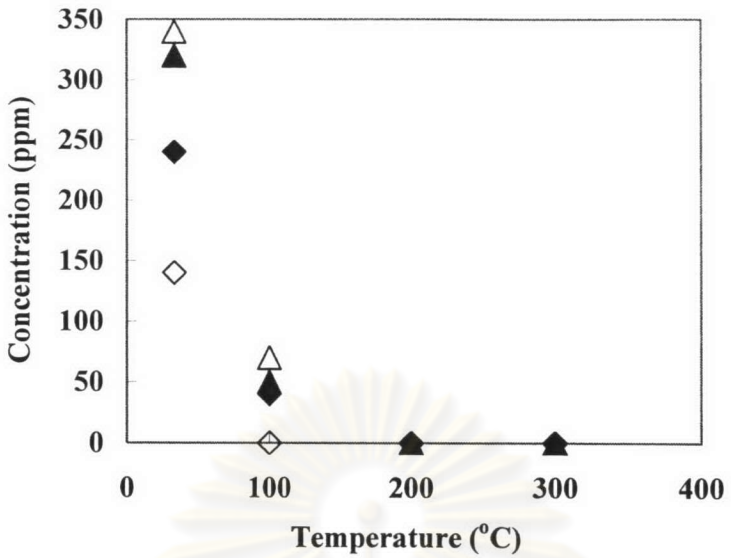

Figure 5.61 Byproduct (O_3) on the simultaneous removal of CH_3CHO and $(CH_3)_3N$ from N_2-O_2-CO_2:
◆ CO_2 (10%) - O_2 (10%),
◇ CO_2 (20%) - O_2 (10%),
▲ CO_2 (10%) - O_2 (20%),
△ CO_2 (20%) - O_2 (20%)

ศูนย์วิทยทรัพยากร
จุฬาลงกรณ์มหาวิทยาลัย

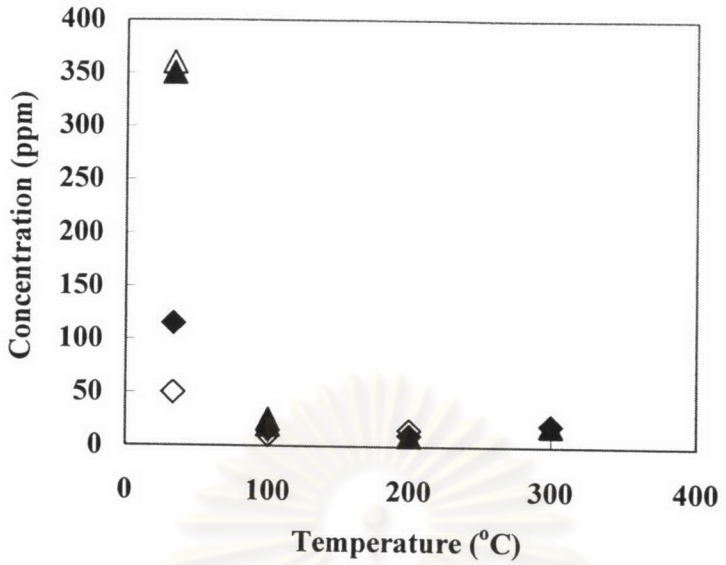

Figure 5.62 Byproduct (NO_x) on the simultaneous removal of CH_3CHO and $(CH_3)_3N$ from N_2-O_2-CO_2:
◆ CO_2 (10%) - O_2 (10%),
◇ CO_2 (20%) - O_2 (10%),
▲ CO_2 (10%) - O_2 (20%),
△ CO_2 (20%) - O_2 (20%)

ศูนย์วิทยทรัพยากร
จุฬาลงกรณ์มหาวิทยาลัย

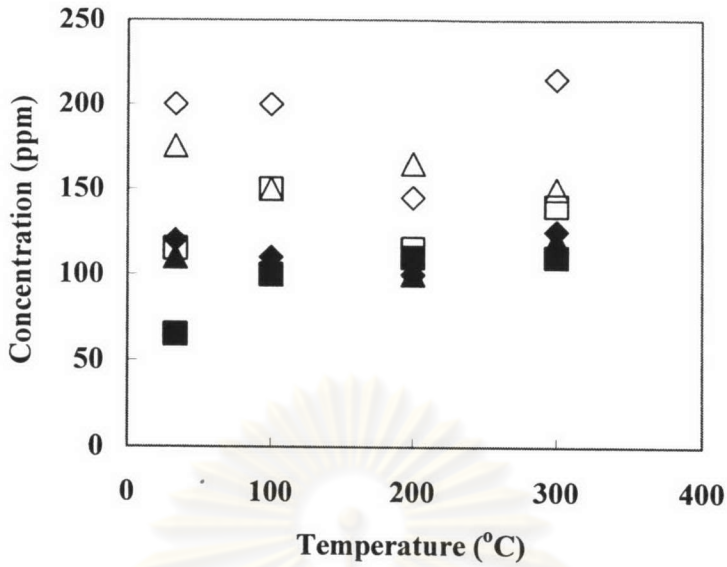

Figure 5.63 Byproduct (CO) on the simultaneous removal of CH_3CHO and $(CH_3)_3N$ from N_2-H_2O-CO_2:
◆ CO_2 (10%) - H_2O (5250ppm),
◇ CO_2 (20%) - H_2O (5250ppm),
▲ CO_2 (10%) - H_2O (10500ppm),
△ CO_2 (20%) - H_2O (10500ppm),
■ CO_2 (10%) - H_2O (21800ppm),
□ CO_2 (20%) - H_2O (21800ppm)

ศูนย์วิทยทรัพยากร
จุฬาลงกรณ์มหาวิทยาลัย

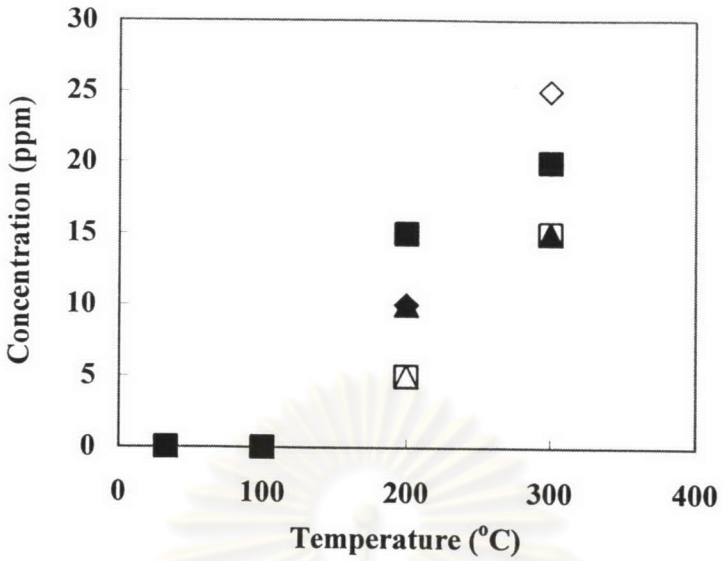

Figure 5.64 Byproduct (NO_x) on the simultaneous removal of CH_3CHO and $(CH_3)_3N$ from N_2-H_2O-CO_2:
◆ CO_2 (10%) - H_2O (5250ppm),
◇ CO_2 (20%) - H_2O (5250ppm),
▲ CO_2 (10%) - H_2O (10500ppm),
△ CO_2 (20%) - H_2O (10500ppm),
■ CO_2 (10%) - H_2O (21800ppm),
□ CO_2 (20%) - H_2O (21800ppm)

ศูนย์วิทยทรัพยากร
จุฬาลงกรณ์มหาวิทยาลัย

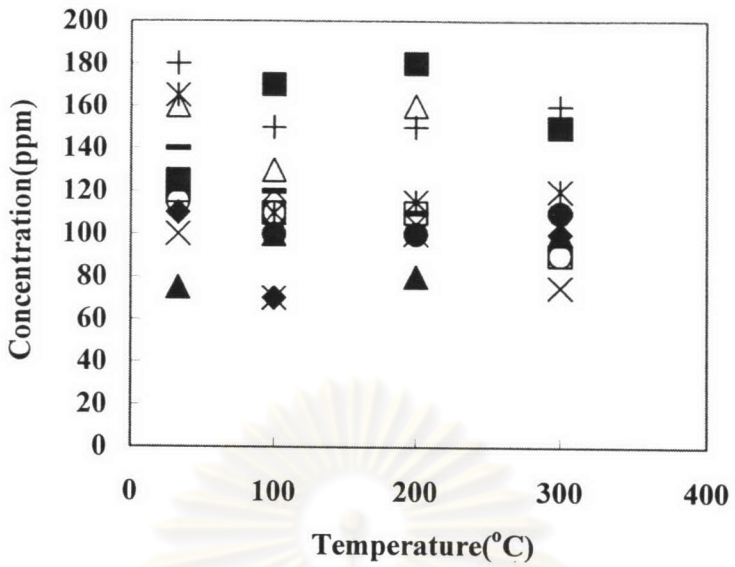

Figure 5.65 Byproduct (CO) on the simultaneous removal of CH_3CHO and $(CH_3)_3N$ from N_2-O_2-H_2O-CO_2:
◆ CO_2 (10%) - O_2 (10%) - H_2O (5250ppm),
◇ CO_2 (20%) - O_2 (10%) - H_2O (5250ppm),
▲ CO_2 (10%) - O_2 (20%) - H_2O (5250ppm),
△ CO_2 (20%) - O_2 (20%) - H_2O (5250ppm),
■ CO_2 (10%) - O_2 (10%) - H_2O (10500ppm),
□ CO_2 (20%) - O_2 (10%) - H_2O (10500ppm),
● CO_2 (10%) - O_2 (20%) - H_2O (10500ppm),
○ CO_2 (20%) - O_2 (20%) - H_2O (10500ppm),
* CO_2 (10%) - O_2 (10%) - H_2O (21800ppm),
× CO_2 (20%) - O_2 (10%) - H_2O (21800ppm),
+ CO_2 (10%) - O_2 (20%) - H_2O (21800ppm),
– CO_2 (20%) - O_2 (20%) - H_2O (21800ppm)

ศูนย์วิทยทรัพยากร
จุฬาลงกรณ์มหาวิทยาลัย

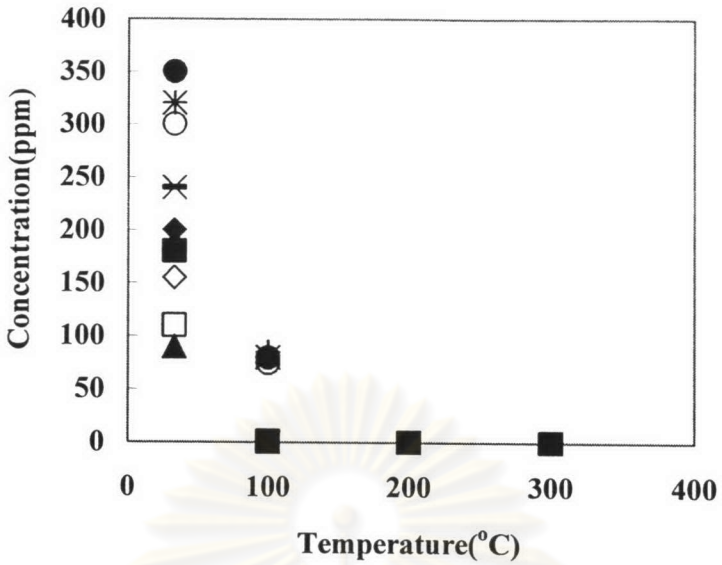

Figure 5.66 Byproduct (O_3) on the simultaneous removal of CH_3CHO and $(CH_3)_3N$ from N_2-O_2-H_2O-CO_2:
◆ CO_2 (10%) - O_2 (10%) - H_2O (5250ppm),
◇ CO_2 (20%) - O_2 (10%) - H_2O (5250ppm),
▲ CO_2 (10%) - O_2 (20%) - H_2O (5250ppm),
△ CO_2 (20%) - O_2 (20%) - H_2O (5250ppm),
■ CO_2 (10%) - O_2 (10%) - H_2O (10500ppm),
□ CO_2 (20%) - O_2 (10%) - H_2O (10500ppm),
● CO_2 (10%) - O_2 (20%) - H_2O (10500ppm),
○ CO_2 (20%) - O_2 (20%) - H_2O (10500ppm),
* CO_2 (10%) - O_2 (10%) - H_2O (21800ppm),
× CO_2 (20%) - O_2 (10%) - H_2O (21800ppm),
+ CO_2 (10%) - O_2 (20%) - H_2O (21800ppm),
— CO_2 (20%) - O_2 (20%) - H_2O (21800ppm)

ศูนย์วิทยทรัพยากร
จุฬาลงกรณ์มหาวิทยาลัย

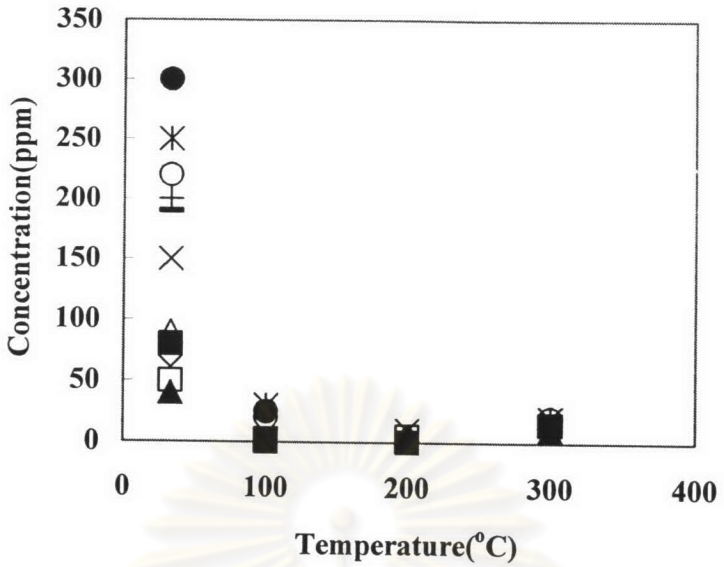

Figure 5.67 Byproduct (NO_x) on the simultaneous removal of CH_3CHO and $(CH_3)_3N$ from N_2-O_2-H_2O-CO_2:
- ◆ CO_2 (10%) - O_2 (10%) - H_2O (5250ppm),
- ◇ CO_2 (20%) - O_2 (10%) - H_2O (5250ppm),
- ▲ CO_2 (10%) - O_2 (20%) - H_2O (5250ppm),
- △ CO_2 (20%) - O_2 (20%) - H_2O (5250ppm),
- ■ CO_2 (10%) - O_2 (10%) - H_2O (10500ppm),
- □ CO_2 (20%) - O_2 (10%) - H_2O (10500ppm),
- ● CO_2 (10%) - O_2 (20%) - H_2O (10500ppm),
- ○ CO_2 (20%) - O_2 (20%) - H_2O (10500ppm),
- * CO_2 (10%) - O_2 (10%) - H_2O (21800ppm),
- × CO_2 (20%) - O_2 (10%) - H_2O (21800ppm),
- + CO_2 (10%) - O_2 (20%) - H_2O (21800ppm),
- − CO_2 (20%) - O_2 (20%) - H_2O (21800ppm)

ศูนย์วิทยทรัพยากร
จุฬาลงกรณ์มหาวิทยาลัย

5.10 Simultaneous removal of ammonia and trimethyl amine

5.10.1 Effect of temperature and coexisting CO_2 on the simultaneous removal of NH_3 and $(CH_3)_3N$ from N_2

Figure 5.68 shows the effect of CO_2 on the simultaneous removal efficiency of NH_3 and $(CH_3)_3N$ from N_2. The inlet concentrations of NH_3 and $(CH_3)_3N$ are 1,000 ppm and 100 ppm, respectively, while the discharge current is 0.3 mA. It is found that the presence of CO_2 has a significant effect on the simultaneous NH_3 removal efficiency ψ' in **Figure 5.68(a)**, as the temperature increases, the NH_3 removal efficiency ψ' decreases from room temperature up to 200°C, then the tendency reverses up to 300°C because this condition, the synthesis occurs of NH_3 again and the mean residence time of the gas mixture inside the reactor decreases as the reactor temperature rises. In **Figure 5.68(b)**, as the temperature increases, the $(CH_3)_3N$ removal efficiency ψ' at 100% from room temperature to 200°C, at 300°C equal to 100% even in blank tests without corona discharge. Obviously, the presence of CO_2 positively affect the removal efficiency $(CH_3)_3N$.

5.10.2 Effect of temperature and coexisting CO_2 and O_2on the simultaneous removal of NH_3 and $(CH_3)_3N$ from N_2

Figure 5.69 shows the effect of CO_2 and O_2 on the simultaneous removal efficiency of NH_3 and $(CH_3)_3N$ from N_2. The inlet concentrations of NH_3 and $(CH_3)_3N$ are 1,000 ppm and 100 ppm, respectively, while the current is 0.3 mA. It is found that the presence of CO_2 has a significant enhancement effect on the simultaneous NH_3 removal efficiency ψ' in **Figure 5.69(a),** as the temperature increases, the NH_3 removal efficiency ψ' remains equal 100% from room temperature to 300°C because effect of O_3, CO_3^- and O^- anion at low temperatures and various radicals at high temperatures. In **Figure 5.69(b)**, as the temperature increases, the $(CH_3)_3N$ removal efficiency ψ' at 100% from room temperature to 200°C and some case, from 200°C to 300°C equal to 100% even in blank tests

without corona discharge. Obviously, the presences of O_2 positively affect the removal efficiency.

5.10.3 Effect of temperature and coexisting CO_2 and H_2O on the simultaneous removal of NH_3 and $(CH_3)_3N$ from N_2

Figure 5.70 shows the effect of CO_2 and H_2O on the simultaneous removal efficiency of NH_3 and $(CH_3)_3N$ from N_2. The inlet concentrations of NH_3 and $(CH_3)_3N$ are 1,000 ppm and 100 ppm, respectively, while the current is 0.3 mA. It is found that the presence of CO_2 has a significant effect on the simultaneous NH_3 removal efficiency ψ' in **Figure 5.70(a),** as the temperature increases, the NH_3 removal efficiency ψ' increases because effect of H^-, OH^-, CO_3^- and O^- anion at low temperatures and at high temperatures, N radicals are consumed by their reaction with CO_2 and H_2O. As the mentioned previously, this condition, the synthesis occurs of NH_3 again. In **Figure 5.70 (b)**, as the temperature increases, the $(CH_3)_3N$ removal efficiency ψ' at 100% from room temperature to 200°C, at 300°C equal to 100% even in blank tests without corona discharge. Obviously, the presence of H_2O positively affects the removal efficiency.

5.10.4 Effect of temperature and coexisting CO_2, O_2 and H_2O on the simultaneous removal of NH_3 and $(CH_3)_3N$ from N_2

Figure 5.71 shows the effect of CO_2, O_2 and H_2O on the simultaneous removal efficiency of NH_3 and $(CH_3)_3N$ from N_2. The inlet concentration of NH_3 and $(CH_3)_3N$ are 1,000 ppm and 100 ppm, respectively, while the current is 0.3 mA. It is found that the presence of CO_2 has a significant enhancement effect on the simultaneous NH_3 removal efficiency ψ' in **Figure 5.71(a),** as the temperature increases, the NH_3 removal efficiency ψ' remains equal 100% from room temperature to 300°C because effect of O_3, CO_3^-, H^-, OH^- and O^- anion at low temperatures and various radicals at high temperatures. In **Figure 5.71(b)**, as

temperature increases, the $(CH_3)_3N$ removal efficiency ψ' at 100% from room temperature to 200°C, at 300°C equal to 100% even in blank tests without corona discharge. Obviously, the presences of O_2 and H_2O positively affect the removal efficiency.

5.10.5 Byproducts from the simultaneous removal of acetaldehyde and ammonia

Figure 5.72 shows the concentration of byproduct CO versus temperature. In **Figure 5.72** as the temperature increases, the byproduct CO increases from room temperature to 100°C, above which the tendency reverses up to 300°C as the mentioned previously, it is known that production of CO by dissociative attachment reaction.

Figure 5.73 shows the concentration of byproduct O_3 versus temperature. In **Figure 5.73** as the temperature increases, the byproduct O_3 decreases. This is because O_3 is unstable at high temperatures.

Figure 5.74 shows the concentration of byproduct NO_x versus temperature. In **Figure 5.74** as the temperature increases, the byproduct NO_x decreases from room temperature up 200°C, then the tendency reverses up to 300°C.

ศูนย์วิทยทรัพยากร
จุฬาลงกรณ์มหาวิทยาลัย

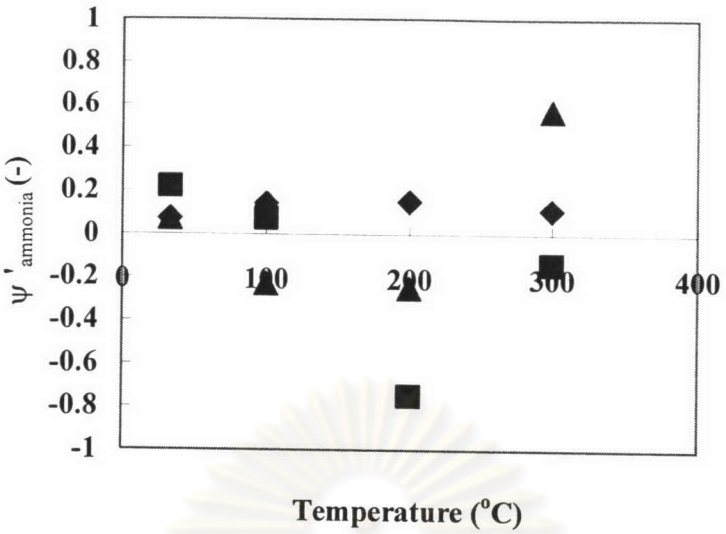

(a)

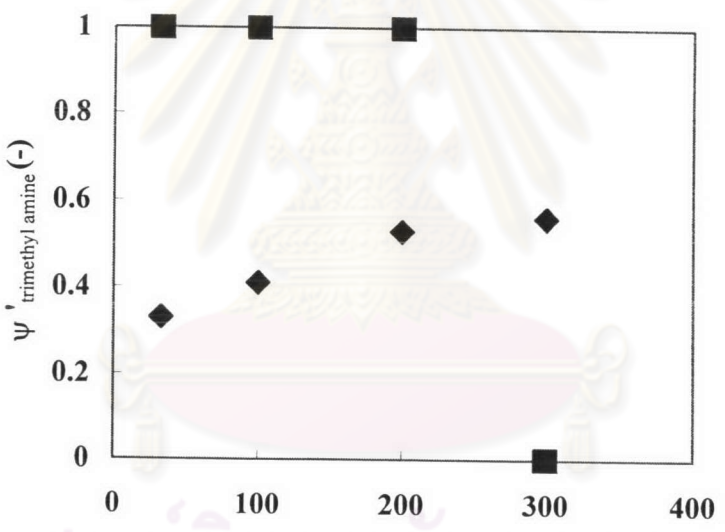

(b)

Figure 5.68 Effect of coexisting CO_2 on the simultaneous removal of NH_3 and $(CH_3)_3N$ from N_2; $C_{in,ammonia}$=1000ppm, $C_{in,trimethylamine}$=100ppm, I=0.3mA, SV=55.8 hr^{-1} at room temperature :

◆ CO_2 (0%), ■ CO_2 (10%), ▲ CO_2 (20%)

ศูนย์วิทยทรัพยากร
จุฬาลงกรณ์มหาวิทยาลัย

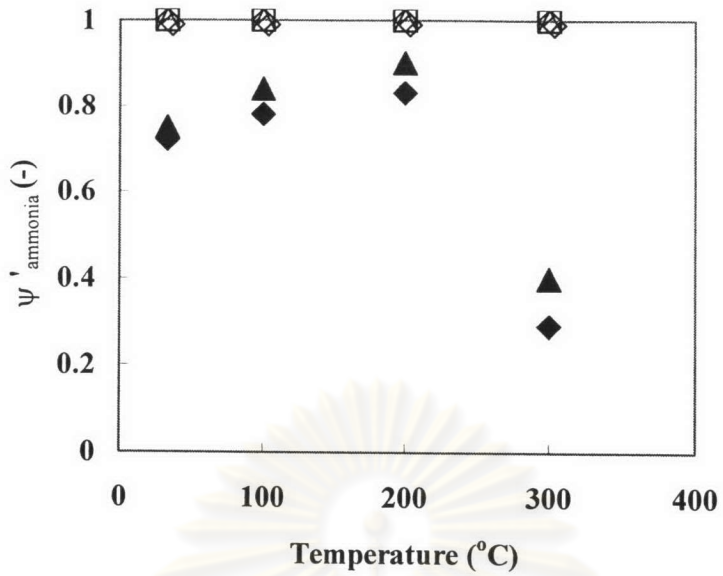

(a)

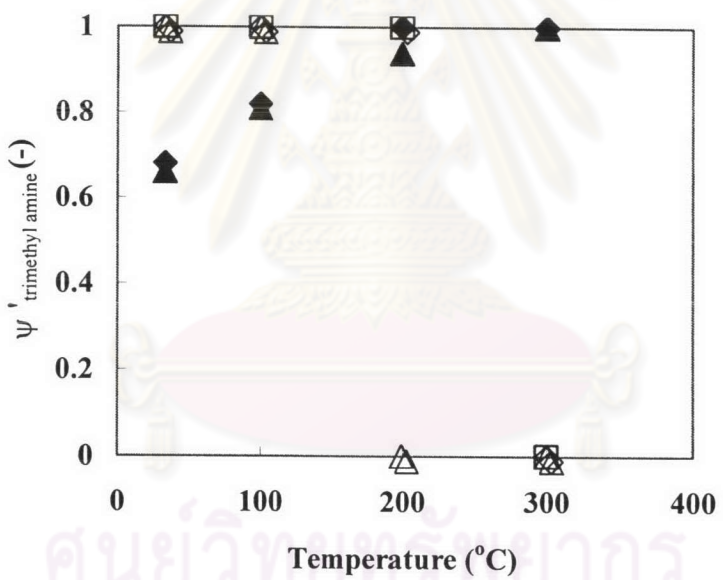

(b)

Figure 5.69 Effect of coexisting O_2-CO_2 on the simultaneous removal of NH_3 and $(CH_3)_3N$ from N_2; $C_{in,ammonia}$=1000ppm, $C_{in,trimethylamine}$=100ppm, I=0.3mA, SV=55.8 hr^{-1} at room temperature :

- ◆ CO_2 (0%)-O_2 (10%),
- ◇ CO_2 (10%)-O_2 (10%),
- □ CO_2 (20%)-O_2 (10%),
- ▲ CO_2 (0%)-O_2 (20%),
- △ CO_2 (10%)-O_2 (20%)

ศูนย์วิทยทรัพยากร
จุฬาลงกรณ์มหาวิทยาลัย

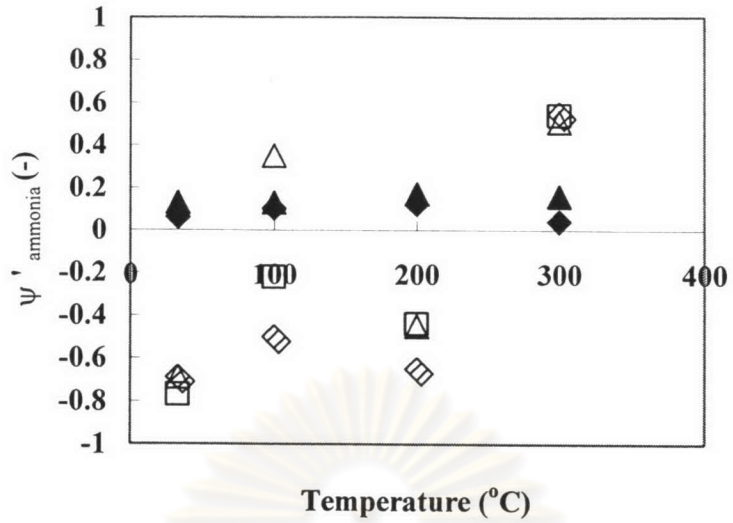

(a)

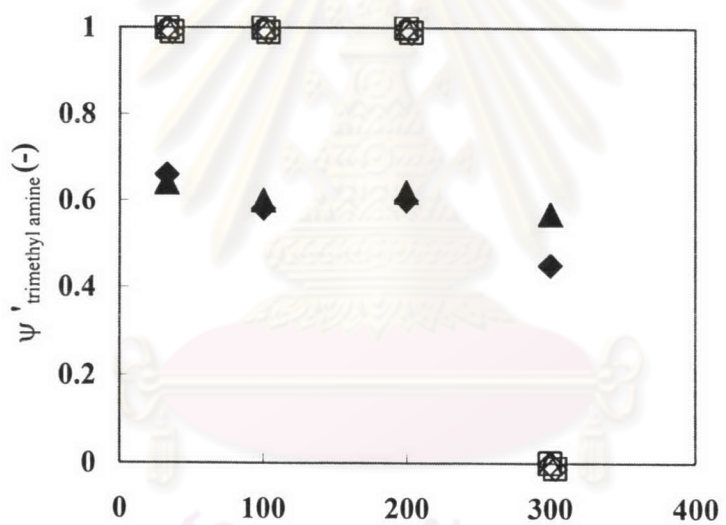

(b)

Figure 5.70 Effect of coexisting H_2O-CO_2 on the simultaneous removal of NH_3 and $(CH_3)_3N$ from N_2; $C_{in,ammonia}$=1000ppm, $C_{in,trimethylamine}$=100ppm, I=0.3mA, SV=55.8 hr^{-1} at room temperature :

- ◆ CO_2 (0%)-H_2O (5250ppm),
- ◇ CO_2 (10%)-H_2O (5250ppm),
- □ CO_2 (20%)-H_2O (5250ppm),
- ▲ CO_2 (0%)-H_2O (10500ppm),
- △ CO_2 (10%)-H_2O (10500ppm)

ศูนย์วิทยทรัพยากร
จุฬาลงกรณ์มหาวิทยาลัย

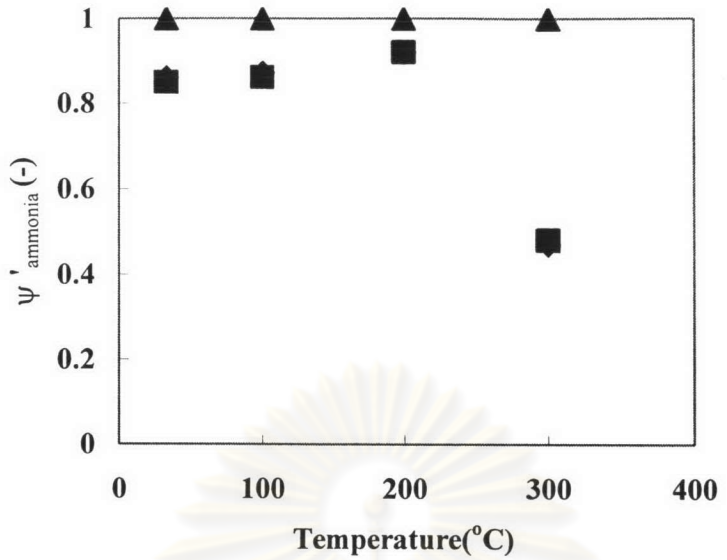

(a)

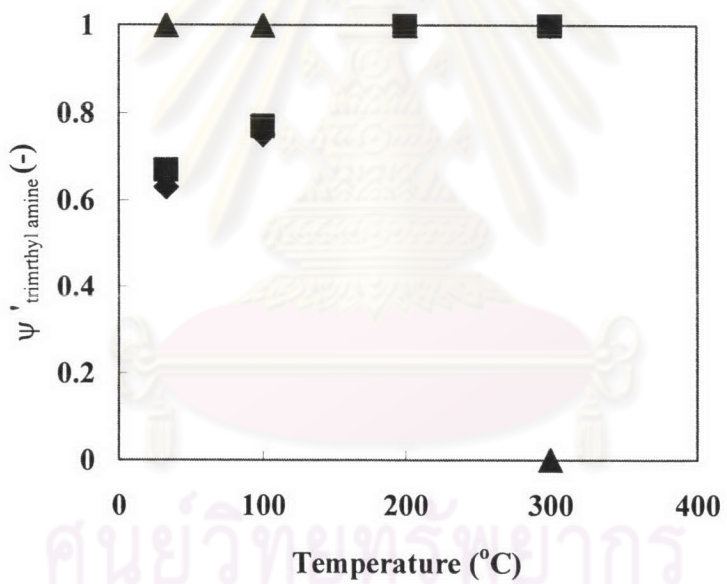

(b)

Figure 5.71 Effect of coexisting O_2-H_2O-CO_2 on the simultaneous removal of NH_3 and $(CH_3)_3N$ from N_2; $C_{in,ammonia}$=1000ppm, $C_{in,trimethylamine}$=100ppm, I=0.3mA, SV=55.8 hr^{-1} at room temperature :
◆ CO_2 (0%)-O_2 (10%)-H_2O (5250ppm),
■ CO_2 (0%)-O_2 (10%)-H_2O (10500ppm),
▲ CO_2 (10%)-O_2 (10%)-H_2O (5250ppm)

ศูนย์วิทยทรัพยากร
จุฬาลงกรณ์มหาวิทยาลัย

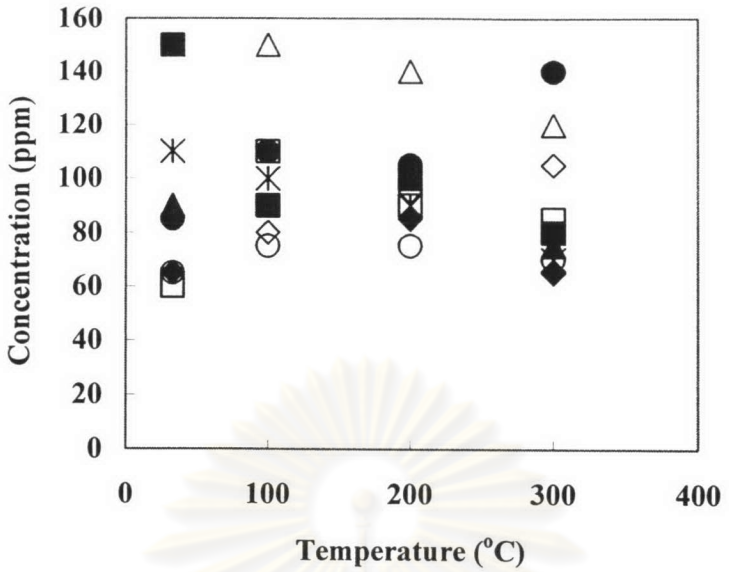

Figure 5.72 Byproduct (CO) on simultaneous removal of NH_3 and $(CH_3)_3N$:

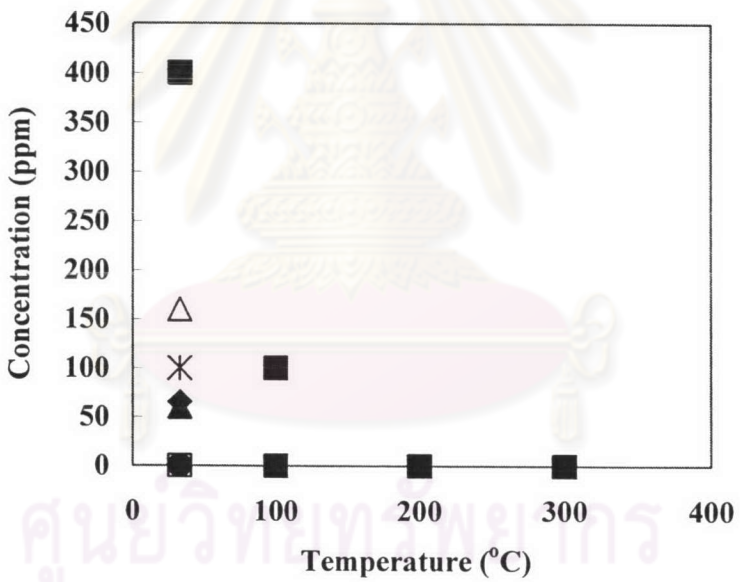

Figure 5.73 Byproduct (O_3) on simultaneous removal of NH_3 and $(CH_3)_3N$:

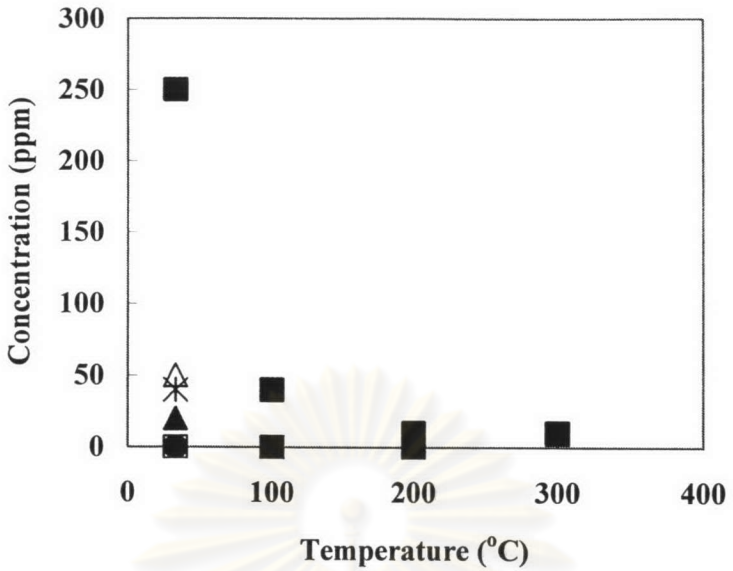

Figure 5.74 Byproduct (NO_x) on simultaneous removal of NH_3 and $(CH_3)_3N$:

ศูนย์วิทยทรัพยากร
จุฬาลงกรณ์มหาวิทยาลัย

5.11 Simultaneous removal of acetaldehyde, ammonia and trimethylamine

5.11.1 Effect of temperature and coexisting CO_2 on the simultaneous removal of CH_3CHO, NH_3 and $(CH_3)_3N$ from N_2

Figure 5.75 shows the effect of CO_2 on the simultaneous removal efficiency of CH_3CHO, NH_3 and $(CH_3)_3N$ from N_2. The inlet concentrations of CH_3CHO, NH_3 and $(CH_3)_3N$ are 150 ppm, 1,000 ppm and 100 ppm, respectively, while the current is 0.3 mA. In **Figure 5.75(a),** as the temperature increases, the CH_3CHO removal efficiency ψ' decreases from room temperature to 300°C. As mentioned previously, this condition, the synthesis occurs of NH_3 again and at high temperature, CO_2 is unstable. In **Figure 5.75(b),** as the temperature increases, the NH_3 removal efficiency ψ' decreases from room temperature up to 200°C, then the tendency reverses up to 300°C because the mean residence time of the gas mixture inside the reactor decreases as the reactor temperature rises. In **Figure 5.75(c),** as the temperature increases, the $(CH_3)_3N$ removal efficiency ψ' remains equal 100% from room temperature to 300°C. As mentioned previously, the presence of CO_2 does significantly enhancement effect the removal efficiency of CH_3CHO and $(CH_3)_3N$ and sinificantly retard removal efficiency of NH_3.

5.11.2 Effect of temperature and coexisting CO_2 and O_2 on the simultaneous removal of CH_3CHO, NH_3 and $(CH_3)_3N$ from N_2

Figure 5.76 shows the effect of CO_2 and O_2 on the simultaneous removal efficiency of CH_3CHO, NH_3 and $(CH_3)_3N$ from N_2. The inlet concentrations of CH_3CHO, NH_3 and $(CH_3)_3N$ are 150 ppm, 1,000 ppm and 100 ppm, respectively, while the current is 0.3 mA. In **Figure 5.76(a),** as the temperature increases, the CH_3CHO removal efficiency ψ' remains equal 100% from room temperature to 200°C, and decreases at 300°C because at high temperature, O_3 and CO_2 are unstable. In **Figure 5.76(b),** in case, no coexisting gas CO_2, as the temperature increases, the NH_3 removal efficiency ψ' increases from room temperature up to 200 °C, above which the NH_3 removal efficiency tends to significantly decrease

because of less O_3 generated from O_2 and in case of the presence coexisting gas CO_2, as the temperature increases, the NH_3 removal efficiency ψ' remains equal 100% from room temperature to 200°C, and decreases at 300°C because at high temperature, O_3 and CO_2 are unstable. In **Figure 5.76(c),** as the temperature increases, the $(CH_3)_3N$ removal efficiency ψ' remains equal 100% from room temperature to 300°C because effect of O_3, CO_3^- and O^- anion at low temperatures and various radicals at high temperatures. Obviously, the presence of CO_2 positively affect the removal efficiency CH_3CHO, NH_3 and $(CH_3)_3N$.

5.11.3 Effect of temperature and coexisting CO_2 and H_2O on the simultaneous removal of CH_3CHO, NH_3 and $(CH_3)_3N$ from N_2

Figure 5.77 shows the effect of CO_2 and H_2O on the simultaneous removal efficiency of CH_3CHO, NH_3 and $(CH_3)_3N$ from N_2. The inlet concentrations of CH_3CHO, NH_3 and $(CH_3)_3N$ are 150 ppm, 1,000 ppm and 100 ppm, respectively, while the current is 0.3 mA. In **Figure 5.77(a)**, in case, no coexisting gas CO_2, as the temperature increases, the CH_3CHO removal efficiency ψ' increases from room temperature up to 300°C and in case of the presence coexisting gas CO_2, as the temperature increases, the CH_3CHO removal efficiency ψ' decreases from room temperature up to 300°C because at high temperatures, CO_2 and H_2O are unstable. In **Figure 5.77(b)**, in case, no coexisting gas CO_2, as the temperature increases, the NH_3 removal efficiency ψ' increases from room temperature up to 200°C, above which the NH_3 removal efficiency tends to significantly decrease and in case of the presence coexisting gas CO_2, as temperature increases, the NH_3 removal efficiency ψ' decreases from room temperature up to 200°C, and then the tendency reverses up to 300°C. As mentioned previously, this condition, the synthesis occurs of NH_3 again. H^-, OH^-, CO_3^- and O^- anions should contribute to the removal of CH_3CHO at low temperatures. At 200°C, the presence of H_2O and CO_2 slightly retards the removal efficiency of CH_3CHO because at low discharge current, the relatively much smaller number of electrons tends to attach mostly to H_2O and CO_2. In addition, N radicals are consumed by their reaction with CO_2 and H_2O at high

temperatures In **Figure 5.77(c),** as the temperature increases, the $(CH_3)_3N$ removal efficiency ψ' remains equal 100% from room temperature to 300°C because at low to moderate temperatures, H^-, OH^-, CO_3^- and O^- anions are expected to be produced by dissociate electron attachment to CO_2 and H_2O molecules at low temperatures (Massay 1976, Moruzzi and Phelps 1996). At 200°C or more, electron detachment would become significant so that radicals of CO_3, O, H, and OH may play a more important role than their anionic counterparts. Obviously, the presence of CO_2 does significantly enhancement effect the removal efficiency of CH_3CHO and $(CH_3)_3N$ and significantly retard removal efficiency of NH_3.

5.11.4 Effect of temperature and coexisting CO_2, O_2 and H_2O on the simultaneous removal of CH_3CHO, NH_3 and $(CH_3)_3N$ from N_2

Figure 5.78 shows the effect of CO_2, O_2 and H_2O on the simultaneous removal efficiency of CH_3CHO, NH_3 and $(CH_3)_3N$ from N_2. The inlet concentrations of CH_3CHO, NH_3 and $(CH_3)_3N$ are 150 ppm, 1,000 ppm and 100 ppm, respectively, while the current is 0.3 mA. It is found that the presence of CO_2 has a significant enhancement effect on the simultaneous CH_3CHO, NH_3, and $(CH_3)_3N$ removal efficiency ψ' in **Figure 5.78,** as the temperature increases, the CH_3CHO, NH_3, and $(CH_3)_3N$ removal efficiency ψ' decreases from room temperature up to 300°C because of less O_3 generated from O_2, effect of H^-, OH^-, CO_3^- and O^- anions from H_2O and CO_2 are unstable and reduction of the mean residence time of the gas mixture inside the reactor at high temperatures.

ศูนย์วิทยทรัพยากร
จุฬาลงกรณ์มหาวิทยาลัย

5.11.5 Simultaneous removal of CH_3CHO, NH_3 and $(CH_3)_3N$ from N_2-O_2-H_2O-CO_2 using two reactors in series

The experiments for simultaneous removal of CH_3CHO, NH_3 and $(CH_3)_3N$ from N_2 - O_2 (10%) - H_2O (10,500 ppm) - CO_2 (10%) were studied using two reactors in series to decreases byproducts and / or increases the removal efficiency.

The first reactor, it was found that $(CH_3)_3N$ was removed completely, but the concentration of NH_3 still remained about 46 ppm and the concentration of CH_3CHO still remained about 12ppm using the single reactor at 300°C and 0.3 mA. Moreover, there were byproducts (CO 100 ppm and NO_x 10 ppm) occurred.

Then the second reactor was added in series with the first reactor in order to decrease byproducts and / or increase the removal efficiency. The experiments were divided into two cases. In the first case, at 100°C, CH_3CHO, NH_3 and $(CH_3)_3N$ were removed completely at 0.1 mA, however, CO, O_3 and NO_x increasesd, when, the current discharge increased. In the second case, At 200°C, CH_3CHO, NH_3 and $(CH_3)_3N$ were removed completely at 0.1 mA, however, CO increased when the current discharge increased, O_3 was non detected and NO_x was removed completely at 0.1 mA.

ศูนย์วิทยทรัพยากร
จุฬาลงกรณ์มหาวิทยาลัย

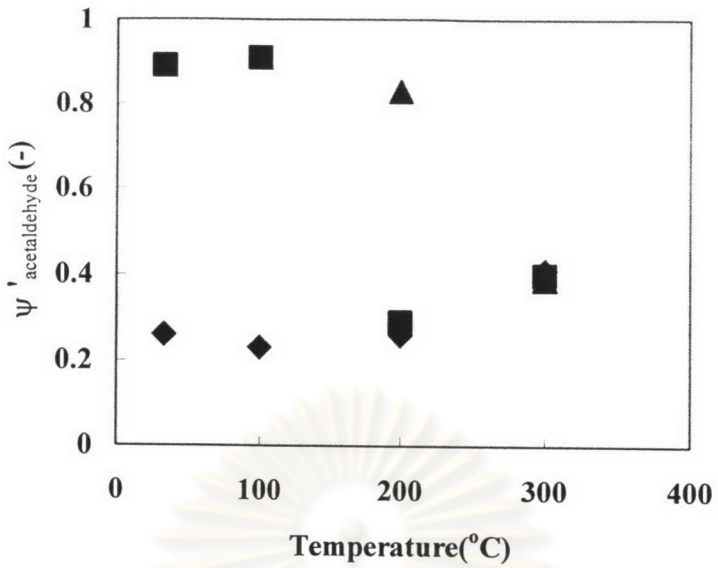

(a)

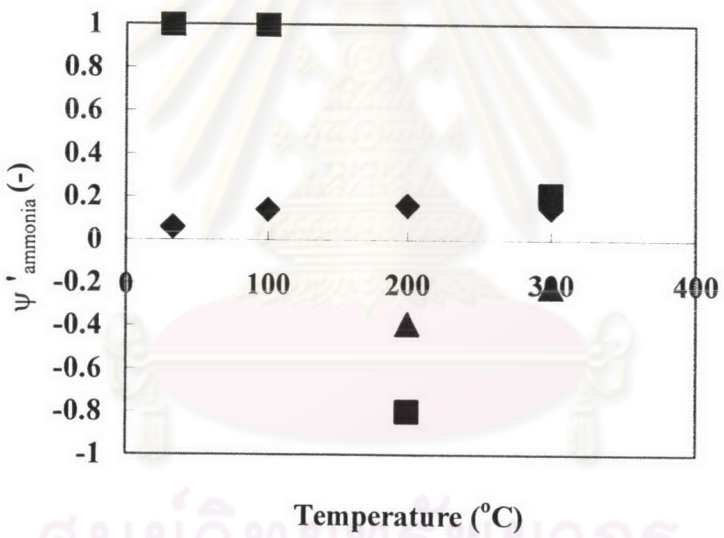

(b)

Figure 5.75 Effect of coexisting CO_2 on the simultaneous removal of CH_3CHO, NH_3 and $(CH_3)_3N$ from N_2; $C_{in,\ acetaldehyde}$=150ppm, $C_{in,ammonia}$=1000ppm, $C_{in,trimethylamine}$=100ppm I=0.3mA, SV=55.8 hr^{-1} at room temperature :

◆ CO_2 (0%), ■ CO_2 (10%), ▲ CO_2 (20%),

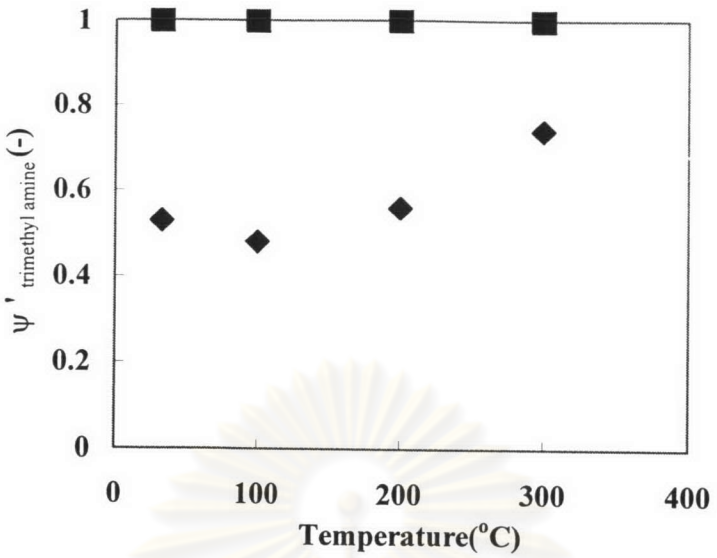

(C)

Figure 5.75 Effect of coexisting CO_2 on the simultaneous removal of CH_3CHO, NH_3 and $(CH_3)_3N$ from N_2; $C_{in,\ acetaldehyde}$=150ppm, $C_{in,ammonia}$=1000ppm, $C_{in,trimethylamine}$=100ppm I=0.3mA, SV=55.8 hr^{-1} at room temperature :

◆ CO_2 (0%), ■ CO_2 (10%), ▲ CO_2 (20%),

ศูนย์วิทยทรัพยากร
จุฬาลงกรณ์มหาวิทยาลัย

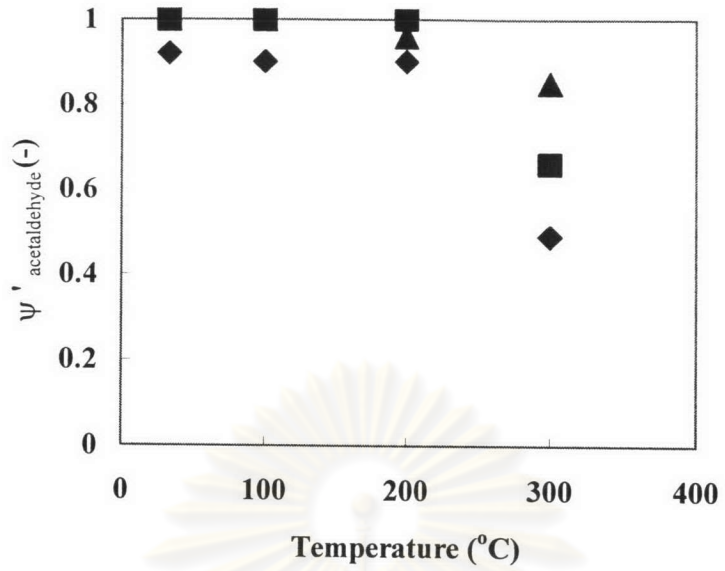

(a)

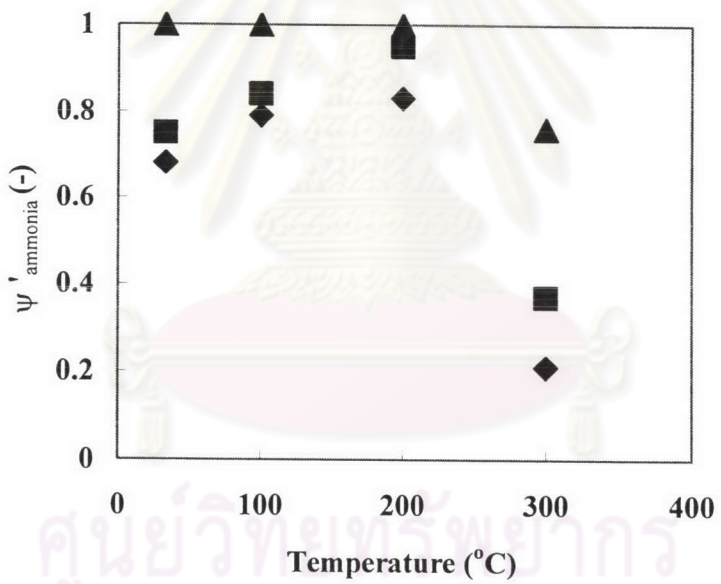

(b)

Figure 5.76 Effect of coexisting O_2-CO_2 on the simultaneous removal of CH_3CHO, NH_3 and $(CH_3)_3N$ from N_2; $C_{in,\ acetaldehyde}$=150ppm, $C_{in,ammonia}$=1000ppm, $C_{in,trimethylamine}$=100ppm I=0.3mA, SV=55.8 hr^{-1} at room temperature :

◆ CO_2 (0%)-O_2 (10%),
■ CO_2 (0%)-O_2 (20%),
▲ CO_2 (10%)-O_2 (10%)

ศูนย์วิทยทรัพยากร
จุฬาลงกรณ์มหาวิทยาลัย

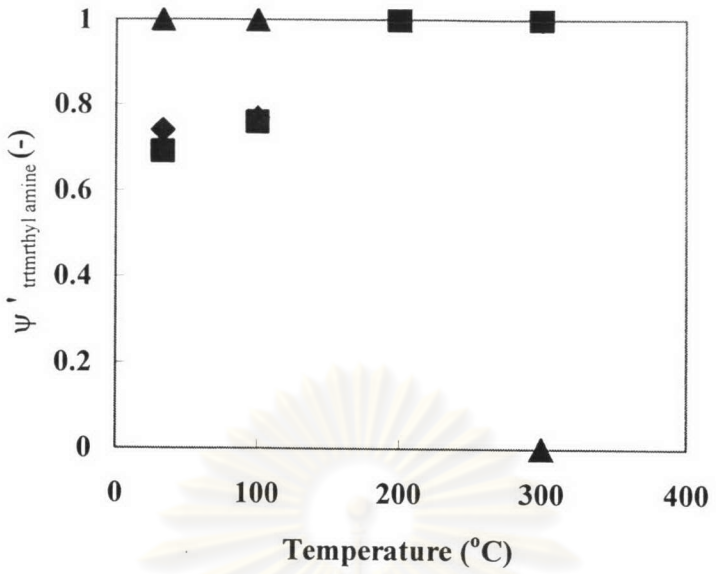

(c)

Figure 5.76 Effect of coexisting O_2-CO_2 on the simultaneous removal of CH_3CHO, NH_3 and $(CH_3)_3N$ from N_2; $C_{in,\ acetaldehyde}$=150ppm, $C_{in,ammonia}$=1000ppm, $C_{in,trimethylamine}$=100ppm I=0.3mA, SV=55.8 hr^{-1} at room temperature :

◆ CO_2 (0%)-O_2 (10%),
■ CO_2 (0%)-O_2 (20%),
▲ CO_2 (10%)-O_2 (10%)

ศูนย์วิทยทรัพยากร
จุฬาลงกรณ์มหาวิทยาลัย

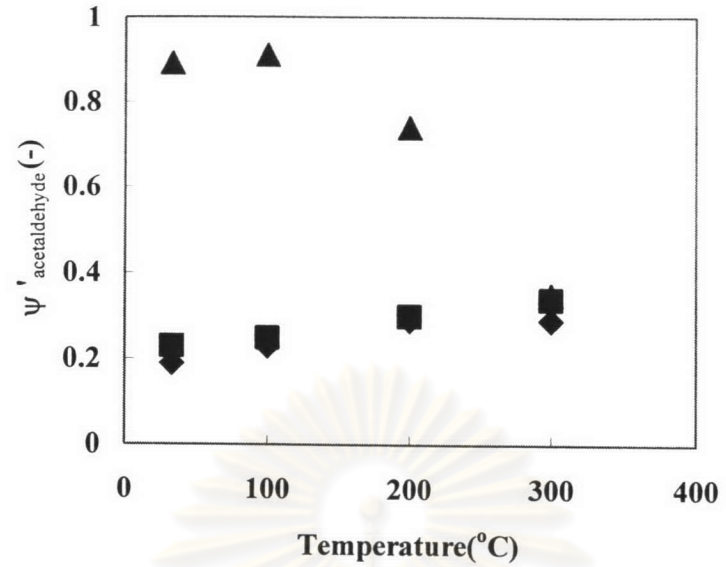

(a)

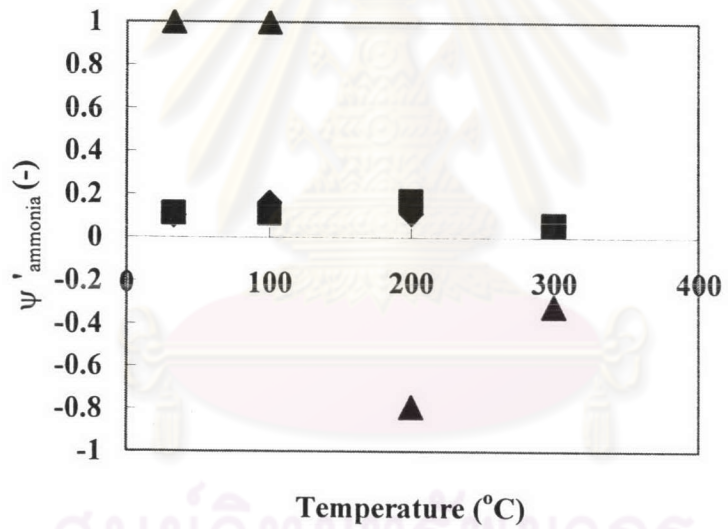

(b)

Figure 5.77 Effect of coexisting H_2O-CO_2 on the simultaneous removal of CH_3CHO,
NH_3 and $(CH_3)_3N$ from N_2; $C_{in,\ acetaldehyde}$=150ppm,
$C_{in,ammonia}$=1000ppm, $C_{in,trimethylamine}$=100ppm I=0.3mA, SV=55.8 hr^{-1}
at room temperature :
◆ CO_2 (0%)-H_2O (5250ppm),
■ CO_2 (0%)-H_2O (10500ppm),
▲ CO_2 (10%)-H_2O (5250ppm)

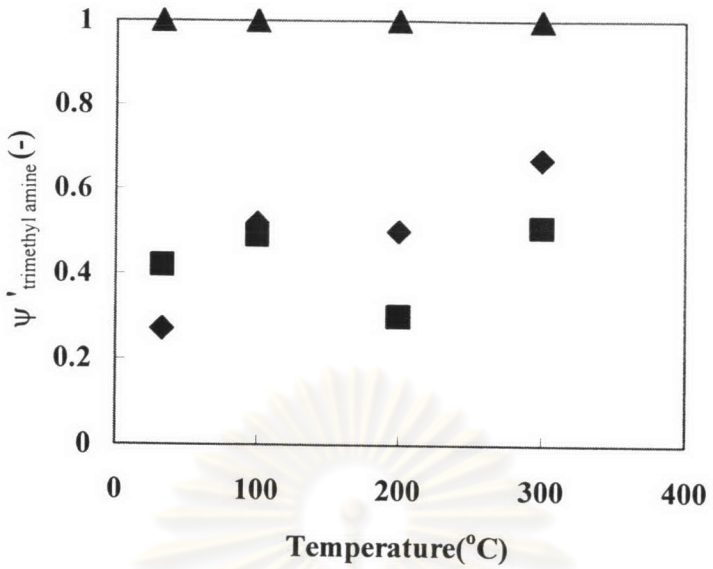

(c)

Figure 5.77 Effect of coexisting H_2O-CO_2 on the simultaneous removal of CH_3CHO,
NH_3 and $(CH_3)_3N$ from N_2; $C_{in,\ acetaldehyde}$=150ppm,
$C_{in,ammonia}$=1000ppm, $C_{in,trimethylamine}$=100ppm I=0.3mA, SV=55.8 hr^{-1}
at room temperature :
◆ CO_2 (0%)-H_2O (5250ppm),
■ CO_2 (0%)-H_2O (10500ppm),
▲ CO_2 (10%)-H_2O (5250ppm)

ศูนย์วิทยทรัพยากร
จุฬาลงกรณ์มหาวิทยาลัย

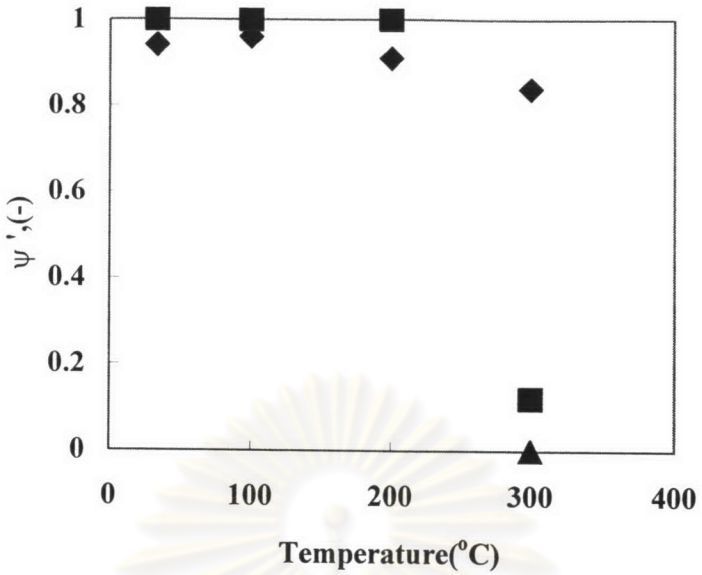

Figure 5.78 Effect of coexisting O_2-H_2O-CO_2 on the simultaneous removal of CH_3CHO, NH_3 and $(CH_3)_3N$ from N_2; $C_{in,\ acetaldehyde}$=150ppm, $C_{in,ammonia}$=1000ppm, $C_{in,trimethylamine}$=100ppm I=0.3mA, SV=77.9 hr^{-1} at room temperature :
◆ (CH_3CHO),
■ NH_3,
▲ $(CH_3)_3N$

ศูนย์วิทยทรัพยากร
จุฬาลงกรณ์มหาวิทยาลัย